University of Southern Queensland

FACULTY OF HEALTH, ENGINEERING AND SCIENCES

Investigation into the Delamination of Composite Laminates on Aircraft Rudders due to Fluid Ingress and Icing

A dissertation submitted by

Samuel Gordon Campbell Pike

In fulfilment of the requirements of

ENG4111 and ENG4112 Research Project

Towards the degree of

Bachelor of Engineering (Mechanical)

Submitted: October 2015

Abstract

Water ingestion into composite structures is one of the many causes of environmental delaminations in the wings of modern composite aircraft. Water ingestion into the composite structure occurs through three distinct pathways; capillary action through cracks in the skin, around fasteners (rivets, bonded joints) and secondary delaminations from previous repairs.

The objective of this research that is being pursued in this research dissertation is to: To investigate fluid ingress into composite aircraft laminate structure, which can lead to the delamination of the primary structure due to icing. To investigate the best methods of crack propagation accumulation progression and detection via fatigue testing by the use of tensile and flexure methods on fibre composite laminates. To compare the established tensile strength of the fibre composite laminates with results from testing and detect how much earlier the samples start crack propagation.

The results of this dissertation are as follows: under tensile testing: optical, thermography and embedded Fibre Bragg Grating (FBG) sensors were the best methods for detecting crack propagation through composite fibre laminates and under flexure testing strain gauges proved to be the best method of detecting crack propagation in composite fibre laminates.

Under tensile loading of 5Hz, the First and Second tensile samples started crack propagation between 80-93% of the ultimate tensile strength of the fibre laminate as determined by material property testing in Chapter 12.0 of 37.5KN. Under flexure testing of 1Hz the flexure sample started crack propagation at 64% of the of the ultimate tensile strength of the fibre laminate as determined by material property testing in Chapter 12.2 of 3.148KN.

As discussed in section 15.1, thermography and thermostress analysis proved to be the most viable, accurate and most importantly, easiest form of crack propagation detection medium out of the three methods of tensile, flexure and thermography testing used in this dissertation.

University of Southern Queensland

Faculty of Health, Engineering and Sciences

ENG4111/ENG4112 Research Project

Limitations of Use

The Council of the University of Southern Queensland, its Faculty of Health, Engineering & Sciences, and the staff of the University of Southern Queensland, do not accept any responsibility for the truth, accuracy or completeness of material contained within or associated with this dissertation.

Persons using all or any part of this material do so at their own risk, and not at the risk of the Council of the University of Southern Queensland, its Faculty of Health, Engineering & Sciences or the staff of the University of Southern Queensland.

This dissertation reports an educational exercise and has no purpose or validity beyond this exercise. The sole purpose of the course pair entitled "Research Project" is to contribute to the overall education within the student's chosen degree program. This document, the associated hardware, software, drawings, and other material set out in the associated appendices should not be used for any other purpose: if they are so used, it is entirely at the risk of the user.

University of Southern Queensland

Faculty of Health, Engineering and Sciences

ENG4111/ENG4112 Research Project

Certification of Dissertation

I certify that the ideas, designs and experimental work, results, analyses and conclusions set out in this dissertation are entirely my own effort, except where otherwise indicated and acknowledged.

I further certify that the work is original and has not been previously submitted for assessment in any other course or institution, except where specifically stated.

Samuel Pike

0061031749

_____

Signature

_____

Date

Acknowledgements

This project was carried out under the supervision of Dr Jayantha Epaarachchi. I would like to offer my sincere appreciation for his support and guidance through the completion of this research and dissertation.

I would like to thank the technical staff especially Wayne Crowell and Martin Geach at the Centre for Excellence in Engineering Fibre Composites (CEEFC) for their assistance in the preparation of the experimental samples and the use of their P11 facilities.

I would like to express thanks to Ayad Kakei for his assistance with Abaqus and Experimental Testing.

Lastly I would like to thank my wife Diana Pike for her love, patience and support in the completion of this degree over the past 5 years.

Table of Contents

List of Figures

List of Tables

Nomenclature

Abaqus	Finite Element Analysis Package designed to handle delaminations, loadings and stress strain and displacement analysis of composite structure.
CEEFC	Centre for Excellence in Fibre Composite Technologies (USQ)
Empennage	The rear part of an aircraft including the vertical and horizontal stabiliser and the associated flight controls such as the rudder and the elevator.
Environmental delamination	Delaminations which occur by use of some environmental factor such as water or biological mechanism
FAR	Federal Aviation Regulations
FBG	Fibre Bragg Grating
FEA	Finite Element Analysis
GAG	Ground Air Ground, the flight cycle of a commercial aircraft
GFRP	Glass Fibre Reinforced Plastic
ISO	International Standards Organisation
NDT	Non Destructive Testing
Primary Structure	Aircraft structure that would endanger the airworthiness of the aircraft if it failed (NSW 2010)

Secondary Structure	Aircraft Structure that would not immediately endanger the airworthiness of the aircraft (NSW 2010)
SHM	Structural Health Monitoring
SRM	Structural Repair Manual
VD	Designed Diving Speed
VMC	Minimum Control Speed for Take-off

Chapter 1.0 Introduction

1.1 A Brief Introduction

Designing aircraft from composite materials is not a new concept. It was first introduced in the 1950's when Boeing covered approx. 2% of their 707 aircraft with fibreglass matting. Because the properties of composites materials were little known at the time, only 20m^2 of the flooring of was made of fibreglass (Environment 2014).

With advancements in the understanding of how composite materials behave and the role that they play in modern aircraft design, more and more, large aircraft manufacturers such as Boeing and Airbus are using composite materials in the designs of their aircraft today.

It is advantageous to use composites over other materials such as Aluminium in aircraft design (Baker & Kelly 2004) as:

- Corrosion problems caused by using Aluminium are removed.
- flight performance as improved damage allowances are improved and the aerodynamics are smoother
- production rates are faster as riveting Aluminium structures are removed
- Significant weight reduction means increased range, lower fuel costs and larger payloads carried.

With the increased benefits of composite materials over traditional Aluminium structures, aircraft designers naturally include as much of this lighter material as possible. Until recently composite materials have only been used in secondary structures such as flaps, fairings, doors and other areas deemed not flight critical.

With an increasing desire to move composite materials into the primary structure of the aircraft, much research has gone into the changes that happen to composite structures when they are damaged and the effect that this has on the structural integrity of the composite fibres. This area of investigation is called structural health

monitoring. Structural health monitoring focuses on various damage mechanisms within the fibre structure of the composite material.

Disbonding which leads to delamination of the composite laminates is the most common form of structural integrity breakdown of a fibre composite structure. It occurs when mechanical forces separate the resin bonds causing a void to form within the fibre structure (Russell & Street 1985). In the case of aircraft operating at high altitudes, this mechanical separation of the resin bonds can be caused by damage to the outside structure of the composite laminate, thus allowing water and icing to affect the internal structural integrity of the material.

The area of study in the structural health monitoring sphere that I wish to investigate further is the effect that icing plays on the water ingestion damage mechanism of delaminations of composite laminates.

1.2 Idea Initiation

The idea to do something in the area of the delamination of composite structures due to icing originally came from working as a Licensed Aircraft Maintenance Engineer on Saab 340 aircraft (see Figure 1). Most of the skin of the aircraft is made from Aluminium with certain areas such as the flaps, empennage, landing gear doors and various other fairings being made from an Aluminium/fibre glass sandwich composite which, although is lightweight, is prone to corrosive damage as well as disbonding if the integrity of the Aluminium covering is compromised.

Areas made of composite structures which are prone to damage due to the ingesting of water into the composite structures include the leading edges of the nose landing gear doors, the leading edge of the flaps and the stabiliser regions. These areas are more prone to ingest water into their composite structures especially if they had been damaged beforehand.

As part of the inspection procedure in the Saab 340 maintenance manual the initial method of inspecting an area for possible delaminations is the carrying out of the "coin tap test" which involves tapping a coin on the composite skin. If the noise

changes to a thud then you have a delamination. The next step is to determine the size of the delamination, repair the delamination in accordance with the SRM (Structural Repair Manual), and check the repair by NDT (Non-destructive testing) methods such as ultrasonic inspection.

I thought this method very crude and when the research project came up I thought it might be interesting to pursue a project in this area. Initial discussions with Dr Jayantha Epaarachchi (USQ School of Mechanical Engineering) my current supervisor confirmed that I could pursue a project in this area that was worth further investigation.

Structural Health Monitoring of Smart Structures is a large component of the (CEEFC) Centre for Excellence in Fibre Composite Technologies work at USQ. They had the resources and the knowledge to assist me in this project and for that reason I choose a supervisor who had a vast knowledge in this area and could effectively assist me in this project.

Figure 1: Saab 340 aircraft (Network 2014)

1.3 Aims, Objectives and Scope

This research aims to cover three important areas of research.

- To investigate fluid ingress into composite aircraft laminate structure, which can lead to the delamination of the primary structure due to icing.

- To investigate the best methods of crack propagation accumulation progression and detection via fatigue testing by the use of tensile and flexure methods on fibre composite laminates.

- To compare the established tensile strength of the fibre composite laminates with results from testing to detect how much earlier the samples start crack propagation.

In order to achieve this project in the given timeframe the following objectives need to be completed.

1. Research background information relating to fluid ingress into composite structure.

2. Research the icing effects of fluid ingress on high altitude flight on laminated composite primary structures.

3. Research the mechanisms of damage propagation in laminated composites due to absorbed fluids during the GAG cycle.

4. Create an appropriate Finite Element Analysis (FEA) model Abaqus or other packages (as available) to model delaminations in aircraft composite laminates.

5. Create a composite panel utilising embedded FBG sensors and strain gauges to laboratory level investigation of how damage accumulation progresses through the GAG cycle of an aircraft.

6. Carry out laboratory experiments to investigate damage propagation in water absorbed composite panel.

7. Carry out Data Analysis to compile, plot and evaluate the collected data obtained from the test samples.

8. Write up the project dissertation.

A more detailed description of the detailed methodology and resource requirements are included in Chapter 3.0 and Chapter 4.0.

1.4 Expected Outcomes and benefits

The project is designed to investigate the internal structure of a composite rudder skin exposed to water ingestion at low temperatures or conditions experienced by a large percentage of commercial and experimental aircraft.

The expected outcomes of this project include:

1. To provide insight into how fluid ingress causes delaminations in composite rudders.

2. To provide insight into how crack propagation occurs via fatigue testing using tensile and flexure methods on fibre composite structure.

3. To compare the established tensile strength of the laminates with the results from testing to see how much earlier the samples start crack propagation.

The expected benefits of this project include

1. A deeper understanding of the environmental impacts of fluid ingress into composite aircraft laminates.

2. Further development resulting from this investigation may open other areas of scientific research into ways of protecting aircraft skins from damage.

3. More information would be available to the engineers working on aircraft around the World who would benefit from further investigation into this phenomenon, and would have better ways of detecting damage before the repairs became too expensive.

Chapter 2.0: Background and Literature Review

2.1 The Evolution of Fixed Wing Aircraft

The first successful controlled powered flight was made by two brothers Wilbur and Orville Wright on December 17th 1903 (History 2015).

Other flight pioneers such as Otto Lilienthal, a German engineer who successfully built and tested over 16 different glider designs in which he made numerous measurements about lift and drag before he was tragically killed testing one of his monoplane designs in 1896 (Gray 2015).

So why was their achievement so special? The Wright Brothers were the first to come up with a way to successfully maintain stable and controlled flight through the use of wing warping and the first to design a successful propeller to propel an aircraft through the air. (Museum 2014)

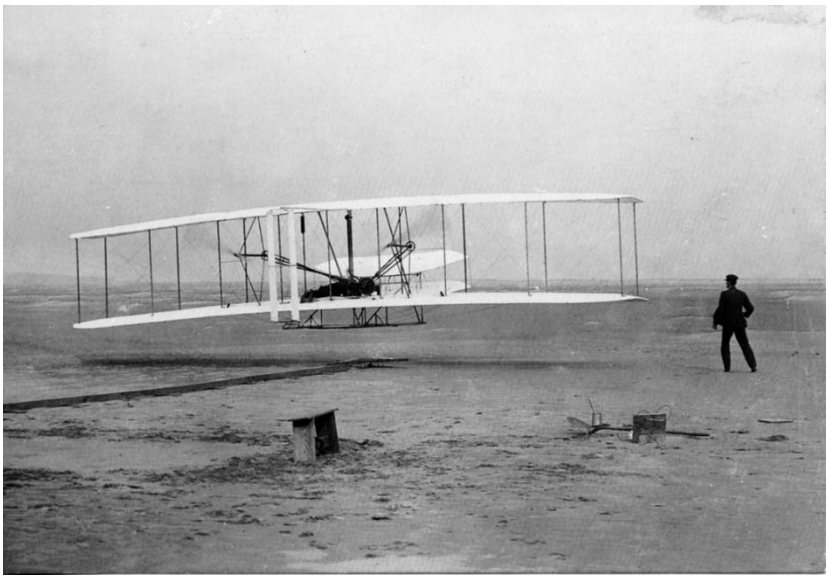

Figure 2: Wright Flyer 1903 (Museum 2014)

The development of aircraft continued slowly between 1907 and 1914 with the advancement in controlling flight such as the use of ailerons, the first production aircraft and a French built aircraft called the Demoiselle, a monoplane design capable of speeds above 100km/h.

With the advent of WW1 aircraft were used first in photo reconnaissance and then increasingly as fighters and bombers with increasing larger bomb loads. After WW1 fabric covered aircraft were seen as outdated, too slow and therefore, the first all-metal aircraft were constructed.

WW2 saw the an increase -in speed, agility and horsepower of the propeller driven aircraft which could reach altitudes requiring oxygen to breathe and also saw the first jet powered aircraft being used at the end of the war in 1945.

In 1940, composite technology was used for the first time in the production of aircraft with the introduction of the de Havilland Mosquito. It used a frameless monologue design utilising sheets of Ecuadorean balsawood sandwiched between layers of Canadian Birch. The combination of the these two materials allowed for a strong lightweight structure only 11mm thick that didn't require any extra stiffening. Problems with this design soon arose when the aircraft was used in tropical conditions causing 'Casein glue' to crack under humid monsoonal conditions (Cook 2010).

2.2 The Use of Composites in Modern Commercial Aircraft Design

Increasingly composite materials were used in commercial aviation in order to increase weight savings and remove many of the corrosion problems associated with Aluminium. From the 1980's onwards, commercial manufacturers started adding composite components to new aircraft designs. As the failure mechanisms of composite weren't really understood by the industry, only secondary structure was made from composite materials such as fairings and nose cones. The 707 was the first aircraft to utilise this new technology in the form of floor boards for the passengers and crew.

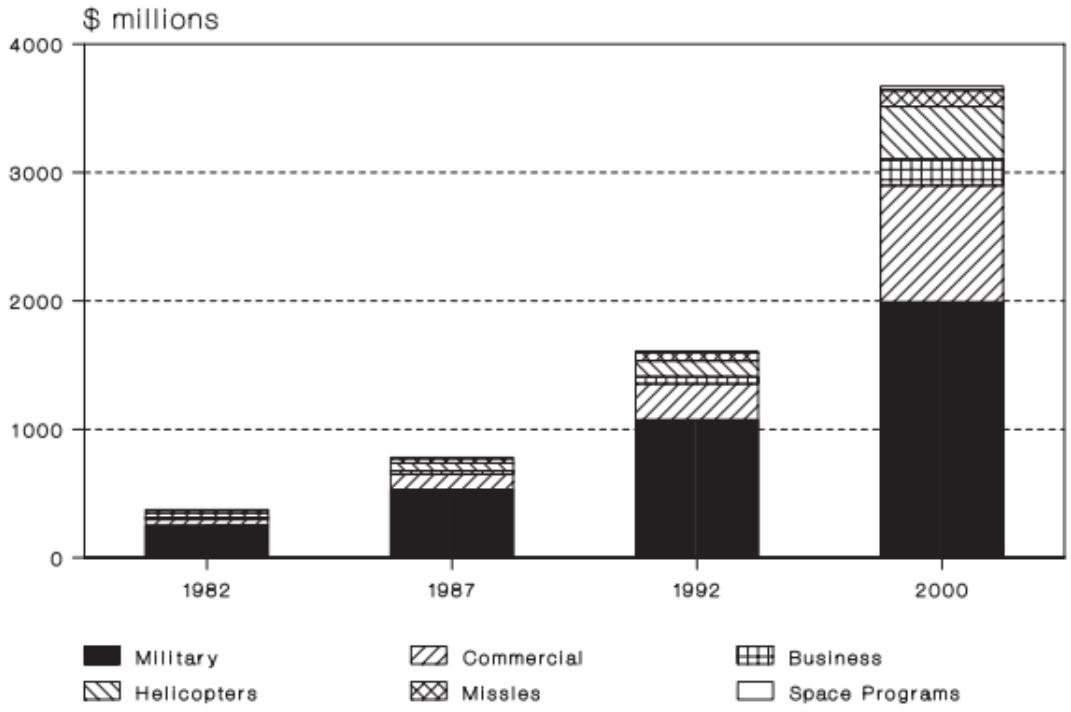

Figure 3: Growth of the Use of Composites in the Aerospace Industry (Ali 2015)

Traditionally, the military has used composite materials more than its civil counterparts mainly because military aircraft with ejection seat could have much higher safety factors. An interesting comparison between military and commercial aircraft composites is shown in the graph shown below (Figure 4).

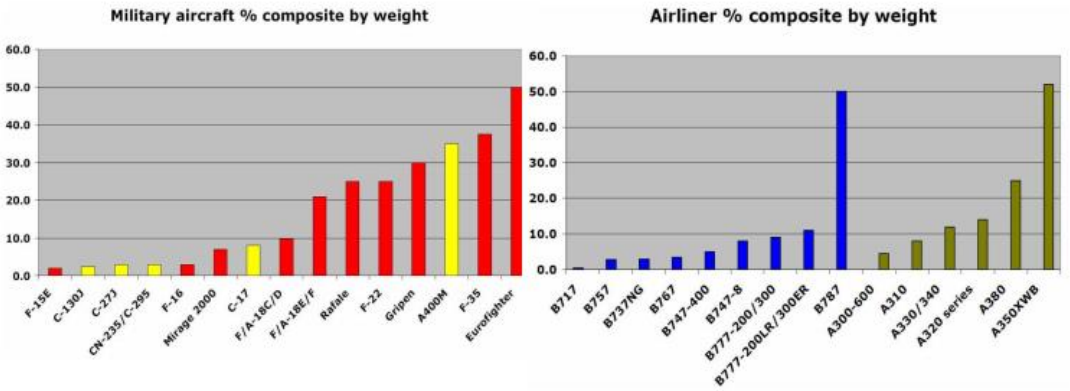

Figure 4: Comparison between Military and Commercial Aircraft Composites content (Smith 2013)

Until recently, only the military with large budgets could afford to develop composite aircraft. In recent years, three things have made commercial companies look at the benefits of using composite materials more closely (Smith 2013, p. 14)

- The increasing price of oil
- The solid predictions of the increase in airline traffic
- A change in attitude about environmental issues

2.3 Composite Materials

Composite materials are fast becoming the material of choice for many engineering applications where traditionally Aluminium or wood had been used previously. The benefits of using composites over more traditional materials are Lighter Weight, Corrosion Resistance, High Strength, Flexibility in Design, many are Non-Conductive electrically, Non-Magnetic and Durable (Australia 2015).

2.3.1 Glass Reinforced Fibre Plastics - GRFP

Fibreglass or GRFP is a lightweight, strong and durable material has a high strength to weight ratio and when impregnated with epoxy resin is stronger than steel based on a per weight basis. Its high strength to weight ratio is the reason why the popularity of GRFP has increased since the 1950's. With an increase in the amount of the combinations available with the addition of other fibre enhancement materials such as Kevlar and Carbon, the fibreglass matrix becomes stronger and stiffer still.

There are many types of Fibreglass reinforcement available. 5 of the most popular are:

- D-glass used in circuit boards with a low dielectric constant
- A-glass offers good chemical resistance, but low electrical properties
- E-glass, the most common type used in fibreglass production, an excellent electrical insulator, inexpensive and appropriate for general usage.
- S-glass, is stronger than E glass, improved mechanical properties, more expensive but has a high modulus of elasticity.
- C-glass is resistant to corrosion and most chemicals.

2.3.2 Weave Styles

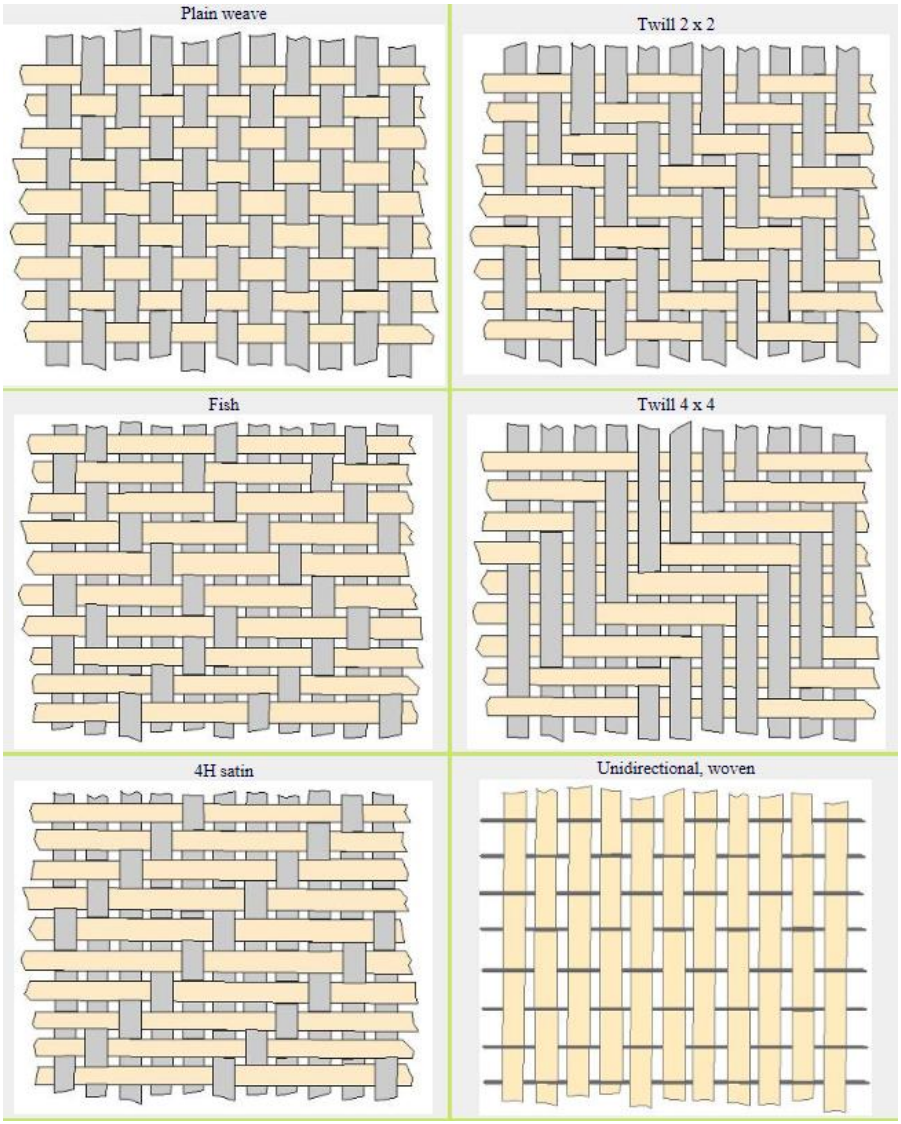

Figure 5: Various Weave Styles found in Fibreglass (Composites, Firemax 2014)

The most common form of fibreglass for aircraft applications is E-Glass for its strength to weight ratio and its low cost. As Figure 5 shows there are many types of Weave Styles available for use in fibreglass production. The Plain weave matting provides the best structural properties for aircraft (Composites, Firemax 2014).

2.3.2 Cores

Aircraft cores are used in aircraft structures to reduce the amount of material needed to form a required shape and reduce the cost and weight to achieve the required outcome. Due to the cost of GRFP and CRFP, the core also acts as a medium for a high Specific Strength in a composite laminate. This gives a high material strength to weight ratio using sandwich- structural composite applications (Choi & Jang 2010). Due to the many and varied properties of aircraft cores, two types are mainly used in the construction of aircraft composites, Nomex Honeycomb and PVC foam.

2.3.3 Nomex Honeycomb

Nomex Honeycomb is a commonly used composite core material manufactured with Nomex paper dipped in heat resistant resin. The material has the form of a beehive hexagonal structure; it has an excellent combination of efficiency and strength, with reducing the overall weight of the component.

Composite fibre reinforcement that uses Honeycomb are Aluminium, Plastics, Carbon fibre reinforced plastics and fibreglass. In the future, the estimated growth of commercial aircraft from 3.4% to 5.4% annually will ensure composites will grow substantial in the future with the use of UAV's, and other future aircraft designs. Figure 5 shows some of the commonly used Nomex Honeycomb Cores thicknesses.

Type	Thickness	Cell size	Density	Strength	Modulus
1	1.5mm	3.2mm	48Kg/m^3	300PSI	18.5KSI
2	2mm	3.2mm	48kg/m^3	300PSI	18.5KSI
3	3mm	3.2mm	48Kg/m^3	300PSI	18.5KSI
4	4mm	3.2mm	48Kg/m^3	300PSI	18.5KSI
5	5mm	3.2mm	32kg/m^3	150PSI	11KSI
6	6mm	3.2mm	32kg/m^3	150PSI	11KSI
7	7mm	4.8mm	32kg/m^3	150PSI	11KSI
8	7mm	3.2mm	32kg/m^3	150PSI	11KSI
9	10mm	3.2mm	48Kg/m^3	300PSI	18.5KSI
10	11mm	4.8mm	32kg/m^3	150PSI	11KSI
11	15mm	4.8mm	32kg/m^3	150PSI	11KSI

Type	Thickness	Weight
1	2mm	90kg/m^3
2	3mm	55kg/m^3
3	3mm	75kg/m^3
4	3mm	90kg/m^3
5	5mm	90kg/m^3
6	10mm	55kg/m^3
7	10mm	75kg/m^3
8	12mm	55kg/m^3
9	12mm	75kg/m^3
10	13mm	75kg/m^3
11	15mm	75kg/m^3
12	15mm	90kg/m^3
13	15mm	200kg/m^3
14	20mm	75kg/m^3
15	20mm	90kg/m^3
16	20mm	200kg/m^3
17	25mm	75kg/m^3
18	30mm	75kg/m^3

Figure 6: Nomex Core and PVC foam Cores Commonly Available (Composites, Fibremax 2014)

2.3.4 PVC Foam

PVC foam is a very popular alternative to honeycomb cores but is mainly used in the interior- of aircraft due to its decreased time life costs and high quality. PVC foam in a hybrid form has been used as a structural component in some aircraft sandwich composites especially close to the fibre reinforcement. This greatly improves the resistance to delamination, impact and fatigue.

PVC foam consist of between 50% to 95% air inside the foam core, which results in a wide range of densities between 55 – 200 kg/m^2. PVC foam can be used with a range of resin from epoxy, polyester and vinyl ester. Various mixes of the of PVC foam have yielded a surprising range of high physical properties which are discussed below (Composites, Fibremax 2014):

Water absorption Ranges: 0.07 to 0.03kg/mm^2
Tensile Modulus: 45 to 180N/mm^2
Tensile Strength: 1.30 to 6.20N/mm^2
Shear Strength: 0.8N/mm^2 till 3.5N/mm^2

Figure 7 shows various forms in which PVC foam can be modelled in order to form an aircraft wing, rudder or horizontal stabiliser.

Sandwich designs preferred in airplane and helicopter construction

Construction concept	Sketch	Rigidity	Weight	Layup cost	Jointing cost
Full sandwich design		++	+	++	++
Skin sandwich		+	++	+	0
Profile reinforcement		+	+	0	+

● ROHACELL®, ● Cover layer, e.g. CFRP, ++ very good, + good, 0 satisfactory

Figure 7: Sandwich design using foam cores (Evonik 2015)

2.3.3 Delamination of Aircraft Composite Structures

A delamination is when a failure of the adhesion has occurred between the adjacent layers within a composite laminate, these can occur in the form of the local separation of two previously adhered layers (Russell & Street 1985). It's the most common of all the failure modes, if the composite matrix cracks then a delamination will probably occur (Bureau 2007).

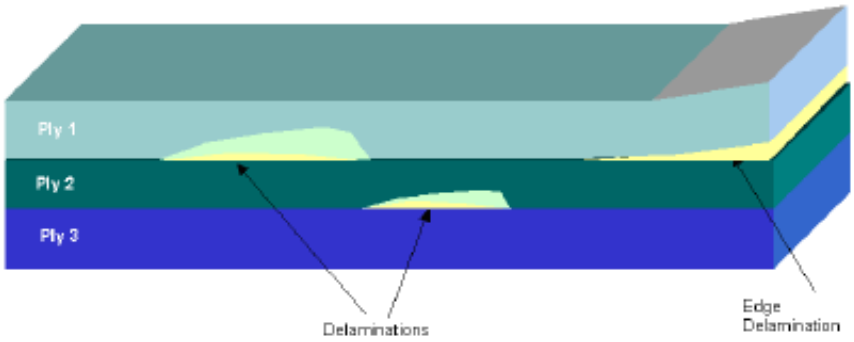

Figure 8: Delamination (Russell & Street 1985)

Delaminations in the fibre composite laminates Figure 8 are caused by many different factors: impact damage and subsequent cracking with the cyclic loads imposed on the airframe wing structure, UV and adhesive degradation after many years of flight loads and sun damage imposed on the airframes, and in the case of sports or experimental aircraft with the use of bonded joints, disbonding can occur when improper manufacturing techniques are carried out on non-pressurised aircraft (Authority 2010).

Manufacturing defects in composites account for a fair percentage of the premature failure of composite structures due to the manual process of "laying up" by hand of the composite materials. This process is still the primary way to manufacture small components, as autoclaves used to cure the composite item are often bulky and required specialist training.

Delaminations are mainly a problem under compression loading; tensile loading is generally a lot smaller. Due to the delaminated area acting like a unfilled hole, the delaminated region has a low modulus reducing its residual strength.(Sih & Hsu 1987)

An incidence where a delamination occurred that almost brought down an aircraft was in 1989. The rudder of a Concorde sustained a rudder separation between the Aluminium skin and the Aluminium honeycomb core caused by the phenolic resin being loosened by the inclusion of water between the laminates. Water was able to leak into the honeycomb core through rivet holes that weren't properly sealed.

2.4 Fluid ingestion in Composite Structure

A literature review was undertaken to understand the problem and to further develop the research project. In the course of the research 3 keys areas were recognized as the main topics that required further research. Below is a summary of the current literature review:

- The Effects of Temperature and Moisture
- Water ingress into the honeycomb core of composite structure on aircraft
- Documented cases where water ingress into the honeycomb core of composite structure damaged an aircraft.
- The use of NDT (Non-destructive testing) and sensors to measure internal environment of composite structure.

2.4.1 Effects of Temperature and Moisture (Ground Air Ground GAG cycle

Moisture Ingress into composite structures is one of the main causes of delamination in composite aircraft. What makes this mechanism especially problematic is what happens to the fluid when it is trapped inside an aircraft component. The Ground Air Ground cycle works by as an aircraft is climbing through 8000 feet, the fluid inside the composite laminate transitions from a liquid to a solid. While the aircraft is in cruise the fluid solidifies into ice, then as the aircraft descends back through 8000 feet the trapped ice thaws into a liquid state again.

Over time this Freezing and Thawing of the trapped fluid with the addition of fatigue on a flight control leads to failure of the laminate and eventually the flight control.

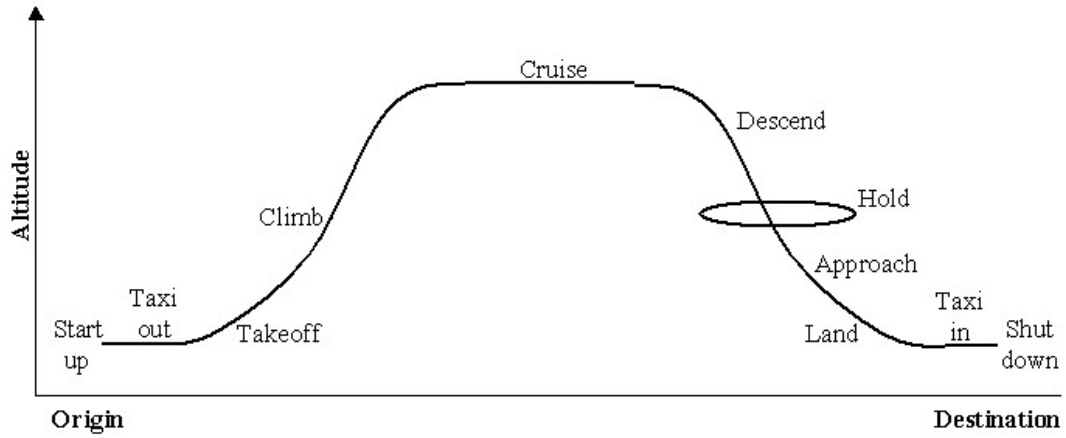

Figure 9: Flight Cycle Profile of Aeroplane (Avionics 2000)

(Figure 9) shows a typical flight profile of an aeroplane. Most aircraft only fly in the troposphere at an altitude of between 0 and 36,000 feet. Aeroplanes spend most of their flight time above the freezing point of water, which is 2300m or 7545 feet according to the US standard atmospheric table below Figure 10.

ALTITUDE (Feet)	TEMP. (°C)	PRESSURE			PRESSURE RATIO $\delta = P/Po$	DENSITY $\sigma = \rho/\rho o$	Speed of sound (kt)	ALTITUDE (meters)
		hPa	PSI	In.Hg				
40 000	- 56.5	188	2.72	5.54	0.1851	0.2462	573	12 192
39 000	- 56.5	197	2.58	5.81	0.1942	0.2583	573	11 887
38 000	- 56.5	206	2.99	6.10	0.2038	0.2710	573	11 582
37 000	- 56.5	217	3.14	6.40	0.2138	0.2844	573	11 278
36 000	- 56.3	227	3.30	6.71	0.2243	0.2981	573	10 973
35 000	- 54.3	238	3.46	7.04	0.2353	0.3099	576	10 668
34 000	- 52.4	250	3.63	7.38	0.2467	0.3220	579	10 363
33 000	- 50.4	262	3.80	7.74	0.2586	0.3345	581	10 058
32 000	- 48.4	274	3.98	8.11	0.2709	0.3473	584	9 754
31 000	- 46.4	287	4.17	8.49	0.2837	0.3605	586	9 449
30 000	- 44.4	301	4.36	8.89	0.2970	0.3741	589	9 144
29 000	- 42.5	315	4.57	9.30	0.3107	0.3881	591	8 839
28 000	- 40.5	329	4.78	9.73	0.3250	0.4025	594	8 534
27 000	- 38.5	344	4.99	10.17	0.3398	0.4173	597	8 230
26 000	- 36.5	360	5.22	10.63	0.3552	0.4325	599	7 925
25 000	- 34.5	376	5.45	11.10	0.3711	0.4481	602	7 620
24 000	- 32.5	393	5.70	11.60	0.3876	0.4642	604	7 315
23 000	- 30.6	410	5.95	12.11	0.4046	0.4806	607	7 010
22 000	- 28.6	428	6.21	12.64	0.4223	0.4976	609	6 706
21 000	- 26.6	446	6.47	13.18	0.4406	0.5150	611	6 401
20 000	- 24.6	466	6.75	13.75	0.4595	0.5328	614	6 096
19 000	- 22.6	485	7.04	14.34	0.4791	0.5511	616	5 791
18 000	- 20.7	506	7.34	14.94	0.4994	0.5699	619	5 406
17 000	- 18.7	527	7.65	15.57	0.5203	0.5892	621	5 182
16 000	- 16.7	549	7.97	16.22	0.5420	0.6090	624	4 877
15 000	- 14.7	572	8.29	16.89	0.5643	0.6292	626	4 572
14 000	- 12.7	595	8.63	17.58	0.5875	0.6500	628	4 267
13 000	- 10.8	619	8.99	18.29	0.6113	0.6713	631	3 962
12 000	- 8.8	644	9.35	19.03	0.6360	0.6932	633	3 658
11 000	- 6.8	670	9.72	19.79	0.6614	0.7156	636	3 353
10 000	- 4.8	697	10.10	20.58	0.6877	0.7385	638	3 048
9 000	- 2.8	724	10.51	21.39	0.7148	0.7620	640	2 743
8 000	- 0.8	753	10.92	22.22	0.7428	0.7860	643	2 438
7 000	+ 1.1	782	11.34	23.09	0.7716	0.8106	645	2 134
6 000	+ 3.1	812	11.78	23.98	0.8014	0.8359	647	1 829
5 000	+ 5.1	843	12.23	24.90	0.8320	0.8617	650	1 524
4 000	+ 7.1	875	12.69	25.84	0.8637	0.8881	652	1 219
3 000	+ 9.1	908	13.17	26.82	0.8962	0.9151	654	914
2 000	+ 11.0	942	13.67	27.82	0.9298	0.9428	656	610
1 000	+ 13.0	977	14.17	28.86	0.9644	0.9711	659	305
0	+ 15.0	1013	14.70	29.92	1.0000	1.0000	661	0
- 1 000	+ 17.0	1050	15.23	31.02	1.0366	1.0295	664	- 305

Figure 10: US Standard Atmosphere (Talay 1975)

Many maintenance organisations have started to use Forward Looking Infrared Imaging Systems (FLIR) systems to detect moisture ingress in composite flight controls post flight. These tests have to be performed within an hour of the aircraft landing while there is a temperature differential between the ambient air and the temperature inside the composite flight control.

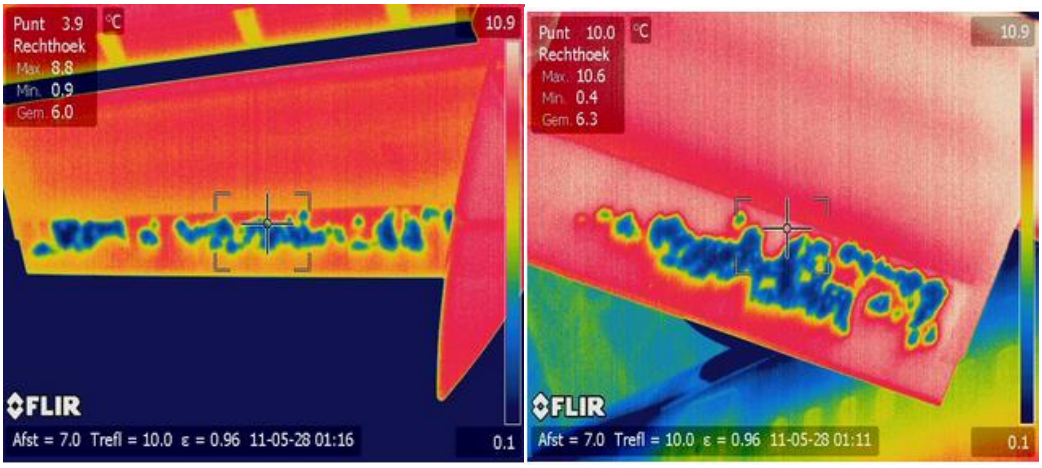

Figure 11: Water Ingress in Flap of B767-200 (BV 2015)

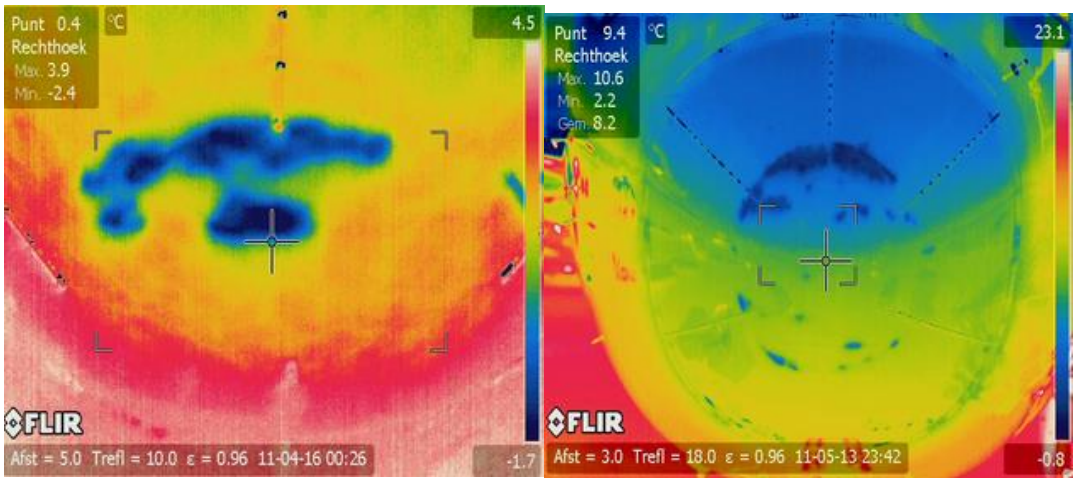

Figure 12: Water Ingress in Radome of B767-200 (BV 2015)

2.4.2 Fluid ingress into the honeycomb core of composite structure on aircraft

There are (three) main ways that Moisture ingress can occur in composite structures:

- Capillary action through cracks in the skin
- Around fasteners (rivets, bonded joints)
- Previous repairs

Capillary action: One of the leading causes of water ingress into composite structures is by damage caused by external forces such as stone and rock damage, the dropping of tools onto the composite structure and manufacturing defects. Once the exterior layer of a composite skin has been damaged, the structural integrity of the composite structure starts to deteriorate and weaken the structure.

Water ingress into the composite layers will start to occur due to the nature of the aircraft flying through the air progressively forcing water into the composite skin. By the action of the water freezing and reheating cracks start to grow within the composite structure (Shafizadeh et al. 2003).

Around fasteners: Most pressurised aircraft require some kind of sealing around rivets and joints in order to reduce leakage of pressurised air from cabin to the outside environment. Over time the sealing material wears away often causing leakage between the rivet and the skin of the aircraft. In the case of composite aircraft structures, the application of adhesive is especially important as any water making its way through into the composite structure could delaminate the various composite skin layers.

Previous repairs: An area that has been previously repaired, whether it is made of Aluminium or composite, will always need to be checked for further issues. In the case of a composite panel, they are susceptible to secondary delaminations. Problems can also occur where there is lack of specialist maintenance personal doing the repair and repairs schemes fall outside the scope of the SRM (Structural Repair Manual). With the lack of NDT (Non Destructive Testing) facilities at maintenance bases, water ingress damage can go unchecked throughout the skin weakening the structure (Authority 2010).

2.4.3 What is an Aircraft Rudder?

In order to successfully control the flight of an aircraft, the pilot needs control about three Axes. They are Roll, Pitch and Yaw. Roll is controlled by the ailerons; Pitch is controlled by the elevators and Yaw by the Rudder.

The vertical stabiliser which is attached to the rudder is used to prevent a yawing motion of the aircraft (Figure 13). The Rudder which is connected to the vertical stabiliser by hinges acts like a small tab varying the amount of force placed on the vertical stabiliser. In this way the yawing motion of the aircraft is controlled (Benson 2014).

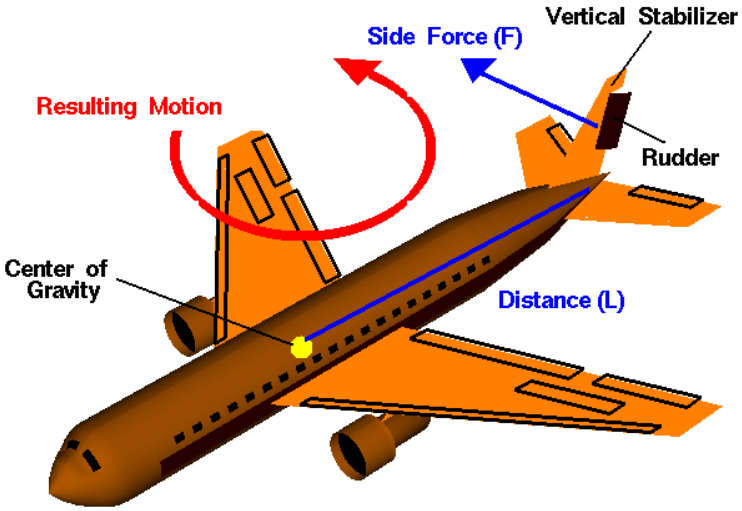

Figure 13: Vertical Stabiliser - Rudder (Benson 2014)

In normal flight conditions, the rudder is sized for the airframe to provide 2 important functions:

- Provide enough lateral control to the aircraft within the scope of crosswind take-offs and landings
- Provide positive aircraft control in engine failure conditions and regions of maximum asymmetric thrust, at any speeds above the minimum speed to control the aircraft on the ground.

2.4.4 Rudder Flight Loads

The rudder of the A310 is designed to handle up to 1.5 times the recommended flight loads ever to be applied to the rudder. According to JAR/FAR 25 requirements 'these loads correspond to the maximum loads expected once in service'. An aircraft rudder is also expected to handle the ultimate flight load and limit loads without

permanent deformation of the structure for at least 3 seconds without failure at any of the flight profiles expected in the life of the structure.

In normal flight conditions, maximum design loads are never supposed to be reached because of a rudder limiting system. This provides reduced movement to the rudder as the speed of the aircraft increases. The operation of this system is as follows; as the speed of the aircraft over the ground increases, the rudder angle required to positively control the aircraft decreases, this is also transmitted through to the rudder pedal and the associated forces applied to the rudder also decrease. Therefore 'Rudder travel is limited as a function of aircraft speed'(IFALPA 2010).

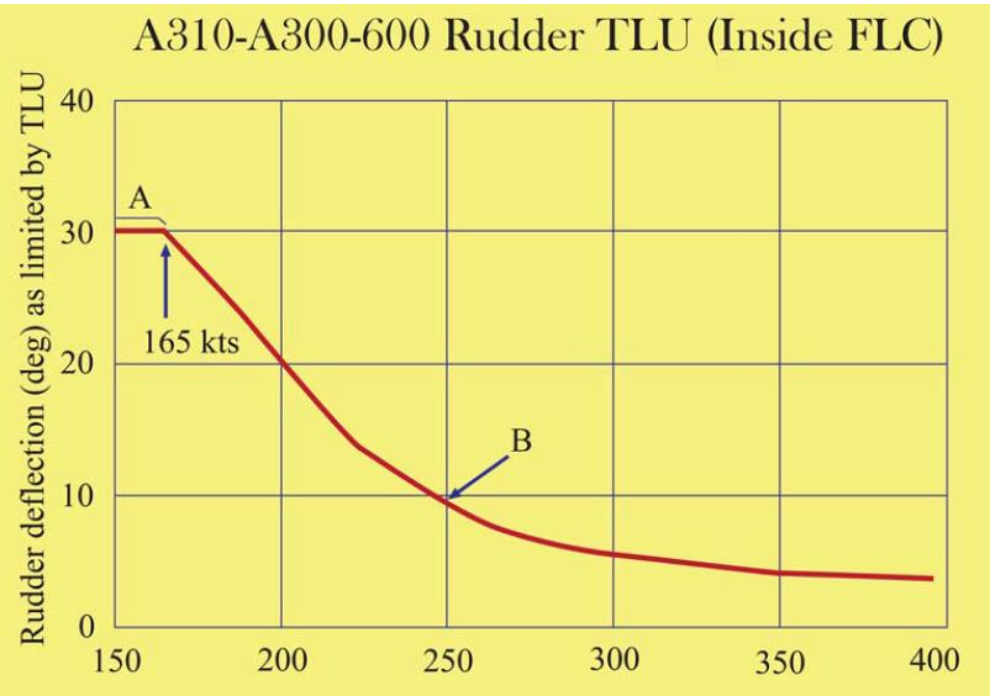

Figure 14: Rudder Limiting System of the Airbus 310 (IFALPA 2010)

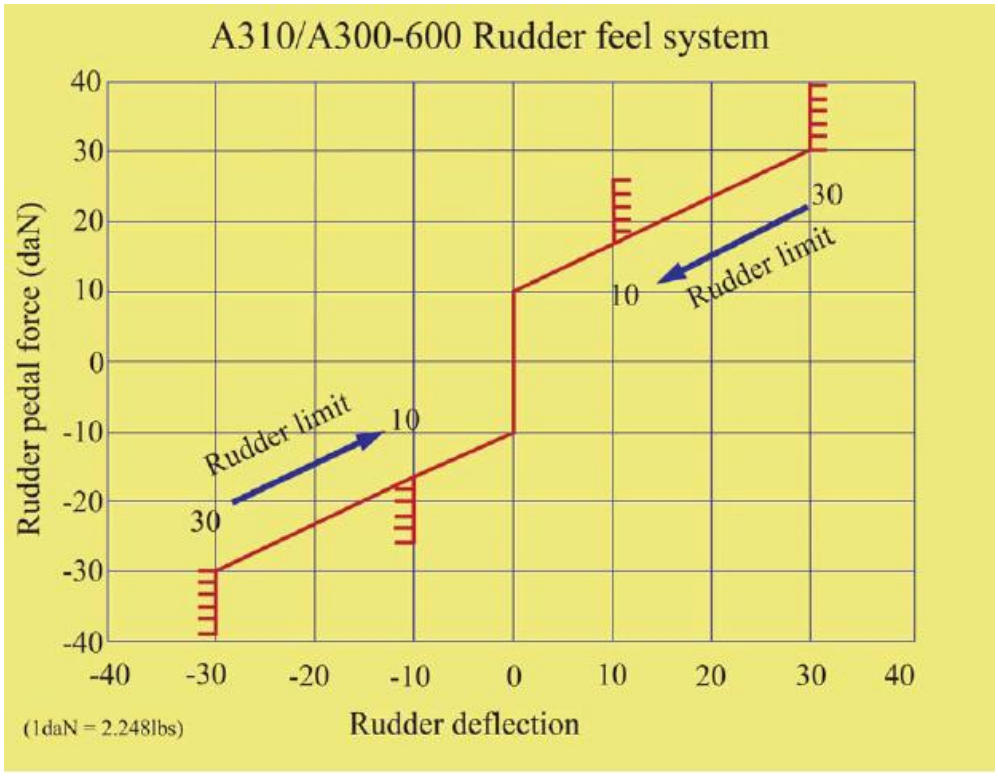

Figure 15: Rudder Feel System on the Airbus A310 (IFALPA 2010).

Due to the proprietary nature of the Airbus aircraft design, the exact design limits of the Airbus aren't readily available for public viewing so accurate test conditions aren't possible and won't be included in this research.

The standard methodology for designing a rudder is spelt out in the FAR 25.351(a) criteria for commercial aircraft design. At speeds from VMC to VD the following must be used for computing tail loads and the yawing velocity = 0. See figure 15 (Lomax 1996).

1. Manoeuvre I: With the aircraft at zero yaw in un-accelerated flight, it can be assumed that the rudder can be deflected to the maximum deflection as limited by the control stops or the 300lb rudder pedal force.
2. Manoeuvre II: The rudder yaws to the resulting sideslip if the rudder is deflected as specified in FAR 25.351(a).
3. Manoeuvre III: The Rudder is assumed to return to neutral with the aircraft yawed to a static sideslip angle corresponding to the rudder specification as specified in FAR 25.351(a)1 (Lomax 1996).

These rudder conditions are labelled in (Figure 16) as Man I, Man II and Man III. In modern aircraft the loads applied on the rudder pedals are further reduced to around the 200lb mark by the advent of hydraulically operated flight controls, which relieves the force required to push the rudder pedals to excite a rudder movement.

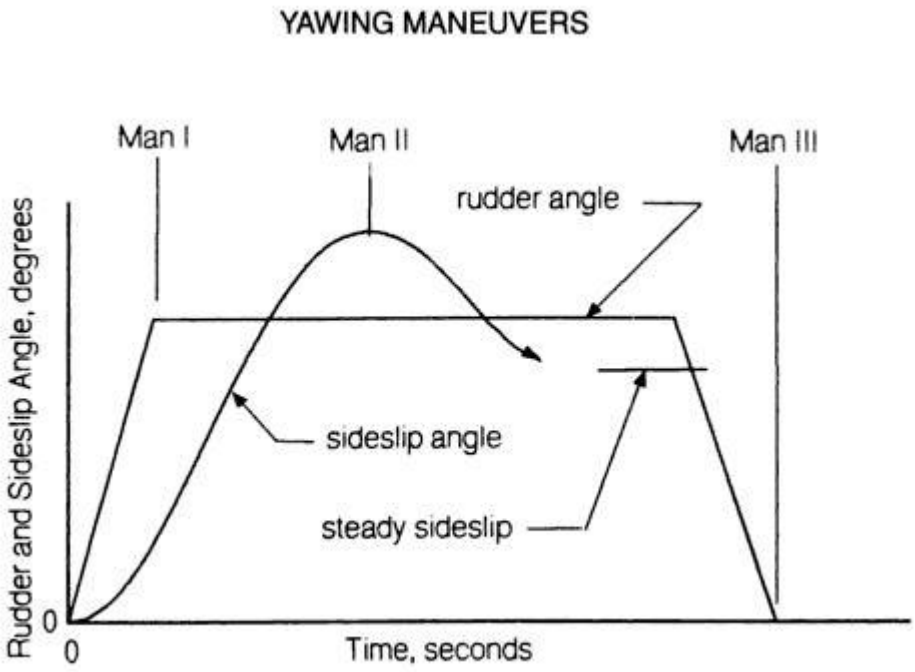

Figure 16: Aircraft Rudder Design according to FAR 25.351(a) (Lomax 1996)

2.4.5 Airbus Rudder

Due to the information available, the rudder system that the project is going to look into comes from an Airbus 310, (part of the Airbus A320 family of aircraft). Below is a CAD model of the empennage of a typical A310 minus the horizontal stabiliser, the height of the vertical stabiliser and rudder assembly is 8.3m tall and 11.238m in length.

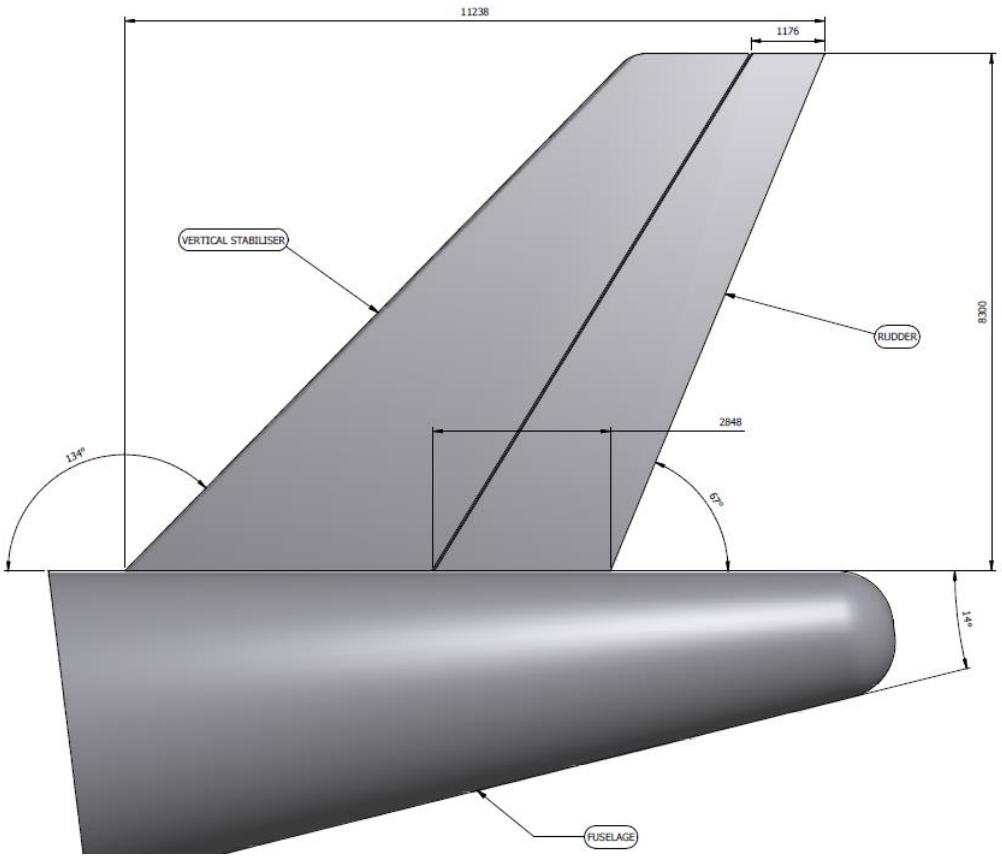

Figure 17: Airbus A310-300 Empennage minus Horizontal Stabiliser (Airbus 2002)

On the Airbus, the vertical stabiliser is called the Vertical Tail plane. The Vertical Tail Plane (VTP) consists of a leading edge fairing; trailing edge panels, a tip and a spar box see Figure 11. The leading edge fairing and the tip are both constructed of sandwich composite of Glass fibre – reinforced plastic (GFRP) and carbon fibre-reinforced plastic (CFRP). The two trailing edge panels are constructed of a series of laminate stiffeners and solid carbon fibre- reinforced plastic (CFRP) skin laminate skin.

The Spar box is an arrangement of trailing edge panels, 2 laminated (CFRP) spars (front and rear) plus a smaller spar extending to rib 5 which have transverse loading fittings on the fuselage side. 18 (CFRP) ribs, including the top and bottom rib encompass the edges of the box arrangement. The trailing edge spar has an aerodynamic fairing attached to it to fill the space between the rear of the VTP and the leading edge of the rudder (Board 2005, p. 5).

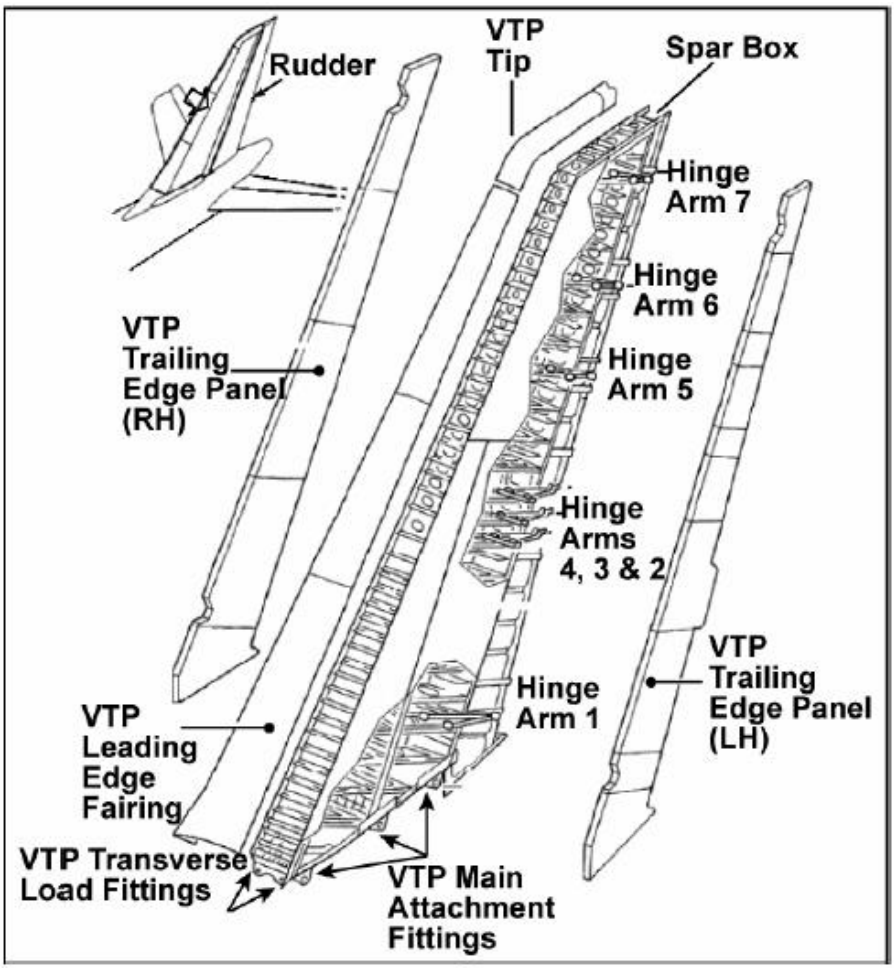

Figure 18: Vertical Tail Plane (Board 2005, p. 5)

The rudder (figure 18) is made up of a front spar and fairing, two side panels made from single piece constructed Nomex aramid – based honeycomb core, (CFRP) face sheets, (GFRP) intermediate layer connecting the honeycomb to the CRFP face sheets and a layer of Kevlar on the interior face to act as a moisture barrier. The thickness of the side panels varies with the location on the rudder because flight loads are different at different locations.

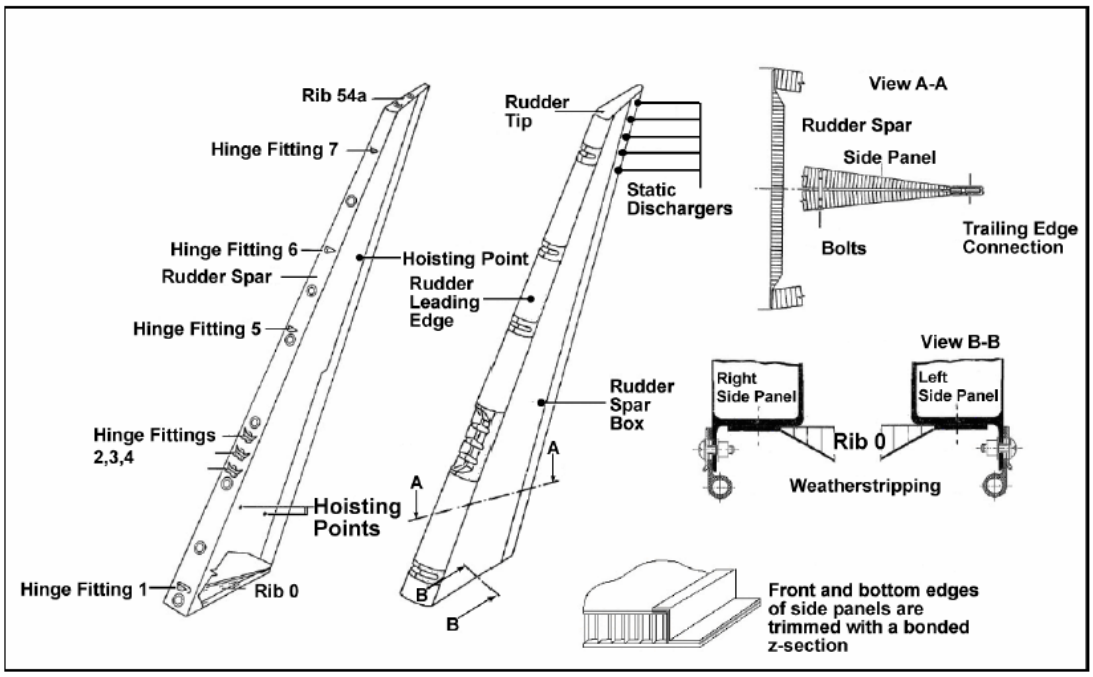

Figure 19: Rudder Design (Board 2005, p. 7)

The construction of the rudder skin (Figure 19) is a composite of an outer layer of CFRP factsheets over a GRFP layer then connected to the Nomex Honeycomb Interior. The CFFP layer acts as the structural layer and the Film Adhesive layer above is a protection against water ingress and corrosion. Lastly, a lightening strip of Aluminium is placed in 11 places along the rudder to act as lightening protection. The purpose of this lightening strip is to act as a sacrificial anode to direct the lightening through the rudder and out to the static wicks thus, dissipating the energy away from the sensitive composite laminates (Board 2005, p. 7).

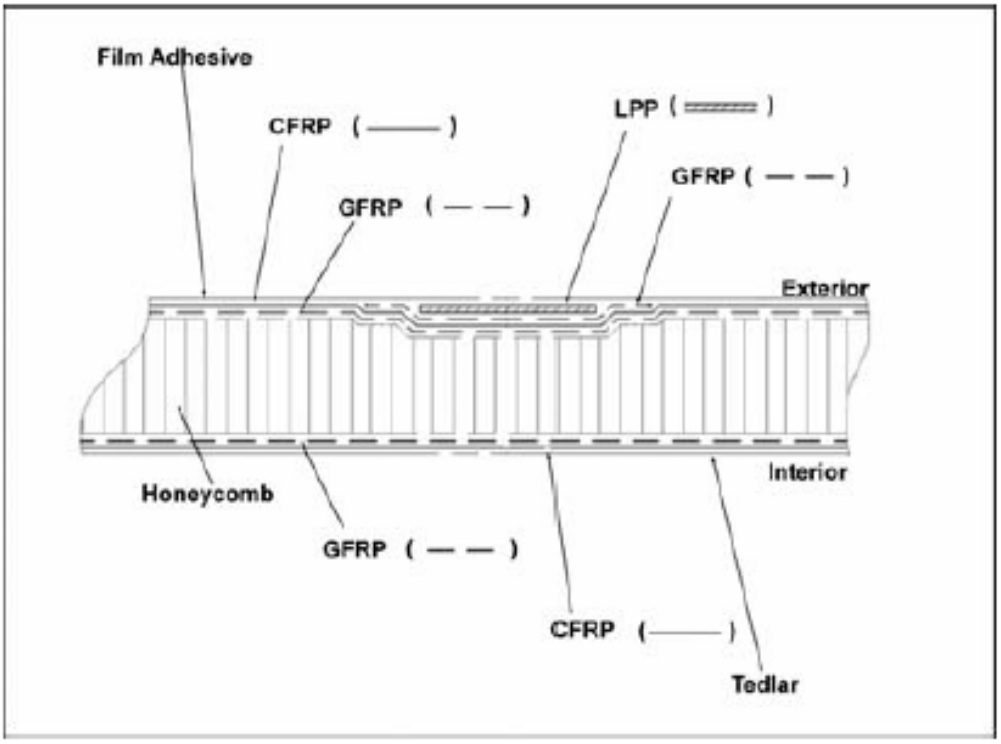

Figure 20: Rudder Side Panel Construction (Board 2005, p. 8)

2.4.5 Documented cases where water ingress into the honeycomb core of composite structure damaged a composite rudder to the point of failure.

There have been two well documented cases where water ingress has occurred in civil and military aircraft causing damage to the structural integrity of the honeycomb sandwich structure (Minakuchi, Tsukamoto & Takeda 2009). Most of this damage is caused by water ingress through the outside of the composite matrix and over time working its way through to the honeycomb core, this has led to the structural integrity of the composite structure deteriorating to the point in which the component has failed due to freeze / thaw action of the trapped water and fluid with led to cracking and separation of the laminates from the honeycomb core.

In 1999, the rudder of an F/A 18 (Figure 21) separated from the aircraft due to long term exposure to water ingression between the Aluminium skin and the honeycomb core. The ingression of water caused the epoxy adhesive to separate the two surfaces and thus lead to the complete failure of the rudder on the vertical stabiliser as seen below (Edwards et al. 2011).

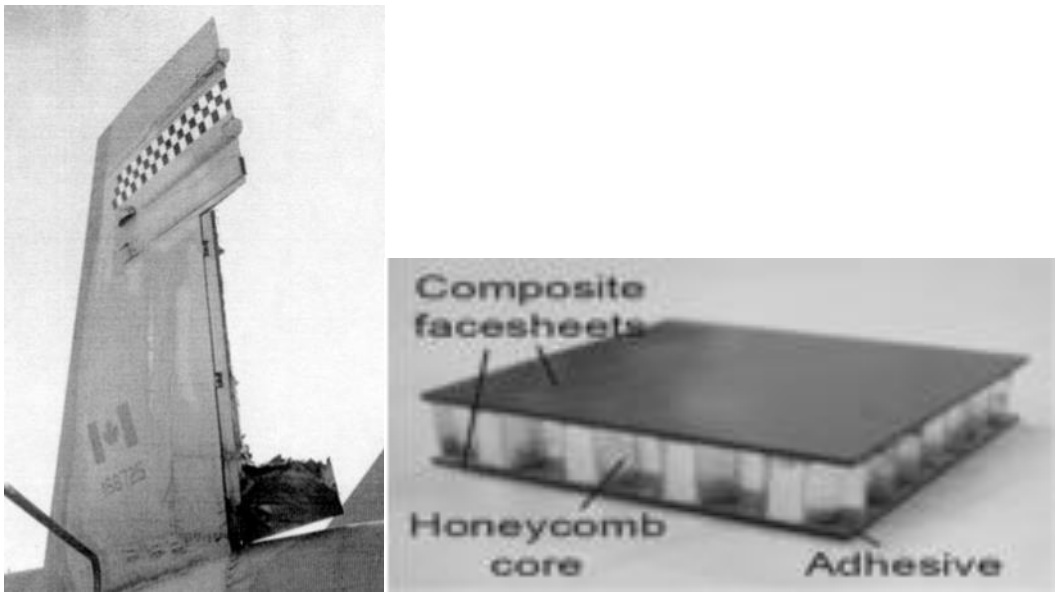

Figure 21: F/A 18 rudder failure (Edwards et al. 2011) and Honeycomb sandwich (Minakuchi, Tsukamoto & Takeda 2009)

On the 6th of March, 2005 the Rudder of an Airbus A319-300 broke off during a flight from Varadero, Cuba, whilst cruising at 35,000 feet. The pilot experienced loss of control in the lateral axis and the aircraft began a slow periodic ("Dutch") roll. The pilot regained control at 12,000 feet and landed the aircraft safely.

Subsequent inspection of the rudder revealed that only 16% of the rudder remained attached to the aircraft. As from the 1999 accident the Air Safety report revealed that fluid ingress resulting from a lightning strike had allowed a large build-up of fluid in the leading edge of the rudder, causing the honeycomb core to fill with fluid (Figure 22). This led to the flight control fluttering uncontrollably at high speed and thus a failure of the rudder flight control (Canada 2005).

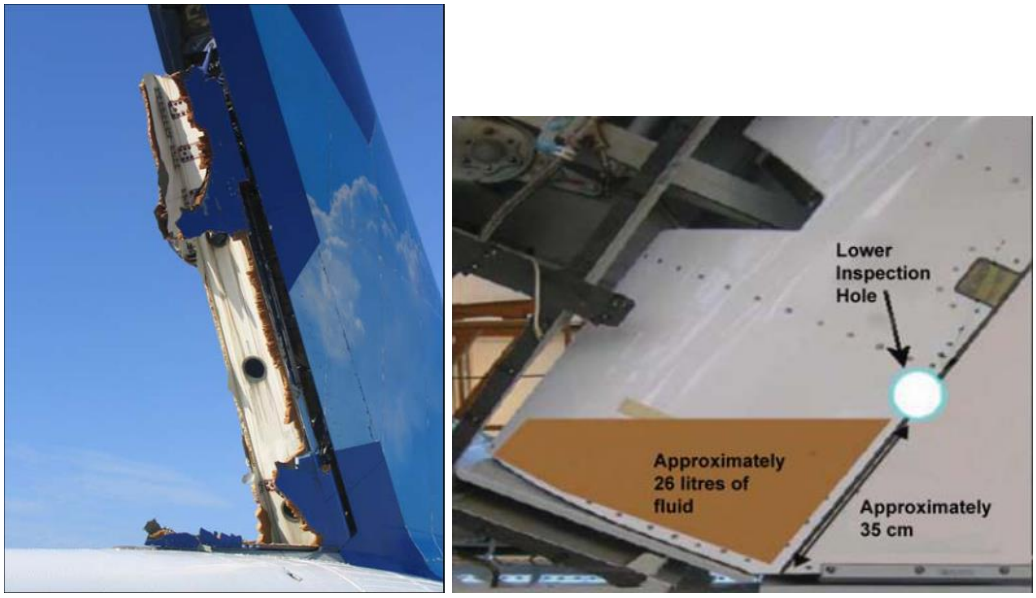

Figure 22: Airbus 319-300 Rudder Separation and Fluid Ingress into Leading Edge of Rudder (Canada 2005)

2.5 Mechanisms for Damage Propagation

2.5.1 Modes of Failure

O'Brian (2001) notes three forms of mode failure in delamination.

- Mode I: Opening Mode
- Mode II: In-Plane Sliding Mode
- Mode III: Tearing / Shearing Mode

These three modes of failure are the major contributors of laminate crack growth in composite structures. In many delaminations, it is common to see geometry's mixed mode cracks.

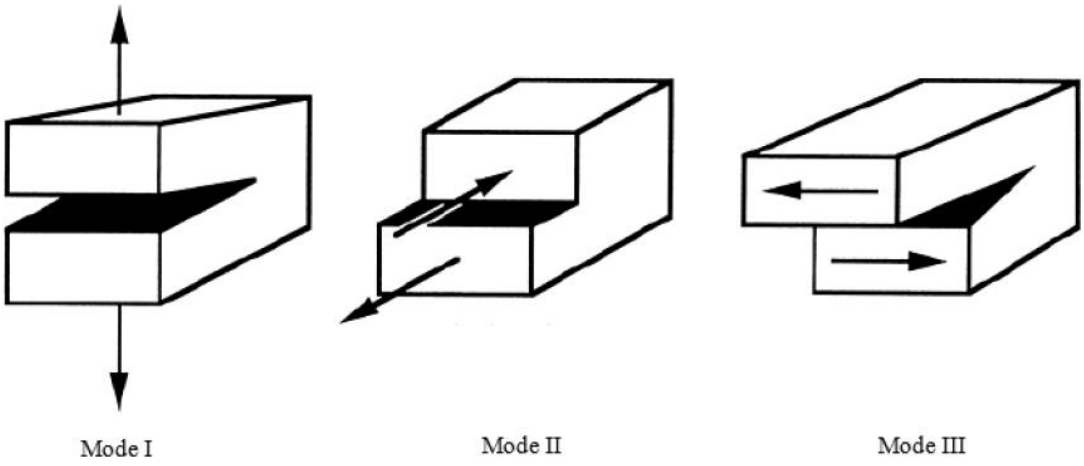

Figure 23: Three Modes of Failure (O'Brien 2001)

In Mode I the body of the laminate is loaded in tensile and compression forces, so that the crack is being pulled apart in the ±y direction. The deformations are symmetrical to one another and this leads to a strain along the axis perpendicular to the loading direction (Roylance 2001).

In this Project I will be examining cracking in the Mode 1 only, due to the complexity of mixed mode analysis see Figure 23.

2.5.2 Fatigue Crack Propagation (Paris Law)

Fatigue crack propagation or Paris Law was first proposed by PC Paris as part of his research into the comet disaster in 1955. He discovered that incremental crack growth was the key to fracture failure. As a result of his research, he created the formula below to explain how the rate of crack growth per cycle should be related to the range of the stress intensity factor (University 2013). The formula for Paris Law is presented below (Pugno et al. 2006):

$$\frac{da}{dN} = C(\Delta K)^m$$

a = crack length

N = number of cycles

ΔK = stress intensity factor range

C, m = experimentally determined

The relationship between the fatigue crack growth rate and the range of ΔK (stress intensity factor) can be presented on a graph as da/dN vs. ΔK. Three regions are presented: Region 1 is the threshold region where cracks don't propagate. This threshold region is where ΔK_{TH} depends on environmental conditions and average stress. Region 2 is where Paris Law comes into effect by taking the logarithm of both sides da/dN which should be proportional to the value of ΔK .Therefore the slope of the line = m and the position on the line can be determined to be C. Region C is where the stress intensity factor approaches the material fracture toughness limit. Therefore at K_{max} the material fractures (Roe & Siegmund 2003).

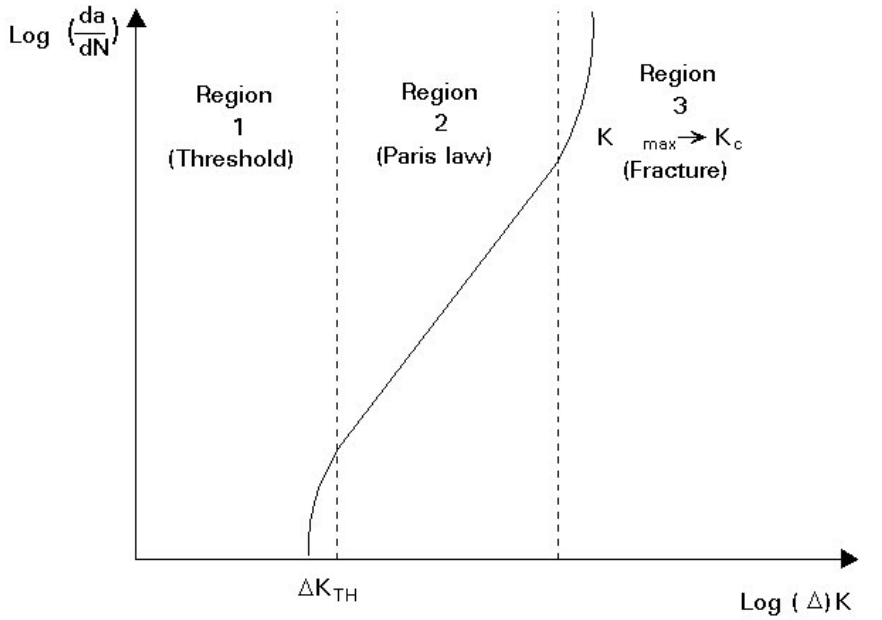

Figure 24: Typical Fracture Mechanics Fatigue crack propagation behaviour (University 2013)

2.6 The use of NDT (Non-destructive testing) and (SHM) Structural Health Monitoring sensors to measure internal environment of composite structure.

Currently, there are a few different NDT (Non-destructive testing) options on the market to detect BVID (Barely Visible Impact Damage) and possibly deeper delaminations in composite structure. A few of them are listed below:

- Coin Tap test: Used extensively in the aviation industry, it is a cheap visual inspection of an area, where a coin is tapped on the outside of the fuselage or wing. A dead sound or noise indicates a delamination (Bureau 2007).

- Ultrasonic Testing: The use of pulse echo techniques which are transmitted through one side of a composite structure to investigate the internal conditions of a particular section of the aircraft. Ultrasonics are particularly good at detecting delaminations but matrix fractures and fibre fractures are more difficult to detect (Adams & Cawley 1988)

- FBG (Fibre Bragg Grating) sensors: The use of FBG sensors imbedded into composite structures as part of Structural Health Monitoring allows a real time evaluation of the condition of an aircraft in flight and on the ground. The challenge is to place the sensors in the correct locations to catch up 95% of the potential delamination areas (Leng & Asundi 2003).

- Thermography: A low cost alternative to the above structural health monitoring options which allows the finding of pockets of water in a composite structure without the use of specialist training. Thermography is partially good at providing a quick check of a composite underlying structure (Kutin et al. 2011).

Chapter 3.0 Project Methodology

This project is designed to be conducted in a variety of phases:

1. Literature Review Phase: Identify by way of an extensive literature review the way damage is caused in composite wing structures due to water ingestion.

2. Modelling Phase: Use Abaqus analytically along with (FEA) Finite Element Analysis Software to determine damage responses to operational loads and changes of structural responses due to damage progression.

3. Sample Testing Phase: Make two tensile samples and a 3 point bending sample. To see how damage accumulation progresses through low temperature operations by the use of experimental composite skin test samples. Additionally, use thermography testing to determine placement of crack propagation throughout the samples.

4. Data Analysis phase: to compile, plot and evaluate the collected data obtained from the test samples.

5. Write up phase: involving the final preparation of the project dissertation.

Further detail in Table 1:

Task	Details	Items
Phase 1	Literature Review Phase	Review of the three Literature Areas • Water ingress into the honeycomb core of composite structure on aircraft • Delamination of aircraft composite structures • The use of NDT (Non-destructive testing) and sensors to measure internal environment of composite structure.

Phase 2	Modelling Phase	Model Proposed Testing Sample • Model fibre composite laminate using Abaqus • Simulate Tensile and Compressive Loadings • Carry out testing of Model using FEA analysis
Phase 3	Sample Testing Phase	Start construction of Laminate samples • Imbed Strain sensors on 1st tensile sample • Imbed FBG and Strain Gauges in 2nd tensile sample • Imbed Strain Gauges in 3 point bending sample • Test all three samples using sensors and thermography
Phase 4	Data Analysis Phase	Collate Data gathered • Compile, plot and evaluate collected data • Look an any variations of the data • Make sure data is verified
Phase 5	Write up Phase	Write dissertation • Write Draft of Dissertation • Get dissertation reviewed • Submit by due date

Table 1: Project Task Descriptions

Chapter 4.0 Resource Requirements

4.1 Resource Requirements

A comprehensive resource analysis was undertaken to determine what resources were required and what resources could be substituted if items were not available. All of the resources used will be obtained from the USQ laboratories or through the (CEEFC) Centre for Excellence in Fibre Composite Technologies laboratories in P11 under the supervision of Jayantha Epaarachchi. Table 2 lists the equipment required to complete the project.

Item	Name	Amount	Location	Cost ($)
1	Optical Spectrum Analyser	1	P2	Nil
2	FBG sensor (1550)	2	P2	$80
3	P3 Strain analyser and tester	1	P2	Nil
4	Strain sensors	2	P2	$50
5	GRFP sheets	10	P11	Nil
6	Epoxy Resin	800ml	P11	Nil
7	Plastic cups	20	P11	Nil
8	Paddle pop sticks	TBA	P11	Nil
9	Paint brush (Disposable)	20	P11	Nil
10	Refrigerator	1	USQ	Nil

Table 2: Equipment Required

Below in Table 3 are items of equipment that will be used for short periods of time due to the nature of the proposed experiments.

Item	Name	Amount	Location	Days
13	Material Testing machine 100KN	1	P9	4
14	Fatigue testing machine	1	USQ	3
15	Optical Microscope	1	USQ	3

Table 3: Equipment required for short durations

Below in Table 4 is a list of Items required if certain materials or equipment cannot be obtained for various reasons.

Item	Name	Amount	Location
16	Refrigerator	1	USQ
17	FBG sensor (830)	2	USQ

Table 4: Alternative Resources

4.2 Alternate arrangements if equipment not available

Due to the nature of the experimentation and testing required for this research project, some alternative resources had to be considered if certain items could not be purchased or used for any reason. Table 3 shows cheaper alternatives for the cooling of the samples and sensors due to the nature of the temperatures required.

For most of the experiments and tests, the samples need to be chilled to around (-56°C) to simulate aircraft flying conditions, hence the reason for using dry ice which is at (-78.5°C)(Gas 2014). Standard FBG (830) sensors can only handle up to (-18°C) (Lobo Ribeiro et al. 1997), hence the reason for more expensive sensors.

If the more expensive FBG sensors cannot be obtained, then the cheaper FBG 830 nm sensors would be used. A normal refrigerator would be set to (-18°C) so that the icing tests could be carried out. The results would not be as accurate as a real aircraft but the data would show if icing and delaminations were occurring inside the composite structure.

Chapter 5.0 Consequential Effect, Ethical Responsibility & Sustainability

The Institution of Engineers Australia holds in high regard the correct application of the Consequential Effects, Ethical Responsibility and Sustainability. As a result of this high standard, Engineers Australia has set out 12 key aspects of the above three virtues that should be considered in any engineering design (Nguyen 1998). The three key aspects that apply to be dissertation are: 4.1 Engage responsibly with the community and other stakeholders, 4.2 Practise engineering to foster the health, safety and wellbeing of the community and the environment 4.3 Balance the needs of the present with the needs of future generations.

For my dissertation, I believe that aircraft companies have an ethical and sustainable obligation to put the concerns of the flying public above profits in regards to aircraft safety and reliability of their services. For many years aircraft manufacturers have adopted a tombstone mentality of "we will fix the problem when someone dies, not before"(Chaddha 2011). Aircraft Safety should be an area which is in the forefront of manufacturer's minds when designing a product, not as a nice a thing to think about after profit (Leybovich 2009).

I believe that my project of Investigation into the Delamination of Composite Laminates Aircraft Rudders due to Fluid Ingress and Icing will highlight the benefit of proper inspection practices and routine maintenance when detecting Fluid Ingress into composite structures. As an engineer, we have a social ethical and morality obligation to incorporate a culture of health, safety and wellbeing of the community, society and the environment in our designs, attitudes and regard to future generations of the flying public (Schmidt 1994).

Chapter 6.0 Project Planning

6.1 Method used to Analysis data and Interpretation of the analysis

The method used to gather data and interpret the analysis gained will be by use of a laptop connected to the FBG and stain gauge sensors. This data will then be analysed and fed into Word.

The graphical results will be presented with either an excel spreadsheet or a Matlab plotting program and for the conference and speech presentation over the September break a PowerPoint presentation needs to be developed, presenting the analysed details of the project into a 20 min talk.

6.2 Project Timeline

A more detailed project schedule will be presented on the following page. But the project schedule incorporates the following details:

1. Project Start November17^{th,} 2014 ending October 29th, 2015 – a total number of 49 weeks

2. A number of milestones are required throughout the project as directed by USQ:

    a. Project Allocation Process 11th March 2015
    b. Project Specification 18th March 2015
    c. Preliminary Report 3rd June 2015
    d. Project Progress Assessment 17th June 2015
    e. Partial Draft Dissertation 16th September 2015
    f. Dissertation submission 29th October 2015

3. Personal project milestones:

    a. Completion of Literature Review 2nd March 2015
    b. Completion of Abaqus modelling 8nd May 2015
    c. Completion of Sample testing 20th July 2015
    d. Completion of Data compilation 14th August 2015
    e. Completion of Draft Dissertation 1st October 2015

4. ENG4903 conference and seminar activities included in 21st September 2015.

5. Data analysis and the write up of the dissertation to be carried out throughout the project so as to not lose momentum and forget aspects of the data collection.

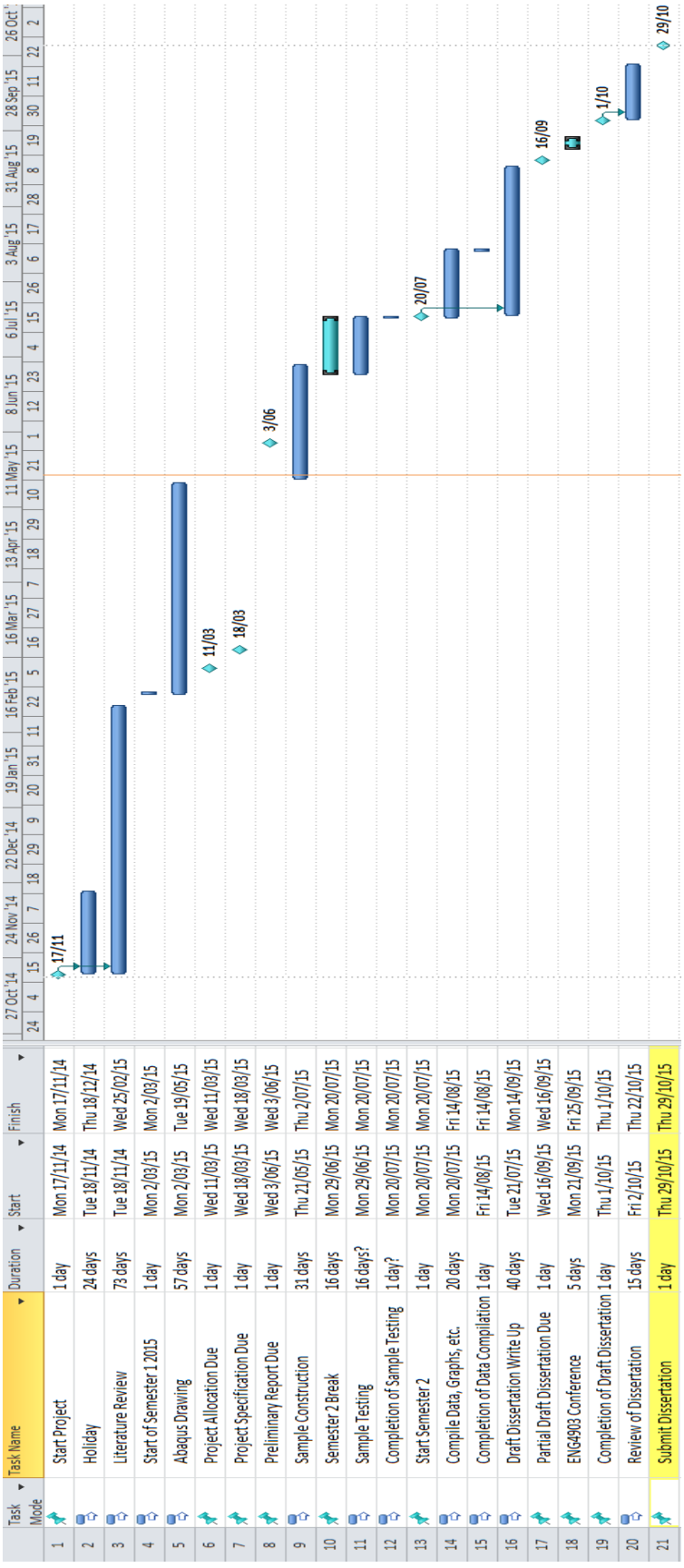

Figure 25: Project Schedule

Chapter 7.0 Risk Assessment

7.1 Experiments Risk Assessment

As part of my project, I will be undertaking activities that carry a low amount of risk. Three potential hazards are the use of lasers, dry ice and the preparation of the GFRP (Glass Fibre Reinforced Plastic) samples. Other pieces of equipment may be utilised in the future and further risk assessments may or may not be needed.

Below is a summary of the risk assessment process carried out to mitigate these risks, the full risk assessment is included in Appendix A –Risk Assessment

University of Southern Queensland

Generic Risk Management Plan

Workplace (Division/Faculty/Section):		
s		
Assessment No (if applicable):	Assessment Date:	Review Date: (5 years maximum)
1	1/05/2015	1/05/2020
Context: What is being assessed? Describe the item, job, process, work arrangement, event etc:		
ENG4111 and ENG4112 Thesis Experiments		
Assessment Team – who is conducting the assessment?		
Assessor(s):		
Samuel Pike		
Others consulted: (eg elected health and safety representative, other personnel exposed to risks)		

The Risk Management Process

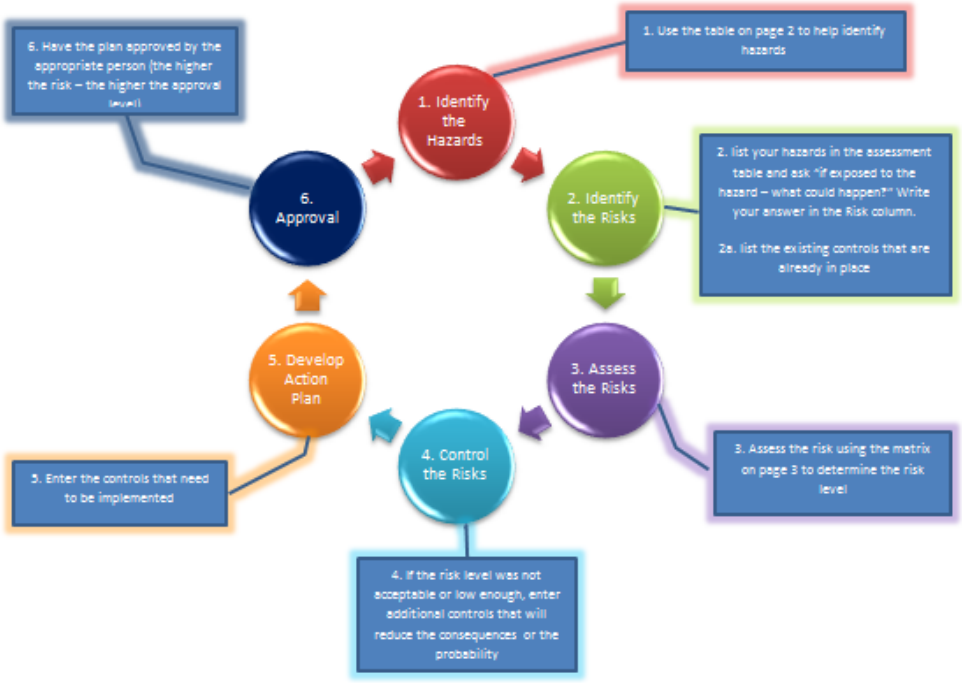

Step 1 - Identify the hazards (use this table to help identify hazards then list all hazards in the risk table)		
General Work Environment		
☐ Sun exposure	☐ Water (creek, river, beach, dam)	☒ Sound / Noise
☐ Animals / Insects	☐ Storms / Weather/Wind/Lightning	☐ Temperature (heat, cold)
☐ Air Quality	☐ Lighting	☐ Uneven Walking Surface
☐ Trip Hazards	☐ Confined Spaces	☐ Restricted access/egress
☐ Pressure (Diving/Altitude)	☐ Smoke	☐
Other/Details:		
Machinery, Plant and Equipment		
☐ Machinery (fixed plant)	☐ Machinery (portable)	☒ Hand tools
☐ Laser (Class 2 or above)	☐ Elevated work platforms	☐ Traffic Control
☐ Non-powered equipment	☐ Pressure Vessel	☐ Electrical
☐ Vibration	☐ Moving Parts	☐ Acoustic/Noise
☐ Vehicles	☐ Trailers	☐ Hand tools
Other/Details:		
Manual Tasks / Ergonomics		
☐ Manual tasks (repetitive, heavy)	☐ Working at heights	☐ Restricted space
☐ Vibration	☐ Lifting Carrying	☐ Pushing/pulling
☐ Reaching/Overstretching	☐ Repetitive Movement	☐ Bending
☐ Eye strain	☐ Machinery (portable)	☒ Hand tools
Other/Details:		
Biological (e.g. hygiene, disease, infection)		
☐ Human tissue/fluids	☐ Virus / Disease	☐ Food handling
☐ Microbiological	☐ Animal tissue/fluids	☐ Allergenic
Other/Details:		
Chemicals Note: Refer to the label and Safety Data Sheet (SDS) for the classification and management of all chemicals.		
☐ Non-hazardous chemical(s)	☒ 'Hazardous' chemical (Refer to a completed hazardous chemical risk assessment)	
☐ Engineered nanoparticles	☐ Explosives	☐ Gas Cylinders
Name of chemical(s) / Details: Kinetix R246TX and H180		
Critical Incident – resulting in:		
☐ Lockdown	☐ Evacuation	☐ Disruption
☐ Public Image/Adverse Media Issue	☐ Violence	☐ Environmental Issue
Other/Details:		
Radiation		
☐ Ionising radiation	☐ Ultraviolet (UV) radiation	☐ Radio frequency/microwave
☐ infrared (IR) radiation	☐ Laser (class 2 or above)	☐
Other/Details:		
Energy Systems – incident / issues involving:		
☐ Electricity (incl. Mains and Solar)	☐ LPG Gas	☐ Gas / Pressurised containers
Other/Details:		
Facilities / Built Environment		
☐ Buildings and fixtures	☐ Driveway / Paths	☐ Workshops / Work rooms
☐ Playground equipment	☐ Furniture	☐ Swimming pool
Other/Details:		
People issues		
☒ Students	☒ Staff	☐ Visitors / Others
☐ Physical	☐ Psychological / Stress	☐ Contractors
☐ Fatigue	☐ Workload	☐ Organisational Change
☐ Workplace Violence/Bullying	☐ Inexperienced/new personnel	☐
Other/Details:		

Step 1 (cont) Other Hazards / Details (enter other hazards not identified on the table)

Risk Matrix

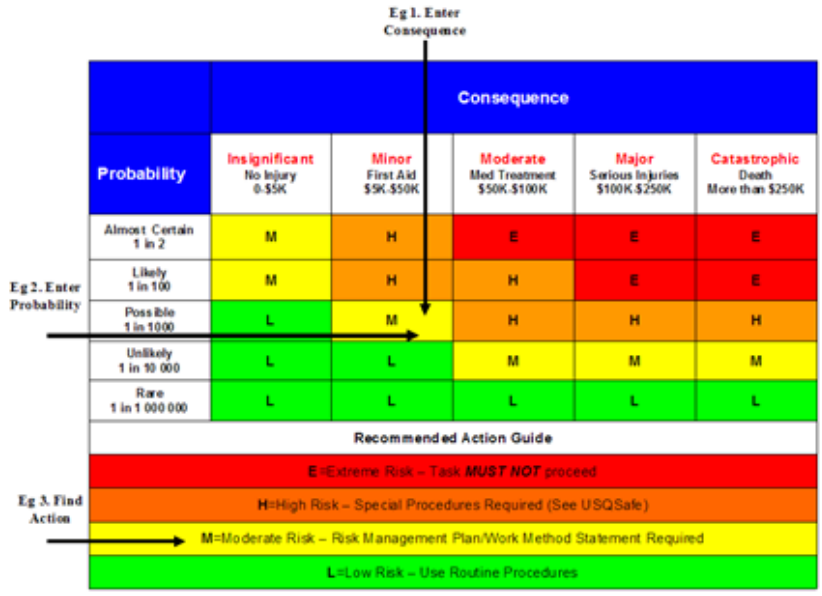

Risk register and Analysis

Step 1 (cont)	Step 2	Step 2a	Step 3			Step 4				
Hazards: From step 1 or more if identified	**The Risk:** What can happen if exposed to the hazard with existing controls in place?	**Existing Controls:** What are the existing controls that are already in place?	**Risk Assessment:** (use the Risk Matrix on p3) Consequence x Probability = Risk Level			**Additional controls:** Enter additional controls if required to reduce the risk level	**Risk assessment with additional controls:** (use the Risk Matrix on p3 – has the consequence or probability changed?)			**Controls Implemented? Yes/No**
			Consequence	Probability	Risk Level		Consequence	Probability	Risk Level	
Example										
Working in temperatures over 35º C	Heat stress/heat stroke/exhaustion leading to serious personal injury/death	Regular breaks, chilled water available, loose clothing, fatigue management policy.	catastrophic	possible	high	temporary shade shelters, essential tasks only, close supervision, buddy system	catastrophic	unlikely	mod	Yes
Preparation of Samples	Fumes	PPE to be worn at all Times	Moderate	Rare	Low		Select a consequence	Select a probability	Select a Risk Level	Yes or No
Working with cold samples	Cold Burns	PPE to be worn at all Times	Minor	Unlikely	Low		Select a consequence	Select a probability	Select a Risk Level	Yes or No
Using FBGs	Eye Damage	PPE to be worn at all Times	Minor	Unlikely	Low		Select a consequence	Select a probability	Select a Risk Level	Yes or No
			Select a consequence	Select a probability	Select a Risk Level		Select a consequence	Select a probability	Select a Risk Level	Yes or No
			Select a consequence	Select a probability	Select a Risk Level		Select a consequence	Select a probability	Select a Risk Level	Yes or No
			Select a consequence	Select a probability	Select a Risk Level		Select a consequence	Select a probability	Select a Risk Level	Yes or No
			Select a consequence	Select a probability	Select a Risk Level		Select a consequence	Select a probability	Select a Risk Level	Yes or No
			Select a consequence	Select a probability	Select a Risk Level		Select a consequence	Select a probability	Select a Risk Level	Yes or No
			Select a consequence	Select a probability	Select a Risk Level		Select a consequence	Select a probability	Select a Risk Level	Yes or No
			Select a consequence	Select a probability	Select a Risk Level		Select a consequence	Select a probability	Select a Risk Level	Yes or No
			Select a consequence	Select a probability	Select a Risk Level		Select a consequence	Select a probability	Select a Risk Level	Yes or No
			Select a consequence	Select a probability	Select a Risk Level		Select a consequence	Select a probability	Select a Risk Level	Yes or No
			Select a consequence	Select a probability	Select a Risk Level		Select a consequence	Select a probability	Select a Risk Level	Yes or No
			Select a consequence	Select a probability	Select a Risk Level		Select a consequence	Select a probability	Select a Risk Level	Yes or No
			Select a consequence	Select a probability	Select a Risk Level		Select a consequence	Select a probability	Select a Risk Level	Yes or No
			Select a consequence	Select a probability	Select a Risk Level		Select a consequence	Select a probability	Select a Risk Level	Yes or No

Step 5 – Action Plan (for controls not already in place)			
Control Option	Resources	Person(s) responsible	Proposed implementation date

Step 6 – Approval

Drafter's Comments:

Drafter Details:

Name: Samuel Pike Signature: Date: 1/05/2015

Assessment Approval: (Extreme or High = VC, Moderate = Cat 4 delegate or above, Low = Manager/Supervisor)

I am satisfied that the risks are as low as reasonably practicable and that the resources required will be provided.

Name: Signature: Date: / /

Position Title:

Chapter 8.0 Finite Element Analysis (FEA) Modelling

8.1 Abaqus Finite Element Analyses

Using an Abaqus CAE 6.13 a model of a Rudder Composite laminate was formed based loosely on the makeup of an Airbus 310 rudder laminate sandwich. An actual rudder laminate was used to base the construct of the Abaqus model as seen from the figure below.

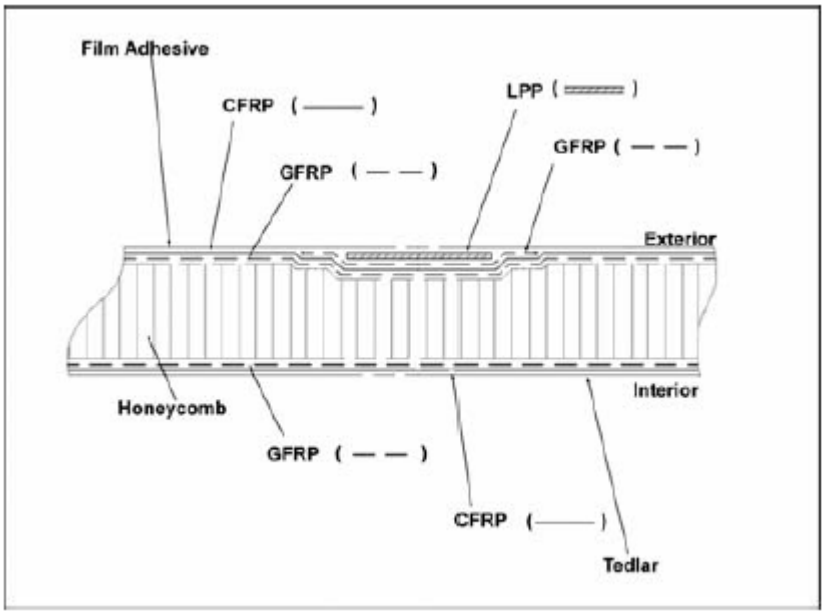

Figure 26: Rudder Laminate Composite to base the Abaqus model (Board 2005)

The figure 26 above provides a to-scale review in order to make a part sketch of the laminate required. Due to the budget constraints of $200 dollars being applied to this project, the CFRP laminates aren't included in the modelling process and only GFRP E- glass sheets are modelled due to cost. The results of the Abaqus model will be compared to the actual experimental results obtained in future chapters and the results explained in Chapter 14.

The Abaqus CAE Model is assigned a 12 ply composite layup consisting of E-Glass properties simulating the construction of layered fibreglass with 0°C to 90°C fibreglass orientation. Boundary conditions are applied to simulate tensile and bending loading on the composite laminate.

8.1.1 Preliminary Modelling

Initial modelling using just top and bottom elements under tensile load gave the following results:

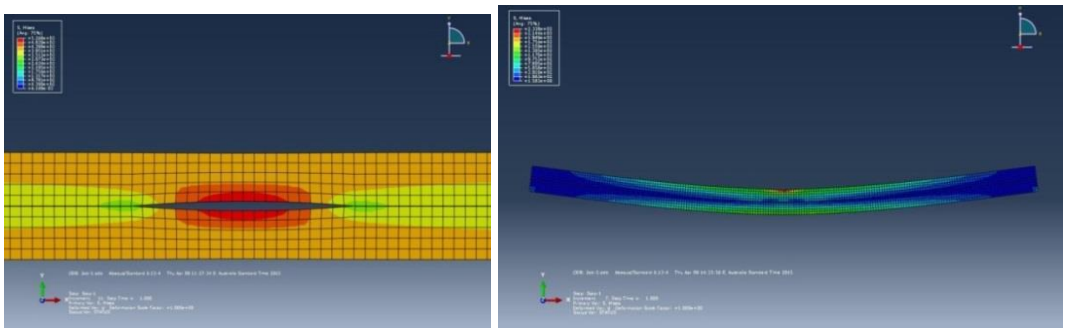

Figure 27: Tensile and Bending 3mm ± Uni-directional loading

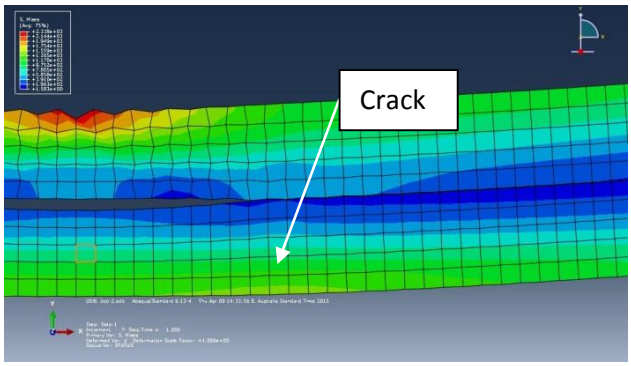

Figure 28: Close up View of crack propagation with 10mm central loading

The above Figures were early attempts at FEA modelling using Abaqus, to determine what was possible with the program and if accurate data could be gathered from the analysis.

8.1.2 Modelling of Rudder Laminates without water inclusion

In order to gain an understanding of the results that I might see during testing, I needed to first do some FEA modelling in Abaqus 6.13. Figures 29 and 30 below simulates via 2D analysis, a fibre composite laminate attached to a honeycomb core sample without ice. As the tensile and compression load is applied to both ends there is a buckling occurring along the fibre laminate. All FEA models were meshed to provide accurate data for further analysis.

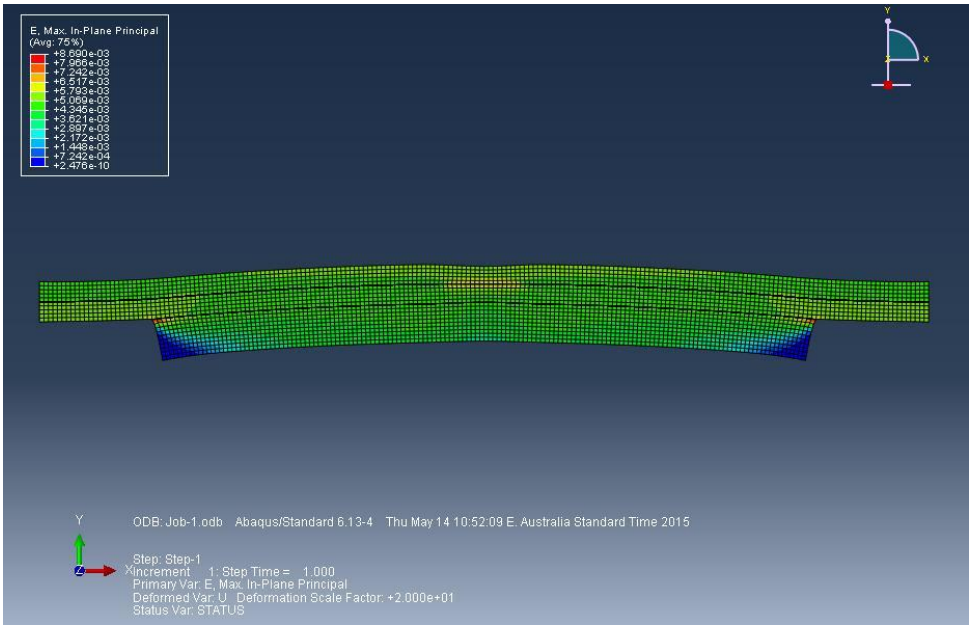

Figure 29: 1mm Tensile Buckling using Abaqus Model (without water)

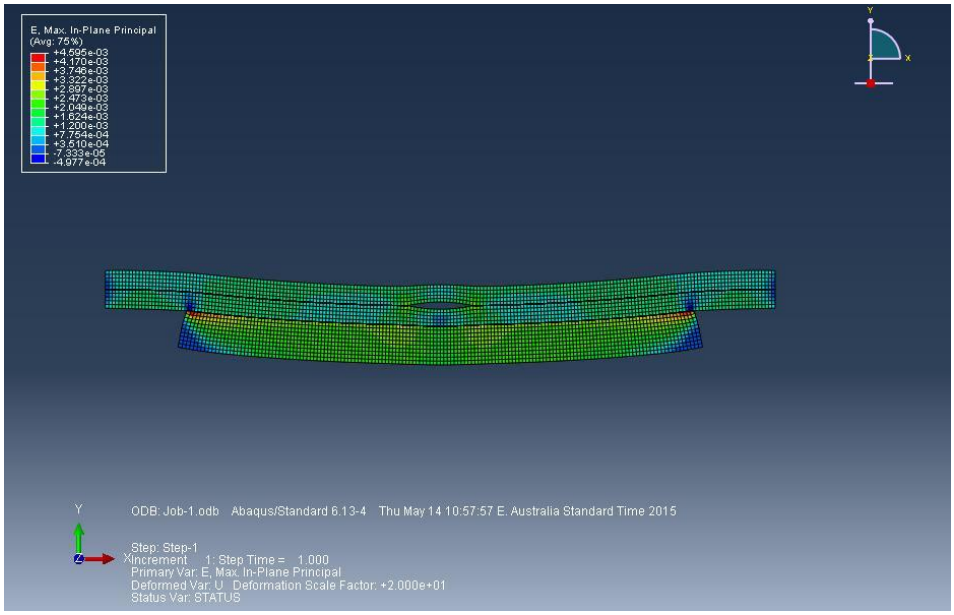

Figure 30: 1mm Compressive Buckling using Abaqus Model (without water)

8.1.3 Modelling of Rudder Laminates with frozen water inclusion

As with the Figures above, buckling is occurring within Figures 31 and 32 and high stresses are also occurring at the ends of the timber inclusion simulating frozen ice. This is an area that will require further investigation within the testing phase of the project.

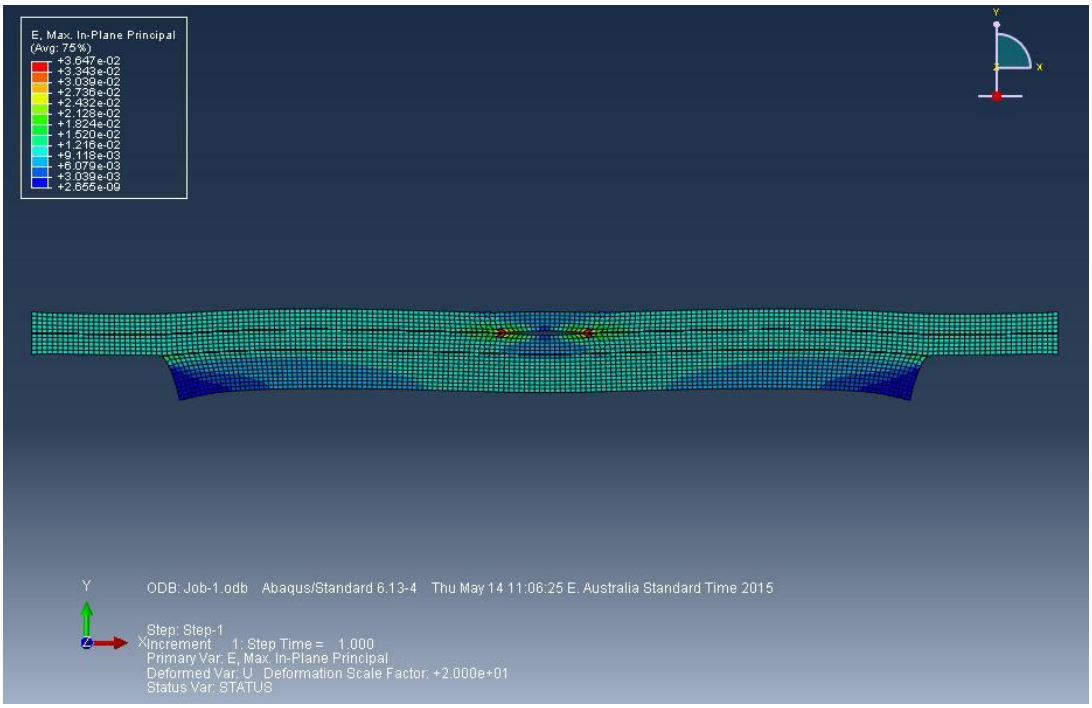

Figure 31: 1mm Tensile Buckling using Abaqus Model (with water)

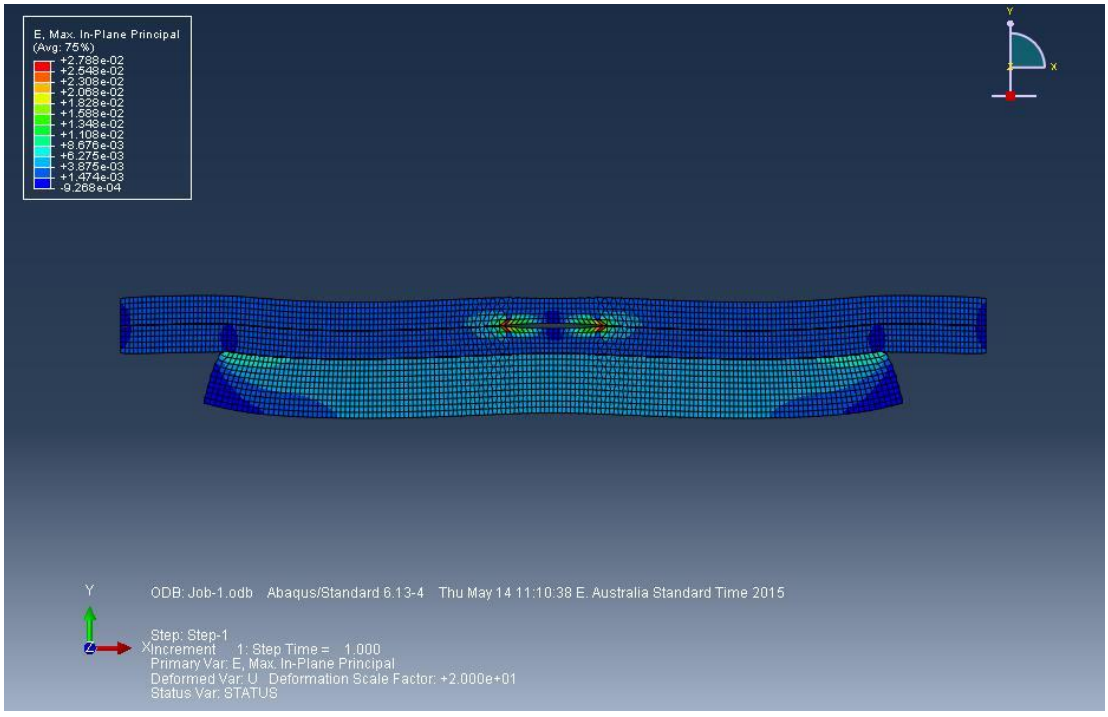

Figure 32: 1mm Compressive Buckling using Abaqus Model (with water)

Chapter 9.0 FBG Sensor System

The FBG (Fibre Bragg Grating) sensor was used to accurately determine the micro strain at the edge of the internal ice simulation wooden block labelled Bending Sample. The FBG sensor system consisted of a laptop containing the Micron Optics ENLIGHT software, a four channel optical sensing integrator (Micron Optics sm125 and a 5mm long 1mm Diameter FBG sensor.

Before testing was carried out the FBG sensor data was recorded below

Technica SA – Fibre Bragg Grating (S/N 101121106066)		
Name	Tolerance	As Tested
Centre Wavelength (CW)	1550 ± 0.3mm	1549.95nm
FBG Length	5.0mm	5.0mm
FWHM Bandwidth (BW)	< 0.5mm	0.32nm
Reflectivity	> 50%	54.710%
Fibre Type	SMF – 28C Fibre	SMF – 28C Fibre
Connector	FC/APC	FC/APC

Table 5: FBG Sensor Data

The three primary components of the FBG sensor system are presented below:

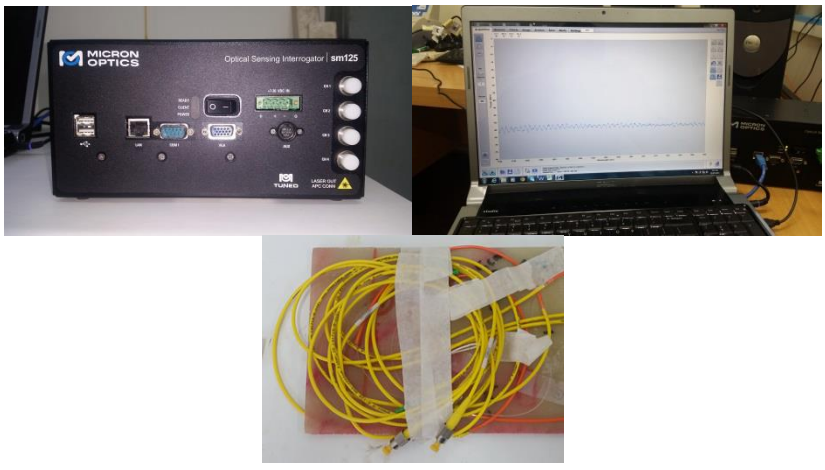

Figure 33: Optical sensing integrator, Laptop and FBG sensor

9.1 Connection of FBG sensor to fibre optic cable

Reconnecting the FBG sensor to the fibre optic cable arose due to the three breakages that occurred in the making and modification of the FBG sample 2. The following process was used to re-splice the sensor back to the fibre optic cable.

1. Cut to length: both ends of the FBG sensor and the Fibre optic cable are trimmed to length. See Figure 37 below

Figure 34: Optical fibre Trimmers

2. Stripping the outer layer of the optical cable: Using the fibre optic wire strippers, remove the outer layer of cladding surrounding the optical cable being careful not to cut the fibre optic cable.

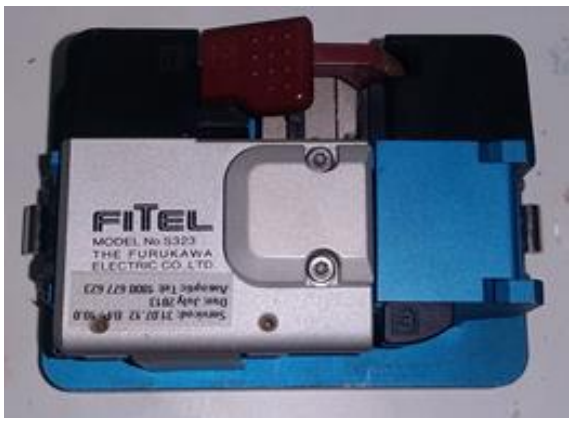

Figure 35: The Vitel high precision fibre optic cleaver

3. Cutting the fibre optic ends square: Align both the fibre optic and the FBG sensor ends in the fibre optic cleaver and hold the fibre whilst the blade cuts the fibre optic cable perpendicular. Both ends need to be squared exactly for accurate splicing (Fig 35).

Figure 36: The Vitel v. 2000 s175 Fusion Splicing Machine

4. Fusion Splicing Machine: Both ends of the sensor are fused together using the Vitel v. 2000 s175 fusion splicing machine as seen in Figure (36). This is achieved via a three part process; the fibres are located and restrained using a magnetic clamp, they are then aligned, any impurities are burnt off, the ends are fused together, then finally a test is carried out across the spliced ends to verify that the fusion process has been successful.

9.2 Position of the FBG sensor on 2nd Tensile Sample

The position and placement of the FBG sensor was determined by the need to measure the high micro strains at the point of crack propagation on the bending sample during tensile testing. Due to budgetary constraints, only one FBG sensor was available for experimental testing.

The 5mm FBG sensor was located between Strain Gauges #1 and #2 in between plies 6-7 in the fibre composite laminate.

Figure 37: Placement of FBG

The FBG sensor was particularity hard to position correctly due to a number of factors:

1. On the day, no one was available to assist me in positioning the sensor and hand layup sample
2. I lacked experience in placing of FBG sensors which lead to the epoxy curing faster than originally anticipated due to the slow pace of work.
3. The fine and delicate nature of the FBG sensors which lead to three breakages of the fibre optic lead.
4. The post curing of the sample after the hand layup was completed prevented proper tension to be maintained on the fibre optic resulting in a kinked wire.

9.3 Signal confirmation from FBG sensor

Before testing with the FBG sensor, two validation tests were performed to detect possible breakages of the FBG sensor in the manufacturing of the 3 point bending sample. This was achieved by attaching the end of the FBG extension cable to a laser light source and then visually seeing the red spot through the fibre laminates at the

end of the extension cable to determine that no part of the optical cable was broken (Figure 38).

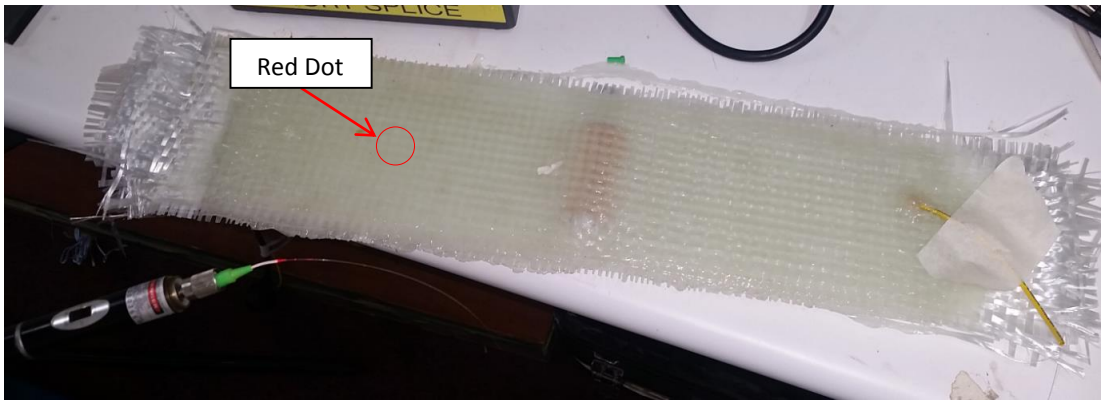

Figure 38: Visual Indication from Laser Light Source

The second test was to connect the end of the FBG optical extension wire to the sm125 interrogator. The return signal could then be analysed via a PC using the ENLIGHT – micron software. As a result of this test, the display returned an unloaded functioning signal as displayed in the figure 39 below.

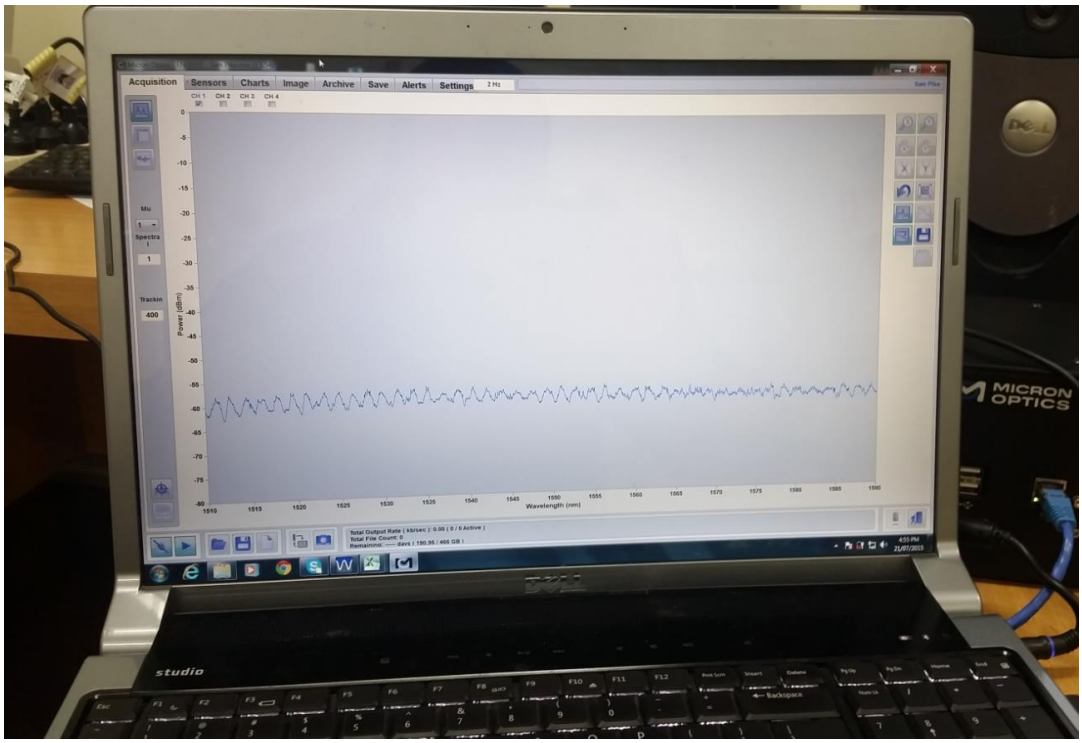

Figure 39: Test signal validating FBG functionality.

Chapter 10 Electrical Strain Gauge Sensors

The average cost of an FBG sensor is around the $200 mark and this project only permitted the use of one of them per student. On the other hand strain gauges are much cheaper and 4 were used on the outside skin of the laminates for both the Tensile and 3 point Bending Samples. Figure 40 and 41 shows the placement of the sensors.

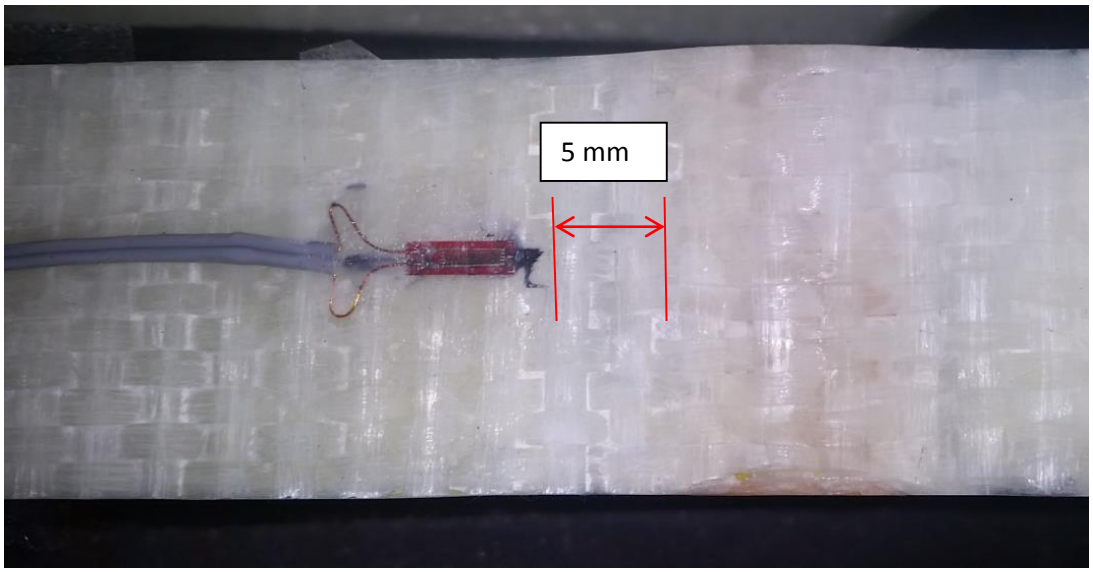

Figure 40: Upper Strain gauge attachment

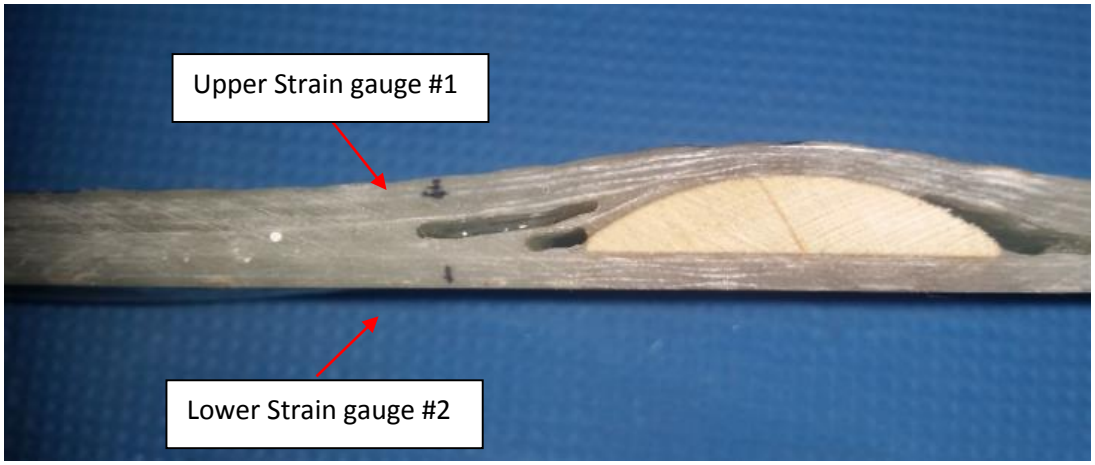

Figure 41: Upper and Lower Strain Gauges #1 and #2

One gauge each was placed on the Upper and Lower Laminates at (Plies 1 and 12) 5mm perpendicular from the edge of the delamination on the centreline of the sample. Each strain gauge was from the same batch and same manufacturer.

Tokyo Sokki Kenkyujo - Strain Gauge	
Type	FLA-5-11-1L
Lot No.	A514611
Gauge Length	5 mm
Gauge Factor	2.13 ± 1%
Gauge Resistance	120.3 ± 0.5 Ω
Temp Compensation For	11x10^-6 / °C
Transverse Sensitivity	0%
Batch No.	0C17P
Lead Wires	10/0.12 1m

Table 6: Strain Gauge Details

10.2 Strain Gauge Electrical Attachment

Each strain gauge has 1m of electrical wiring to attach to an electrical connection in this case the Vishay Micro Measurements P3 Train Indicator and Recorder was used to convert electrical resistances into usable data to be displayed on an LCD display. Two strain gauges were used per sample labelled Channel 1 and 2. Figure 44 shows the digital readout of each of the strains for both channels. These numbers were put into graphs which are displayed in Chapter 14.0 Results and Conclusion.

Figure 42: Micro Measurements P3 Train Indicator and Recorder and LCD display.

Chapter 11.0 Thermoelastic Stress

Thermoelastic Stress Analysis or (TSA) is a method by which solids, when compressed, are heated. When the solid is released, it returns to its original shape and its original temperature. This is called elasticity and thermo-elasticity. This change in temperature can be represented by the thermoelastic equation below (Brischetto & Carrera 2008).

$$\Delta T = \frac{-\alpha T}{\rho C_p}(\Delta\sigma)$$

$\Delta T = change\ in\ Temperature$

$\alpha = coefficent\ of\ thermal\ expansion$

$\rho = density$

$C_p = heat\ capacity\ at\ constant\ pressure$

$\Delta\sigma = sum\ of\ principle\ stress$

This equation assumes adiabatic conditions throughout the solid (No heat loss). The adiabatic conditions are assumed to be fatigue loads acting on the structure. For this project, this is the tensile fatigue cycle exerted on sample 1 (Boyce 1999). Due to the lack of literature available on cyclic loading due to fatigue loading, the predictive fatigue life of composite components is difficult to accurately determine even with the addition FBG and strain gauges. Hence, the inclusion of thermoelastic stress data gives a visual reading of the thermal stresses acting on the component.

Various methods have been employed for the detection of crack propagation in composite materials in the past such as coin tap testing, ultrasonic and magnetic particle. These methods are called non-destructive testing and have been used with varying success, but require the removal of flight control components but do not give an accurate picture of the inside of the component.

Infrared thermography has seen increased use in this area due to its non-contact, non-destructive testing methodology that uses the surface temperature as well as the

inside temperature to accurately determine the thermal and mechanical load on the component (Vergani, Colombo & Libonati 2014, p. 2).

11.1 Thermoelastic techniques applied to composite materials

When a static tensile load is applied to a composite homogenous material, an initial decrease in surface temperature occurs as the material stretches elastically. This effect relates to the change in volume of the composite material. As the load increases, the temperature rises linearly till the minimum fatigue limit is reached, then the temperature increases till the material reaches a critical failure point. At the point of failure, the temperature climbs rapidly again. These three stages of thermoelastic stress are shown in Figure 45.

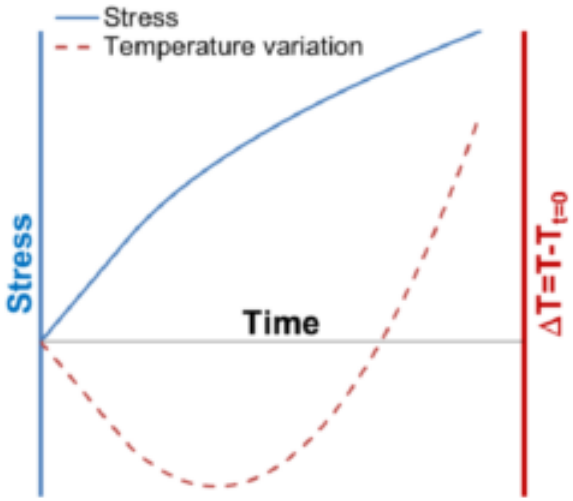

Figure 43: Stress and Temperature Stress as a function of time (Vergani, Colombo & Libonati 2014)

Due to the nature of the experiments required for this project, dynamic loading needed to be taken into effect as well as static loading. This would show the temperature increase of the outside surface and thus show crack propagation through the sample. As seen in Figure 44, the solid line is a solid homogenous material without the inclusion of any addition materials and the dotted line is a non-homogenous material and a closer representation of the inclusion of ice in a fibre composite sample.

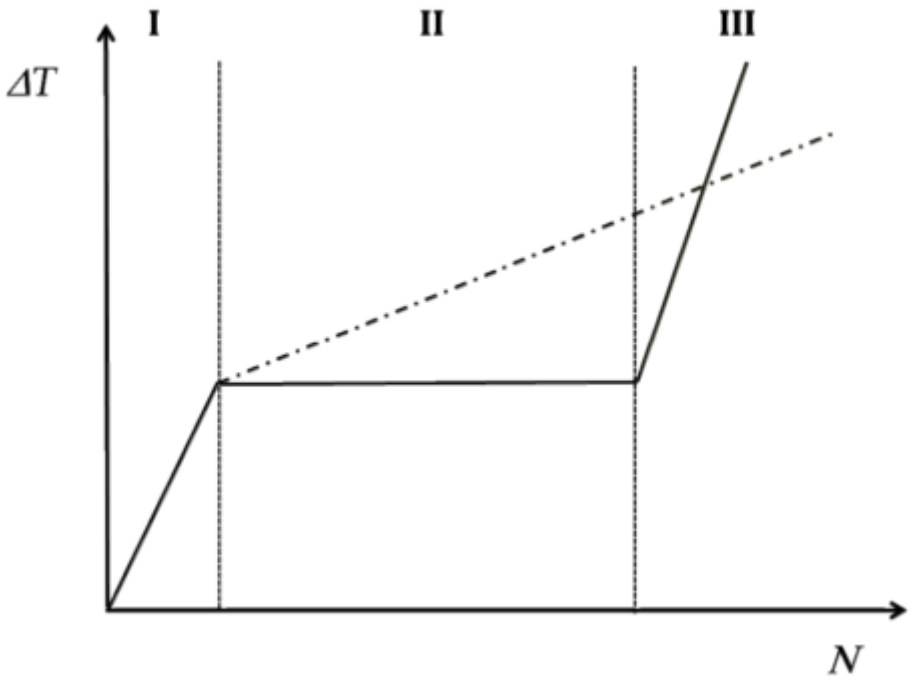

Figure 44: Thermal profile of each interval (Vergani, Colombo & Libonati 2014)

Stage 1 shows the initial linear thermal interval until the fatigue limit is reached, Stage 2 is the plateau region where the temperature varies due to the nature of the material, Stage 3 is the region of failure.

To accurately draw a plot of the damage propagation, only a single area needs to be analysed thoroughly. A typical example of the image that you would see by thermography is shown below in Figure 45. This shows a visual representation of the thermal stress inside a turbine blade and thus can be used as a quick reference tool to see if any further action needs to be undertaking on the component.

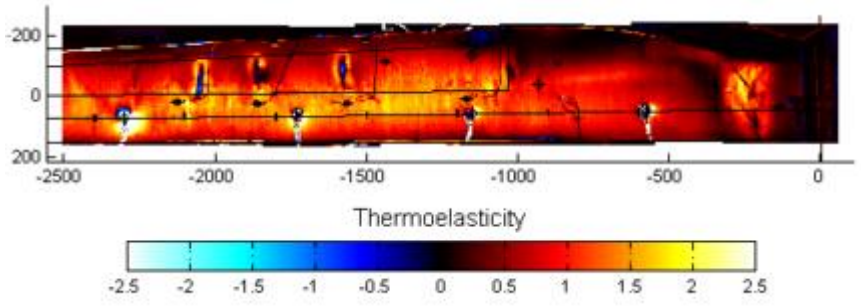

Figure 45: Thermography data of a turbine blade (Dutton 2004).

Chapter 12.0 Determination of Material Properties for Testing of the Rudder Laminates

12.1 Tensile Testing Procedure and Results

The following procedure was used to determine the material properties of the rudder laminates in regards to tensile properties.

12.1.1 Sample Testing manufacture

The Methodology used to determine the size of the test samples is specified in ISO 527-4. p5 (ISO) where the width is to be 25mm and thickness is between 2mm and 10mm.

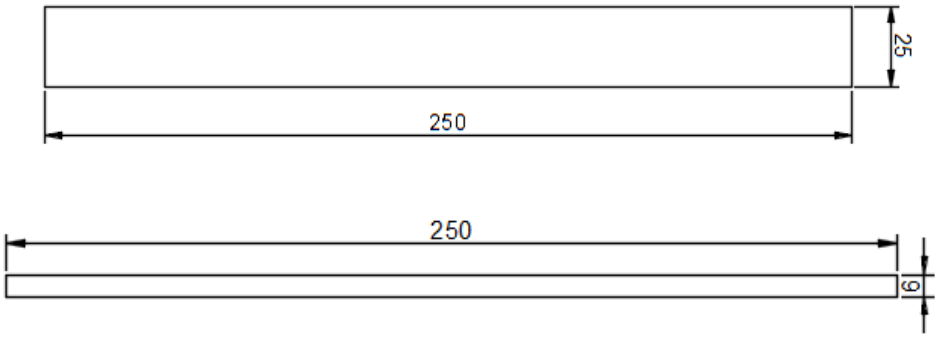

Figure 46: Test Sample Size

As a result of ISO 527-4, a sample width of 25mm was chosen and 3 x 12 ply samples (6mm thickness) were made from AR145140 Woven Roving E-glass of Density 400g/m^2, then machined to size using a diamond blade table saw. The samples were sanded along the edges to reduce the effects of edge delamination then each sample was visually inspected. No samples were discarded.

Dimension	ISO Requirement	Actual	Remarks
Thickness (mm)	2.0 – 10	6.0 (nominal)	OK
Width (mm)	25.0 ± 0.5	25.0 (nominal)	Ok
Length (mm)	>250	250	Ok
Distance Between Grips (mm)	150±0.25	150±0.25	OK

Table 7: Test specimen dimensions summary

12.1.2 Determination of Tensile Properties:

ISO 527-1 p9 (ISO 1996) requires that 5 samples be tested for each of the required testing parameters and more samples to be used if a more accurate mean value is required. In accordance to ISO 2602 it is possible to evaluate this by means of a 95% probability confidence interval. Due to the limited availability of materials for testing, only 3 test samples were able to be made – see Figure 34. Looking at Figure 47, the mean value for the Modulus of Elasticity was determined using these three samples.

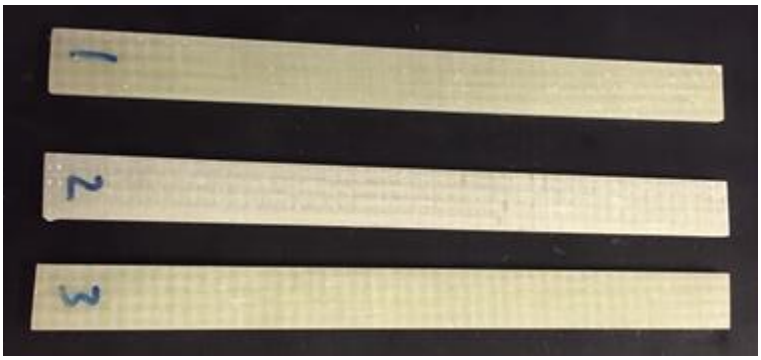

Figure 47: Material Property samples 12 ply 3 x (25 x 250)

Testing Procedure

The tensile testing procedure was conducted as closely as possible to ISO 527-1 and ISO527-4. The USQ CEEFC MTS Insight Tensile Testing Machine was used for the tensile testing as seen in Figure 48.

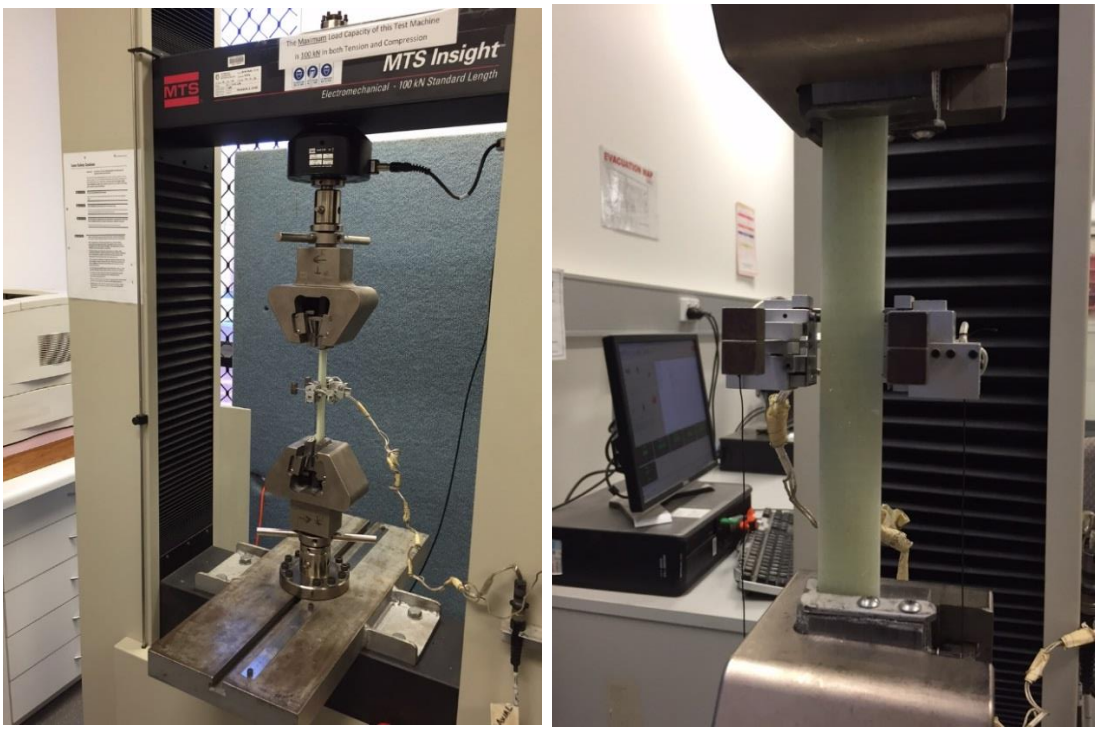

Figure 48: Tensile Testing Machine (MTS Insight 310).

The Figure above shows the placement of the extensometer on the test samples. This was removed when the strain reached 0.03, so that the ultimate strength could be determined by the failure of the sample. The speed of the test was 2mm/min; this was based upon the guidelines set out in ISO 527-1.

Equipment	Part No.	Serial No.	USQ No.
MTS Tensile Testing Machine	Q.AC/258-V-6	-	009-9009
Extensometer	632.85F-14	305	999-9637

Table 8: List of Equipment Used

12.1.3 Results from Tensile Testing

No	Thickness 1 (mm)	Thickness 2 (mm)	Thickness 3 (mm)	Width 1(mm)	Width 2(mm)	Width 3(mm)	Peak Stress (N)
1	6.17	6.17	6.17	25.17	25.17	25.17	244.5
2	6.04	6.04	6.04	25.05	25.05	25.05	250.5
3	6.00	6.00	6.00	25.18	25.18	25.18	252.9
Mean	6.07	6.07	6.07	25.13	25.13	25.13	249.3
Std. Dev	0.07	0.07	0.07	0.05	0.05	0.05	3.07

Table 9: Results from Samples Testing

Figure 49 below gives an indication of the stress strain curve for the three samples tested.

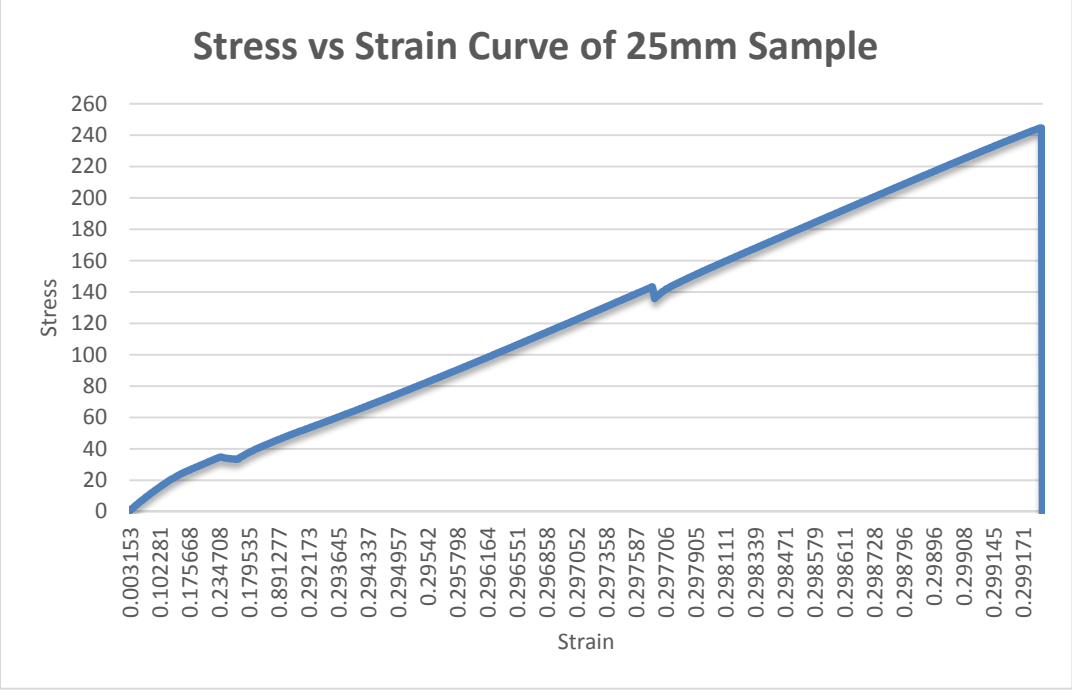

Figure 49: 25mm Sample Stress vs Strain Graph

The first dip at the 40Mpa range was caused by the removal of the extensometer; the second dip was caused when the fibres straightened suddenly at the 140Mpa mark. With the increase in stress, the fibres continued to strain eventually causing the sample to fail at an average Ultimate tensile strength of approximately 250Mpa.

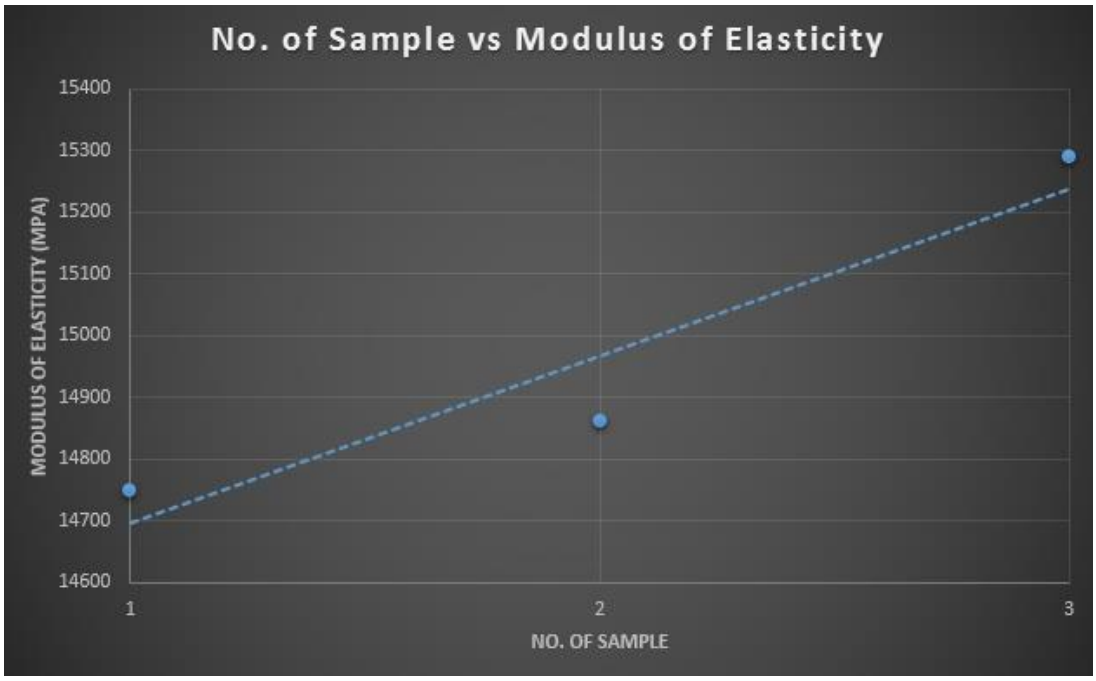

Figure 50: Average Modulus of Elasticity across 3 samples

No.	Possions Ratio	Modulus of Elasticity (Mpa)
1	0.126	14750
2	0.126	14861
3	0.126	15289

Table 10: Possions Ratio and Modulus of Elasticity for Each Sample

For the purposes of the tensile data from Table 6 and 7, the average results are summarised below.

	Modulus of Elasticity (Mpa)	Possions Ratio	Peak Stress (Mpa)
Mean	14967	0.126	249.3
Std. Deviation	201.3	0	3.065

Table 11: Average and Standard Deviation Results

Failure Modes

As can be observed in the Figure below, the tensile samples experienced a separation of the fibres in the transverse direction due to stress, fracture and ply failure. It can be assumed therefore that surface fibres were displaced and fractured when they were no longer constrained by the surrounding plies.

12.1.4 Summary

As a result of the tensile material testing, the following table summarises the accumulated data gleaned from the material testing. The Shear Modulus was calculated using (Moore, Williams & Pavan 2001, p. 21).

Material Property	Value
Modulus of Elasticity	14967 Mpa
Possions Ratio	0.126
Density	398 g/m^3
Ultimate Tensile Stress	248.45 Mpa
Shear Modulus	6527.53 Mpa
Ultimate Tensile Load	37500N

Table 12: Summary of Tensile Testing Results

12.2 Flexure Testing Procedure and Results

12.2.1 Determination of Flexural Properties

The 3 samples needed to determine the flexure material properties were manufactured in accordance with the ISO 14125 – Fibre Reinforced Plastic Composites – Determination of flexural properties. Subsequently, the 3 point bending test was adopted based on the formulae covered in the standard.

Due to the late addition of the 3 point bending flexural testing to be undertaken as part of this research project, the left over samples used in the tensile testing were used to conduct the flexural testing. As a result ISO 14125 was used as a basis for the testing, but the samples used were slightly thicker and wider than what is required to conform to the letter of the standard.

The Figure 51 below is a representation of the fixture needed to carry out the flexure testing.

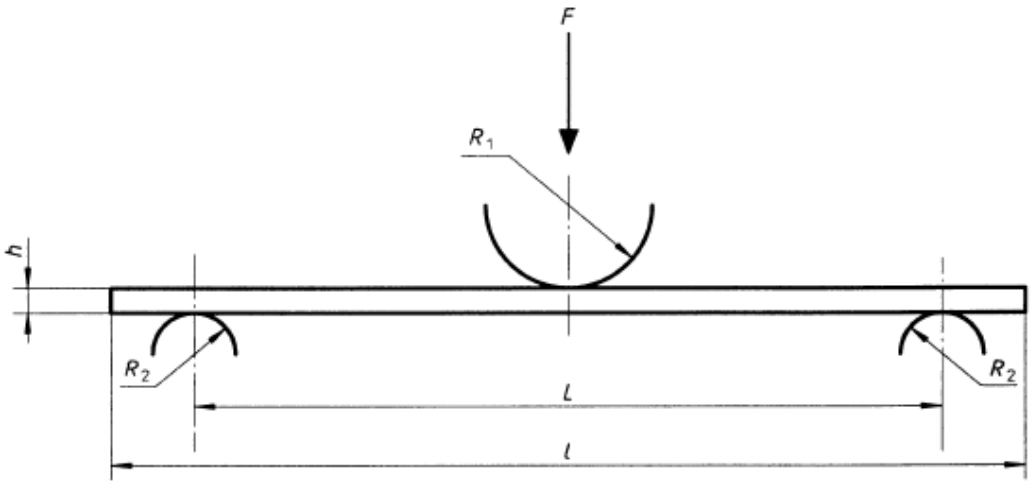

Figure 51: Three point bending fixture (ISO 1998)

Due to the limited availability of samples and time required to finish the testing material class II was selected to be used as a basis for the ideal length between the lower supports.

	Width (mm)	Thickness (mm)
Sample 1	24.5	5.48
Sample 2	24.82	5.43
Sample 3	24.48	5.56

Table 13: Sample Dimensions

The formula below is a representation of material class II Table A1 (ISO 1998, p. 9) calculation. This formula was used to determine the optimum distance of 88mm between the lower supports using the average thickness of 5.52mm (Hibbeler).

$$16 * t = L$$

$t = average\ thickness\ of\ samples\ (mm)$

$L = Distance\ between\ supports\ (mm)$

Second Moment of Inertia formula for a rectangle beam (Hibbeler)

$$I = \frac{bd^3}{12}$$

Modulus of Elasticity formula for three point bending (Hibbeler)

$$\delta = \frac{PL^3}{48EI}$$

δ = Deflection (mm)

P = Load (Newtons)

L = Length between supports (mm)

E = Modulus of Elasticity (Mpa)

I = Second Moment of Area mm^4

Using the above Equation the Modulus of Elasticity for Flexural Properties is 14089 Mpa

12.2.2 Flexural Testing Procedure

The flexural testing was carried out as close as possible to ISO 14125. The size and quantity of the samples were different compared to the standard due financial constraints. As the force required to break the samples was below 4KN, the MTS 310 testing machine was used instead of the much larger MTS 810 which was used for the tensile material properties testing.

Figure 52: Three Samples Tested in three point bending

A closer view of the flexural testing setup is seen below in Figure 52.

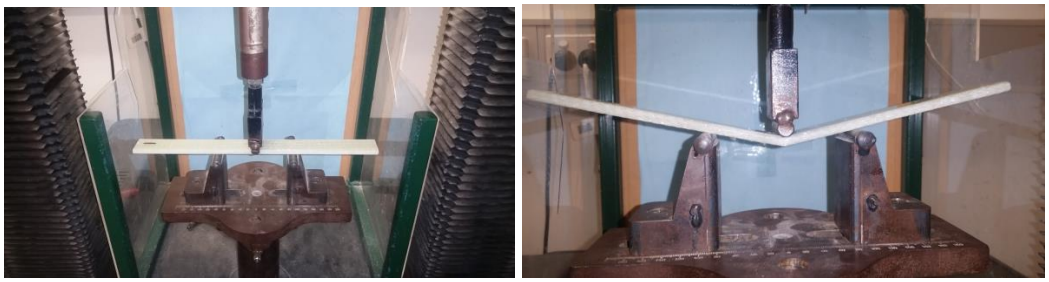

Figure 53: Flexure Test Pre and Post Test

12.2.3 Results from Flexure Testing

No	Thickness 1 (mm)	Thickness 2 (mm)	Thickness 3 (mm)	Width 1(mm)	Width 2(mm)	Width 3(mm)	Peak Load (N)
1	5.56	5.56	5.56	24.48	24.48	24.48	2455
2	5.43	5.43	5.43	24.82	24.82	24.82	2539
3	5.56	5.56	5.56	24.48	24.48	24.48	2460
Mean	5.52	5.52	5.52	24.59	24.59	24.59	2485
Std. Dev	0.08	0.08	0.08	0.20	0.20	0.20	47.1

Table 14: Flexure Sample Testing Results

12.2.3 Results of Three Samples

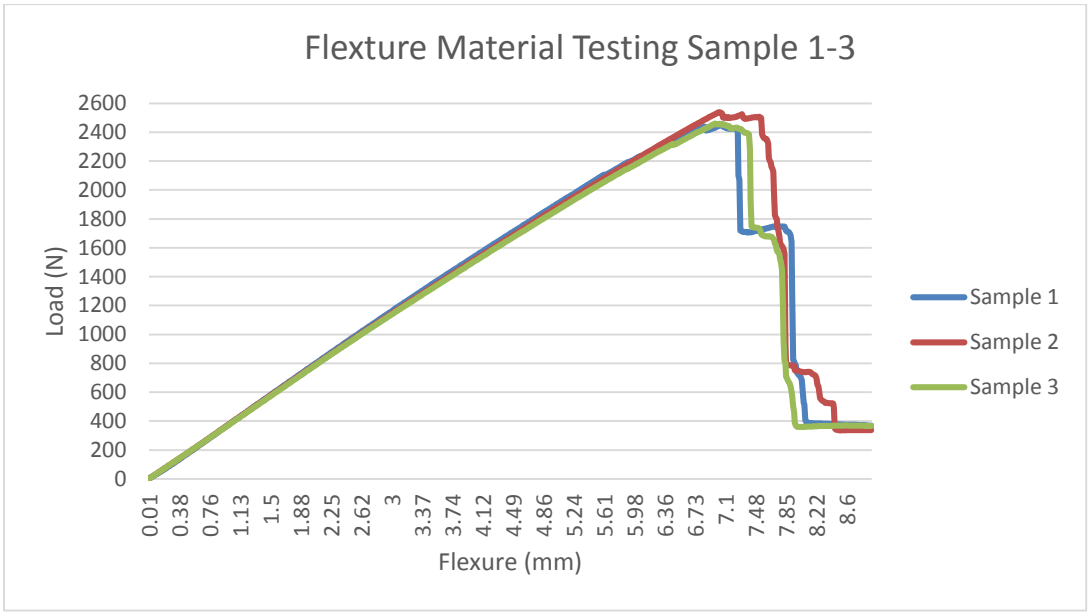

Figure 54: Flexure vs Load Plot of Three Samples

12.2.4 Possible Failure Modes

Some typical failure modes for three point bending are shown below. Due to the nature of the experiments and the standardisation of the testing procedure, it is reasonable to assume that the failure mode would be one of the modes seen below in Figure 55.

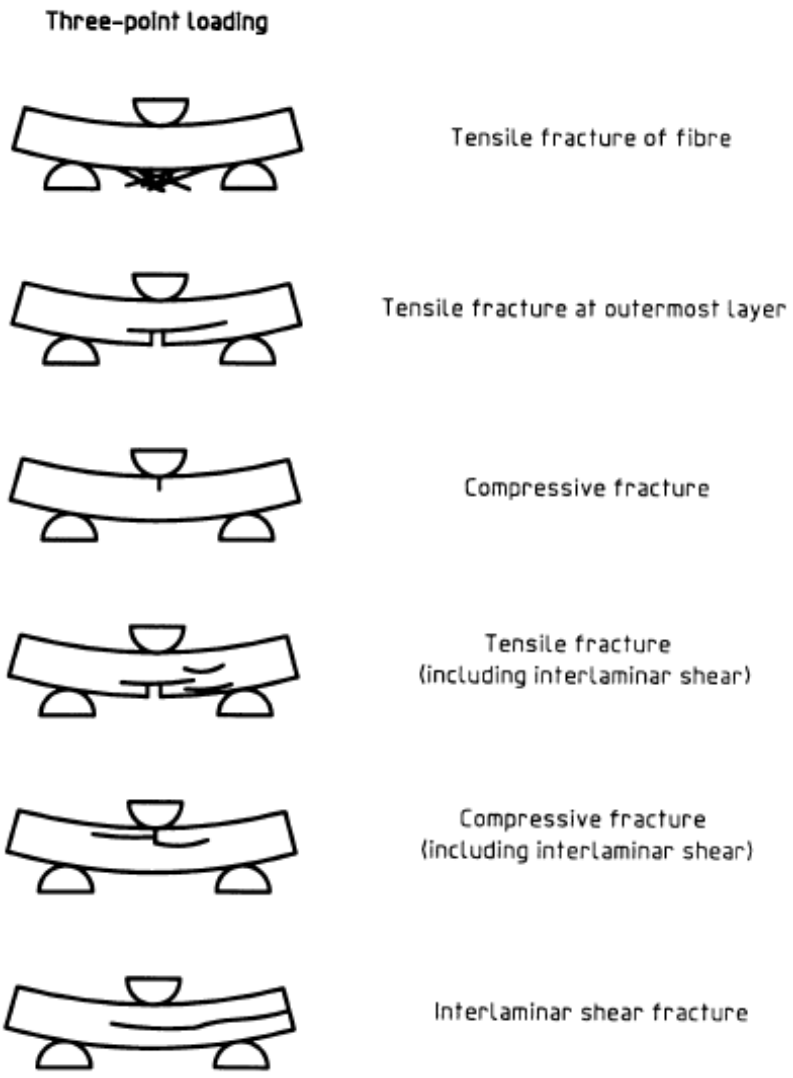

Figure 55: Failure Modes

Due to the low Load required (under 3.2KN) the 310 MTS machine was used to carry out the three point bending tests. The 310 testing machine was used to provide a detailed report detailing the primary mode of failure. The results for each sample are presented below.

Sample	Failure Mode
1	Tensile Fracture at Outermost Layer
2	Tensile Fracture at Outermost Layer
3	Tensile Fracture at Outermost Layer

Table 15: Sample Failure Points

The test equipment used found tensile fractures at the outermost layer as Figure 56 shows below. On further inspection several modes of failure were found to contribute to the failure of the sample such as fracture of the upper surface due to compressive loads.

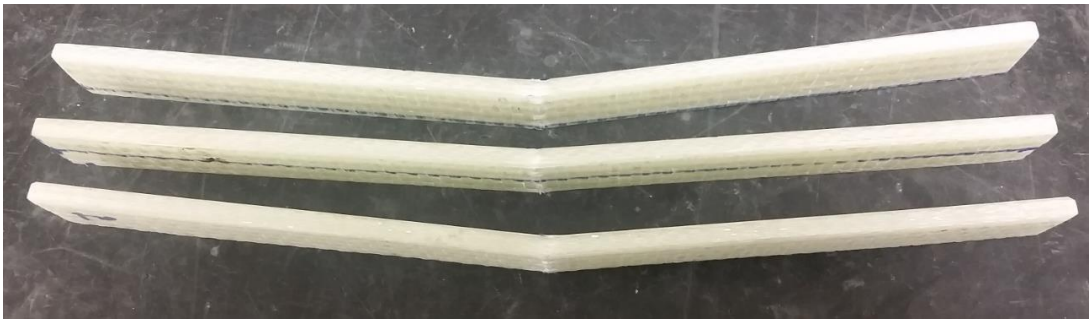

Figure 56: Flexure Fracture at Outermost Layer.

12.2.5 Summary of Results

Material Property	Value
Average Maximum Load	2.485 KN
Modulus of Elasticity	14089 Mpa

Table 16: Summary of Flexure Results

Chapter 13.0 Experimental Testing

13.1 General Overview

The best way to replicate the conditions experienced on a rudder laminate when icing occurs in the composite laminate was to use a GAG (Ground Air Ground cycle) series of tests. Due to the nature of the problem and the high cost of replicating the actual conditions on board an aircraft, a series of experiments were carried out on 12 ply GRFP samples, in two configurations of testing; tensile and three point bending.

All three samples were made from 12 plies of AR 145 woven E-glass and infused with 100/26 mixture of R246TX epoxy resin. Then post cured for 4 hours at 80ºC in an oven.

The testing regime consisted of 5 tensile tests and 1 3 point bending test. As found in Chapter 12, the Ultimate Tensile Load was 37500N and the Ultimate bending Load was 2485N.

13.1.2 Assumptions

During the planning of the manufacturing of samples a couple of assumptions of sample making needed to be made due to the scope of the project such as:

- Funding limited to the project: $200
- Time allocated to the manufacturing of samples
- Amount of experimental samples
- Amount of material available to make samples
- The samples representing frozen ice were replaced with wood (Tasmanian Oak).
- The amount of time allocated to testing was limited

Due to the amount of fatigue cycles needed to accurately determine the rate of crack propagation in a frozen water panel and the problem of the melting fairly quickly, the frozen water was replaced with pieces of Tasmanian Oak.

Also both samples (1&2) did not include the honeycomb core modelled in the original Abaqus FEA modelling, and, as such, the experiments conducted were as true as the budget would allow.

13.2 Tensile Testing

Tensile Testing was performed on two fibre composite samples.

1. An initial sample to determine the failure points of a sample with two timber inclusions in the fibre composite
2. A final sample which combined a more accurate wooden block and a FBG sensor with strain data to accurately determine crack propagation under low fatigue cycles.

13.2.1 First Tensile Sample

The initial tensile testing sample incorporated two pieces of timber 18mm wide placed horizontally perpendicular to the longitudinal axis at the midpoint of the sample. Two strain gauges were later placed 5mm from the ends of the timber inclusion on plies 1 and 12 on the upper end of the sample.

Figure 57: First Tensile Sample Top View.

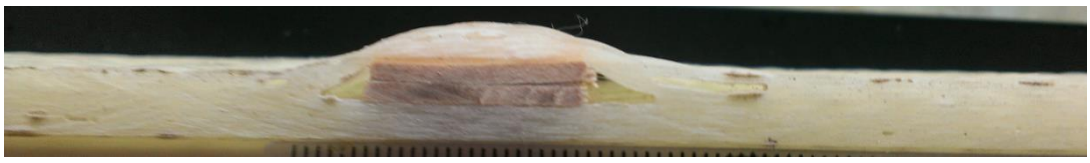

Figure 58: Second Tensile Sample Front view

Dimensions (mm)	
Length	340
Width	40
Thickness	6

Table 17: Dimensions of Tensile Samples

Based upon the results found in the materials testing in Chapter 12, the stress of 250Mpa was used as a basis for the ultimate tensile strength of the 12ply (40mmx6mm) fibreglass sample (Hibbeler).

$$\sigma = \frac{F}{A}$$

$\sigma = Stress$ (Mpa)

F = Force (Newtons)

A = Cross sectional area of sample (mm^2)

Using the formula above and the results from the materials testing in chapter 12, the ultimate strength of the fibreglass sample was determined to be 37500N. As a starting point for the fatigue testing, the ultimate strength was reduced by 70% to give an approximate yield point to the fibre composite first sample; this was determined to be 26200N.

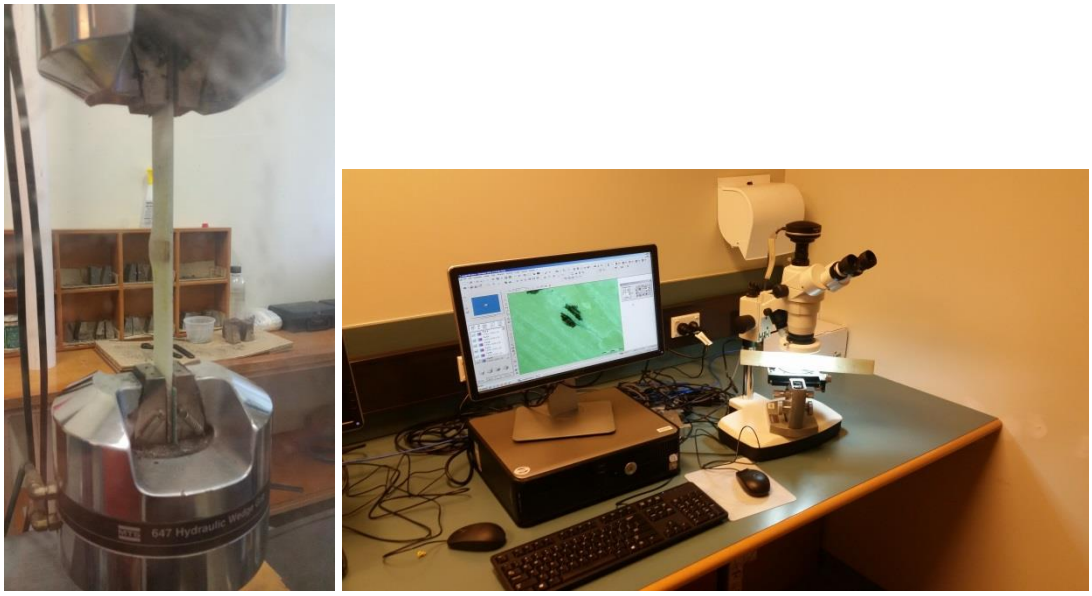

Figure 59: Initial Testing using 1st Sample and Optical Measurement of Crack Propagation

The Table below shows the fatigue cycle loads applied to the First tensile sample. A course ratio of 0.1 was used on all samples to show crack propagation within 5000 cycles.

Loading (KN)	Max (KN)	Min (KN)	Mean (KN)	Amp (KN)	Ratio
25	25	2.5	13.75	11.25	0.1
30	30	3.0	16.50	13.5	0.1
35	35	3.5	19.25	15.75	0.1

Table 18: Fatigue Loads

After each fatigue loading, the sample was inspected under an optical microscope to visually determine if any crack propagation had occurred. The results are shown in Figure 75.

13.2.2 Second Tensile Sample

The second tensile sample incorporated a half moon piece of single piece of Tasmanian oak (Fig 60) to simulate a more realistic block of ice for use in the fatigue testing. This was used to detect the presence of fatigue cracking and as a measure of possible crack propagation from the edge of the timber.

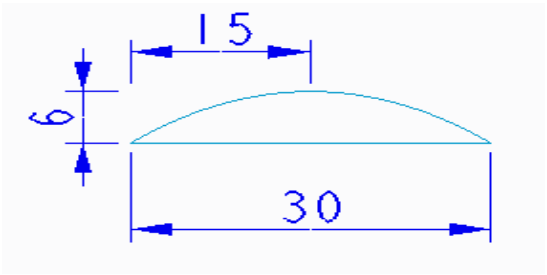

Figure 60: Tasmanian Oak profile used to simulate Icing

Figure 61: 2nd Tensile Sample Top View

The Second tensile sample incorporated an FBG sensor placed 15mm from the edge of the block of timber between plies 6 and 7. 4. Strain gauges were placed on both upper and lower surfaces of the samples to detect any cracks over a 5000 cycle time period. An attempt was made with the sample to control the position of the top fibreglass layers over the piece of wood embedded in the sample. This was done with pieces of wood weighed down with a 10lb weights while the sample dried as seen in Figure 62.

Figure 62: Controlling the shape of the 2nd Tensile Sample

While the pre testing delaminations of the previous sample were eliminated, as seen in Figure 63, the edges were reduced in thickness from 6mm – 4mm. This made for a reduction in the ultimate tensile strength.

Figure 63: 2nd Tensile Sample Side View

As a result the new ultimate strength was calculated to be:

$$\frac{4.5}{6} * 100 = 75\%$$

Therefore the ultimate strength was reduced from 37500N to 28125N.

Based on previous tests with the first tensile sample, a load of 20KN or 70% of 28125N was used for the initial fatigue testing over 5000 cycles using the values shown in Table 19. Further testing was not required as crack propagation began during the 5000 cycle period. Table Number 19 shows the loading conditions of the test. The results are presented in Chapter 14.

Loading (KN)	Max (KN)	Min (KN)	Mean (KN)	Amp (KN)	Ratio	Hz
20	20	2.0	11	9	0.1	5

Table 19: Fatigue test values of Second Sample

13.2.3 Failure Modes

Under flexure testing, the sample failed under interlaminar shear. This was due to the position of the sample relative to the load applied.

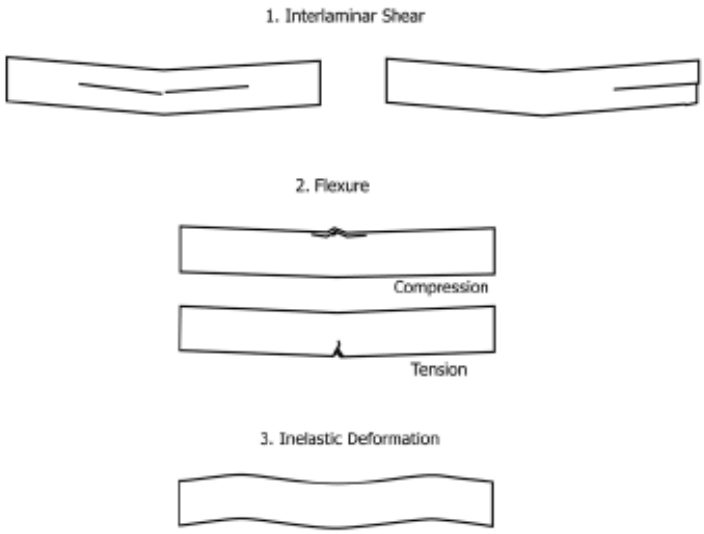

Figure 64: Failure Modes for Tensile Testing (Standard 2000)

13.3 Flexure Tests

The three point bending testing or flexure sample incorporated a single piece of half-moon Tasmanian oak as seen in the second tensile sample. It was placed horizontally perpendicular to the longitudinal axis at the midpoint of the sample. Two strain gauges were later placed 5mm from the ends of the timber inclusion on plies 1 and 12 on the upper end of the sample.

Flexure sample Dimensions

Figure 65: Top View of Bending Sample

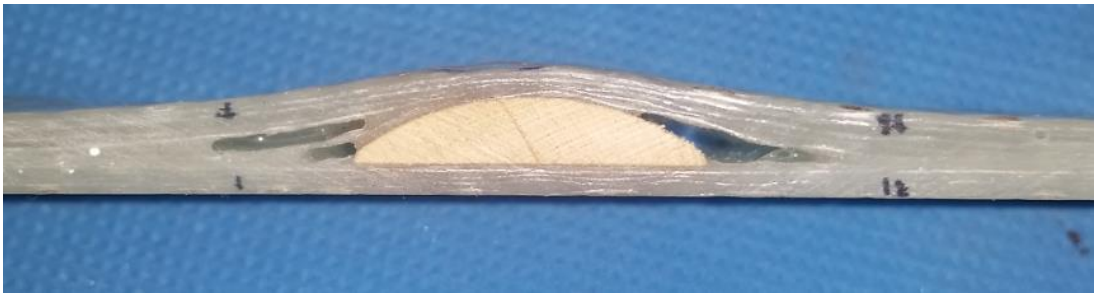

Figure 66: Front view of Bending Sample

Dimensions (mm)	
Length	400
Width	40
Thickness	6

Table 20: Dimensions of Flexure Sample

13.3.1 Placement of Strain Gauges

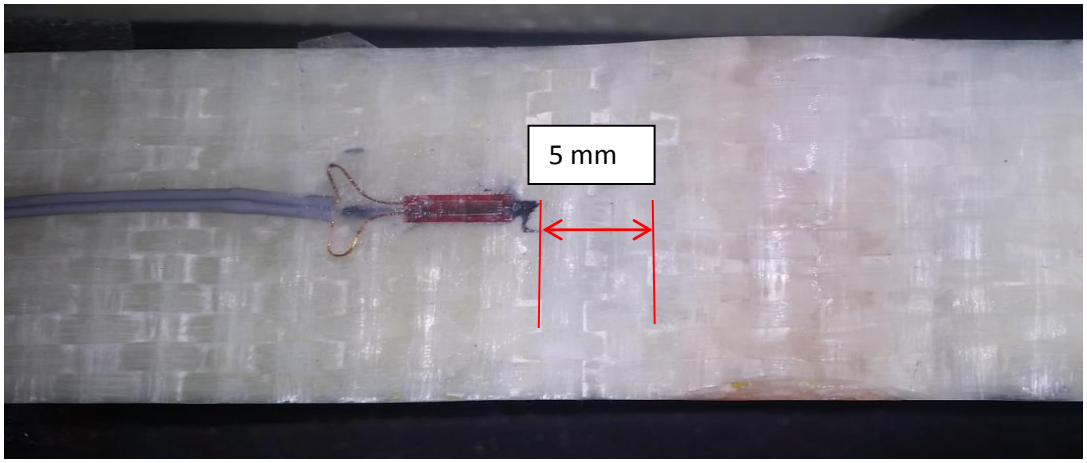

Figure 67: Upper Strain gauge attachment

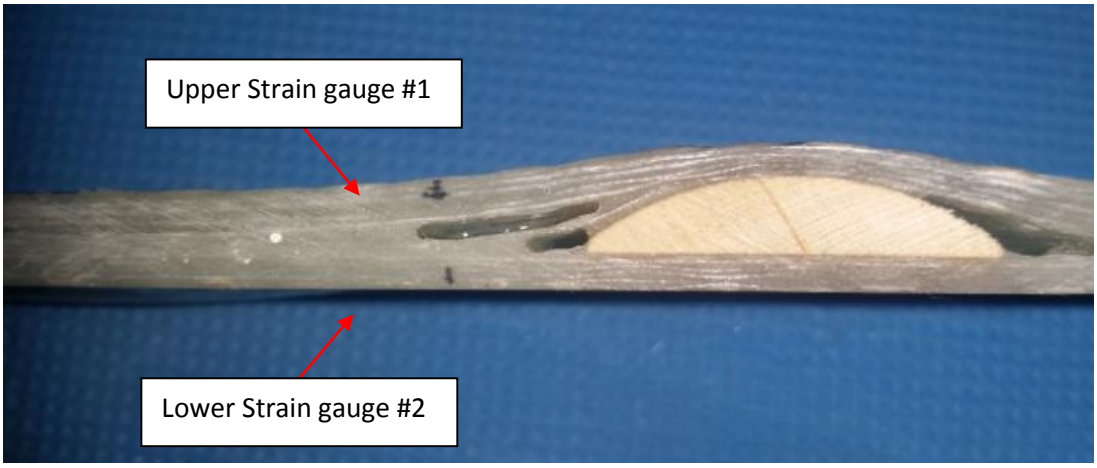

Figure 68: Side view of sensor placement

13.3.2 Fatigue and Strain Testing

Due to the placement of the strain gauges on the three point bending sample, the lower supports were moved from 88mm apart to 120mm.The testing procedure was modified slightly to handle the increased distance. This increased the ultimate tensile load of the sample from 2.485KN to 3.148KN thus strains were taken in 2KN intervals from 1.600 – 2.400KN see Figure 69.

Figure 69: Flexure Sample in fixture

13.3.3 Failure Modes

Under flexure testing the sample failed under interlaminar shear. This was due to the position of the sample relative to the load applied.

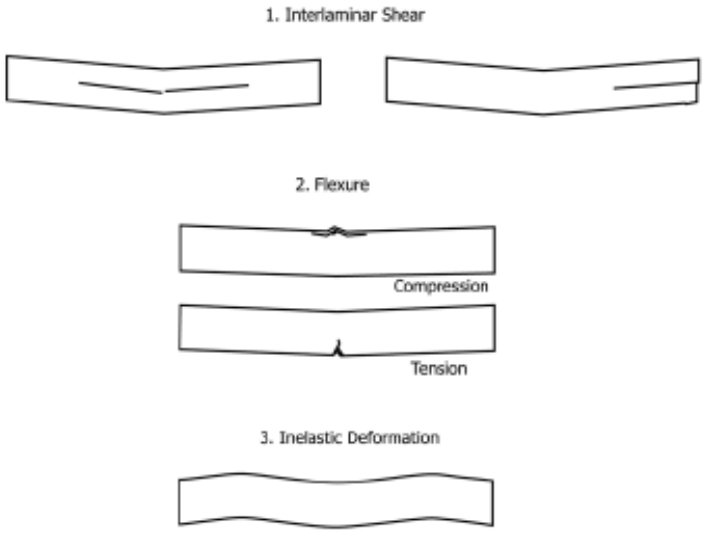

Figure 70: Failure Modes for flexure testing (Standard 2000)

13.4 Thermographic Testing

13.4.1 Preparation of Samples

In order to accurately show heat accumulation within the structure of the composite laminate, the first and second tensile samples and the flexure samples were sprayed with enamel matt black topcoat as seen below in Figure 71.

Figure 71: All three Samples Sprayed Black in preparation for thermographic testing

This was done to increase the emissivity of the fibre composite which in turn increased the heat transfer between the two black bodies to retain any heat generated through fatigue testing cycles. The tensile samples were the only samples that could be used for thermography testing as the thermographic camera provided was unable to be positioned perpendicular to the sample. This is illustrated in the Figure 72.

13.4.2 Testing

Figure 72: First and Second Tensile Samples during thermographic testing

The setup for Thermography testing with the 810 MTS machine is shown below in Figure 73.

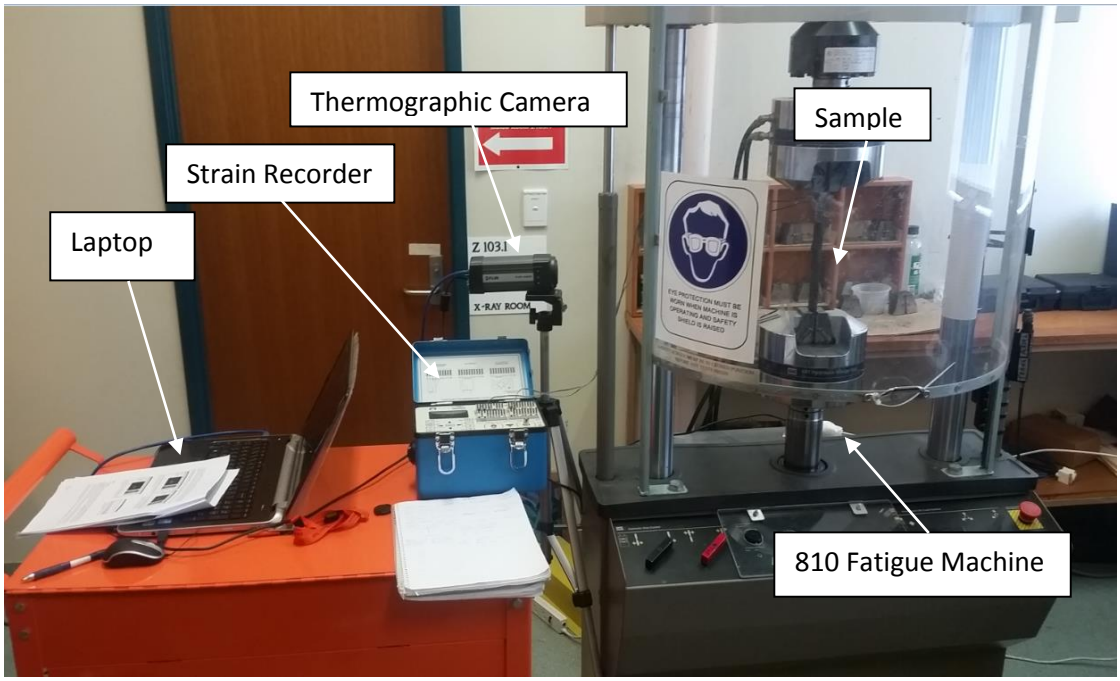

Figure 73: Setup of 810 Fatigue Machine

13.4.3 Failure Modes

As with the tensile and 3 point bending samples, the failure modes during thermographic testing was interlaminar shear. The benefits of using thermographic images in Thermoelastic stress analysis (TSA) is shown in Figure 74 with red in the left of Figure 74 and green in the right of Figure 74. The images were taken with a computer and an A325 Thermographic camera.

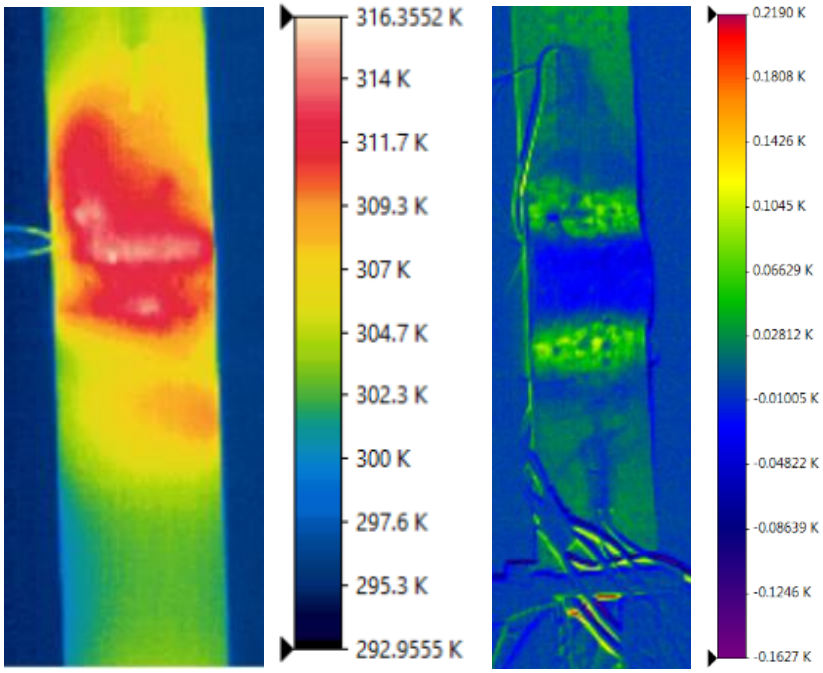

Figure 74: Thermoelastic Stress Analysis

Chapter 14.0: Results

14.1 First Tensile Test Sample

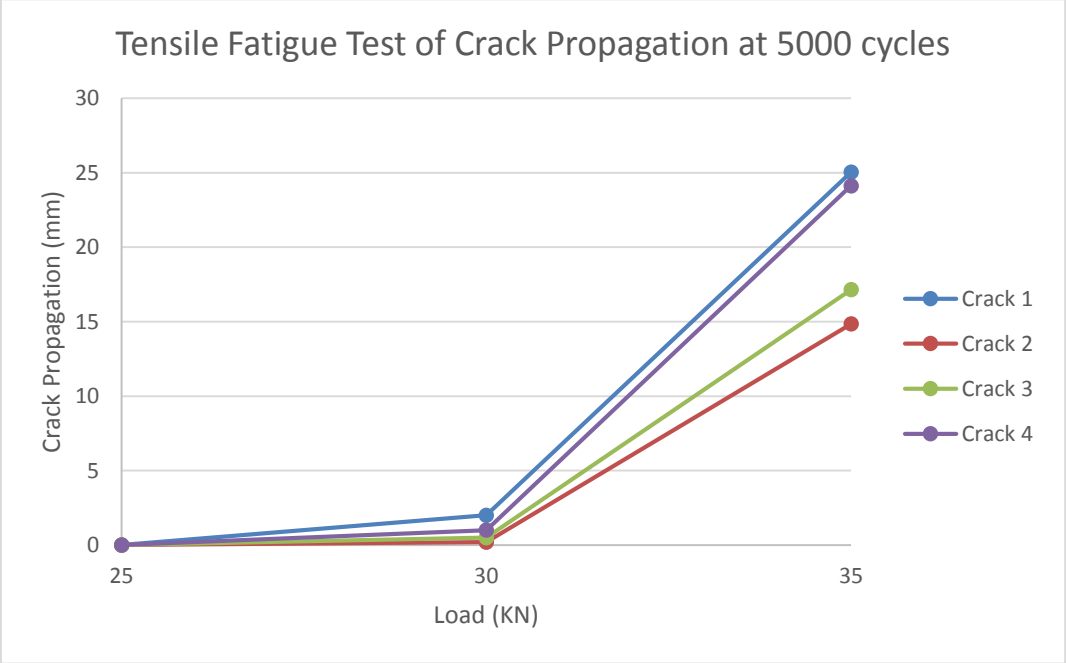

Figure 75: Tensile initial testing

As seen in figure 75, the tensile sample began to crack at the 30KN load mark, but was very difficult to measure optically with the electron microscope. Bearing blue or Prussian blue was used to bring out the crack in the same way that dye penetrant is used to bring out cracks in metal components. As the cracks were very small, it was decided to increase the load to 35KN to ascertain a positive crack reading and to form a basis for further fatigue testing.

Due to the initial crack propagation at the 30KN mark or 80% of the ultimate tensile strength of the composite material, further studies are needed in this region to determine more accurate data. The results in terms of percentage failure are shown below.

	Ultimate Tensile Strength	Percentage Failure
Undamaged	37.5 KN	100%
Test 3	35.0 KN	93%
Test 2	30.0 KN	80 %

Table 21: Percentage Failure of Tensile Samples

The second round of testing on the first tensile sample involved the use of thermography to determine the thermoelastic stresses within the sample as it was cycled up to 5000 cycles. The graph below, Figure 76 shows the change in temperature over the 5000 cycles of the first sample under tensile load.

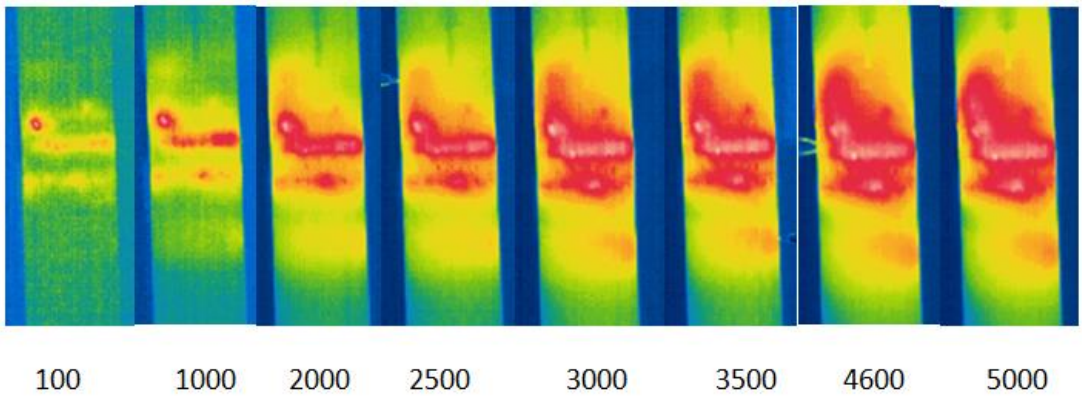

Figure 76: Thermography Pictures in Cycles

The data from Figure 76 was collated and placed in a graph to illustrate the change in temperature vs the fatigue cycles; this was determined by choosing a fixed point on the camera, at the end of the simulated inclusion and measuring the associated temperature at that position and graphing the results.

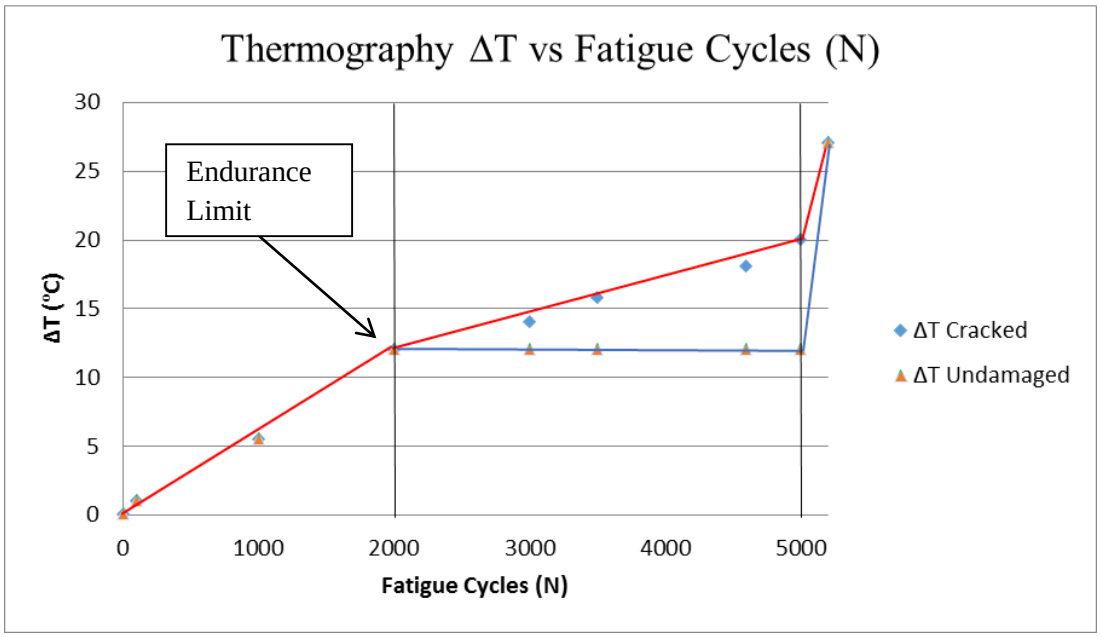

Figure 77: Thermographic Results

According to (Vergani, Colombo & Libonati 2014) the position between the first and second linear line is called the fatigue limit or endurance limit. This corresponds to the arrow in Figure 77 which is positioned at the 2000 cycle mark. The red line corresponds with the cracked sample and the blue dotted line is an undamaged sample. This information is important because finding the fatigue limit of a fibre composite laminate was extremely difficult using strain data or FBG analysis.

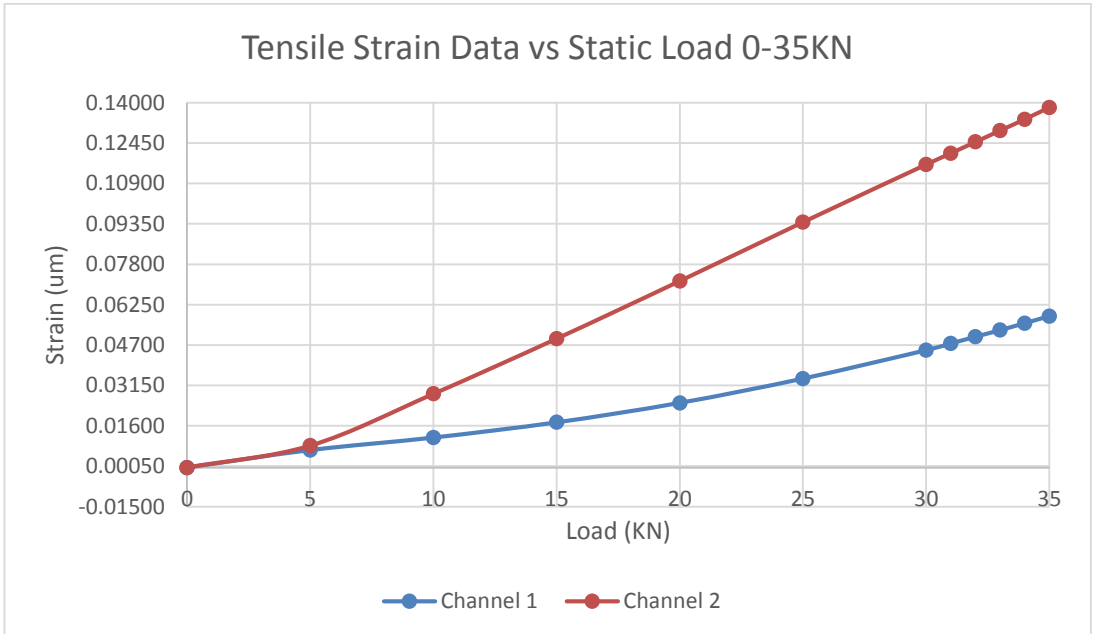

Figure 78: Visual Crack initiation

Determining where a crack had started in each sample was one of the biggest challenges with this project. The most accurate way was to draw a graph using the strain data. If the line was straight then no cracks had appeared but if the line was curved, then the place where the curve had originated was the location of the first micro cracking. Figure 78 is a good representation of this phenomenon.

14.2 Second Tensile Sample

Testing for the second tensile sample involved gaining results from three sources:

1. Strain gauges
2. FBG sensors
3. Thermography data

Comparison between Strain, FBG and Thermography Data

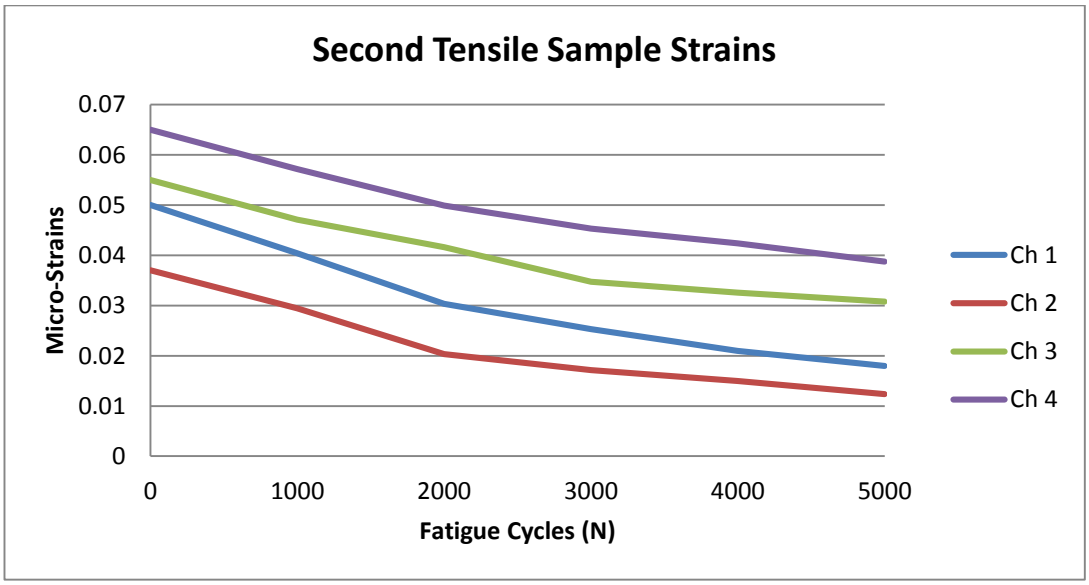

Figure 79: Strain Data from Second Tensile Sample

Testing for the Second Tensile Sample involved the use of FBG as well as strain gauges to accurately determine at what point crack propagation started under tensile load. As with the results from thermography testing for the First tensile sample, there is a definite change of macro-strain values across all strain gauges at the 2000 cycle mark. This was further illustrated with the data obtained with the FBG sensors between 2000 and 3000 cycles as seen below in Figures 80-81.

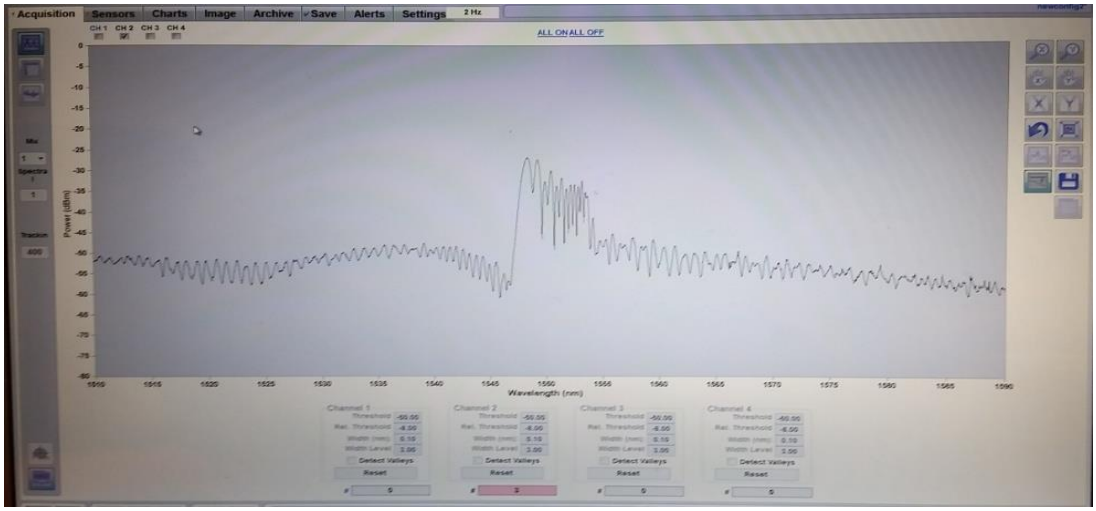

Figure 80: FBG data at 2000 Cycles

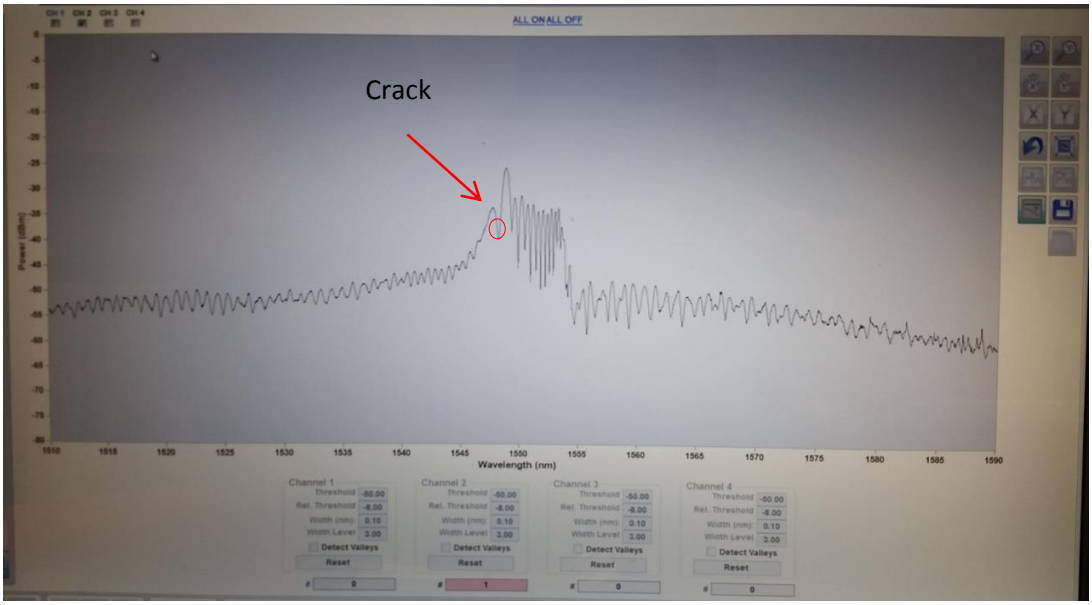

Figure 81: FBG data at 3000 cycles

The red arrow painted in Figure 81 shows where a crack has formed at 3000 cycles, due to the fact that pictures were only obtained at 1000 cycle intervals it is likely that the crack formed between cycles 2000 and 3000. The best representation of crack propagation and visual confirmation of the existence of a micro crack was under Thermoelastic stress as seen in the figure 82 below.

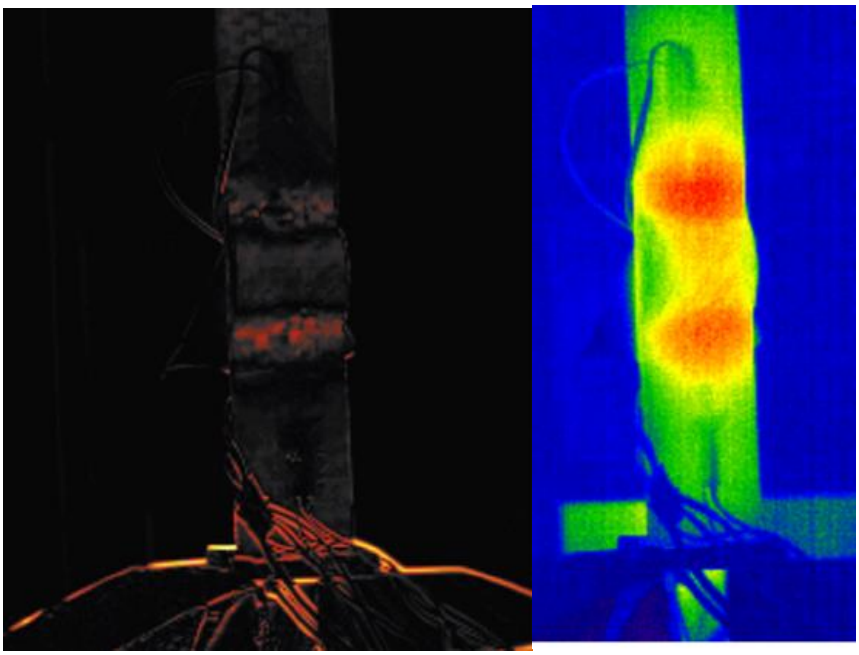

Figure 82: Thermoelastic Stress under Tensile Load

Although strain and FBG data show the existence of a crack, the advantage of Thermoelastic Stress Analysis is that the location and severity of interlaminar cracking can be quickly determined by visual means.

14.3 Flexure Test Sample

The flexure or three point bending test was carried out to see if there was any substantial change with subjecting a sample to flexure testing. For this test, only strain readings were taken due to the cost of FBG sensors. Figure 83 below shows a spread of the two channels of strain gauge which were glued to the outside of the sample. Channel 1 provided the best data due to its fixture on the upper face of the sample and thus was able to register the greatest deflection in stain values.

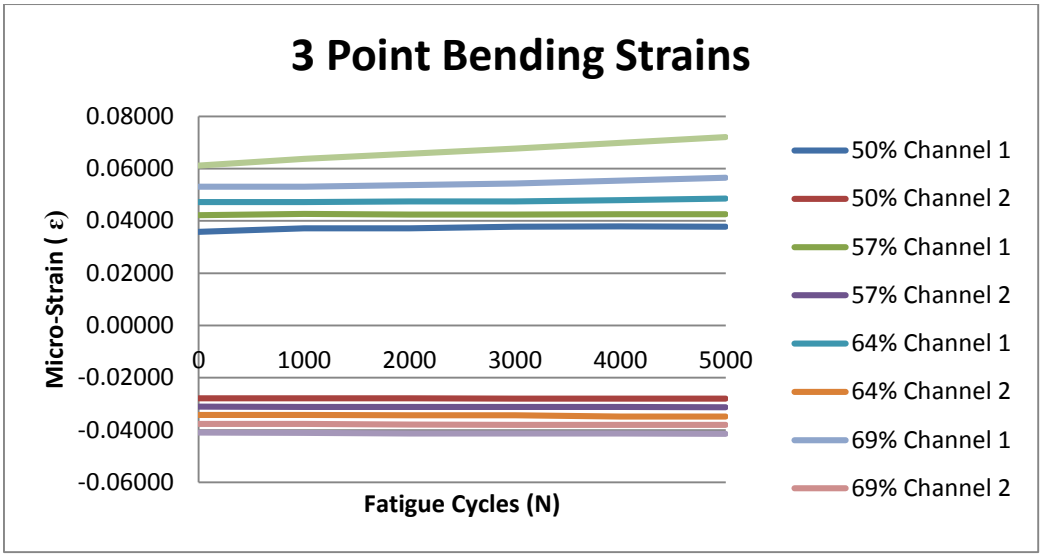

Figure 83: Three point bending Strain vs Fatigue Cycles

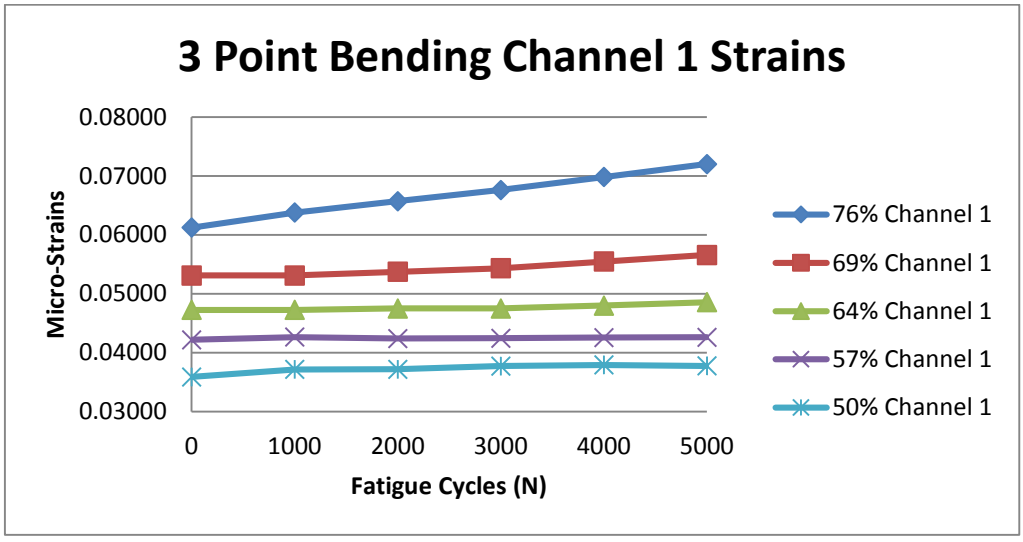

Figure 84: Three point bending Channel 1 Strains

Looking at Figure 84 above it is clearly seen that crack propagation has started by 64% at 3000 cycles of the ultimate strength of the fibre composite material. This is a 16% difference from the tensile test above., Possible reasons for this was the slow frequency rate of 1Hz that had to be applied to the sample during flexure testing because the machine used for testing was not designed for loads below 5KN.

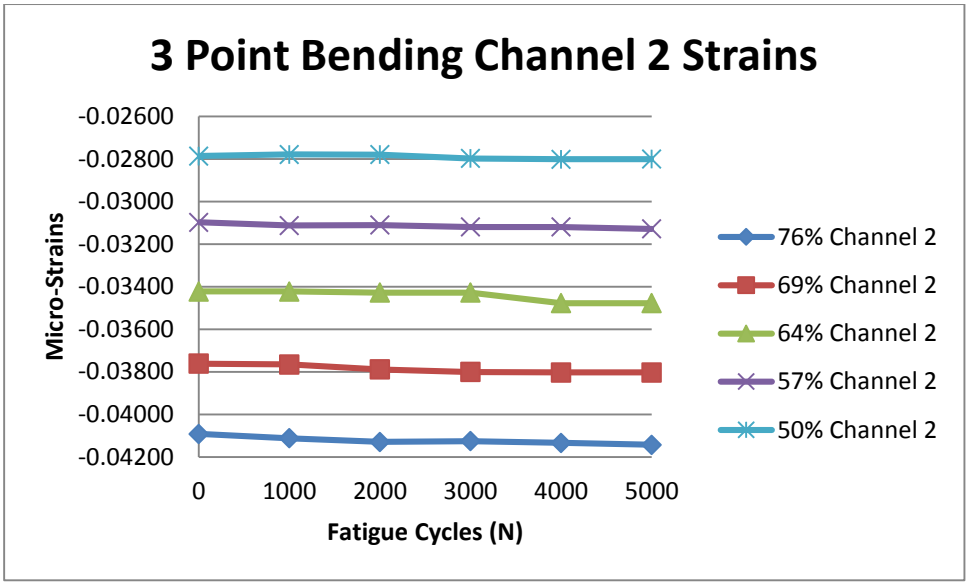

Figure 85: Three point bending channel 2 Strains

Figure 85 shows the channel 2 strains that were gathered during flexure testing. Interestingly, the 64% strain drops at the same point as the 64% Channel 1 data is increasing strain due to the presence of a micro-crack.

Chapter 15.0: Discussion and Conclusion

15.1 Discussion

This chapter compares the research aims with the results of the project and data for further discussion.

This research aims of this dissertation were to cover three important areas. Plus an additional aim if time permitted.

1. To investigate fluid ingress into composite aircraft laminate structure, which can lead to the delamination of the primary structure due to icing.

2. To investigate the best methods of crack propagation accumulation progression and detection via fatigue testing by the use of tensile and flexure methods on fibre composite laminates.

3. To compare the established tensile strength of the fibre composite laminates with results from testing and detect how much earlier the samples start crack propagation.

4. If time permitted: Investigate crack propagation through composite laminates through the use of a Thermography and Thermoelastic stresses

As seen in the extensive literature review undertaken at the beginning of this project, there is ample evidence to suggest that there is a current and very real need to look further into fluid ingress into fibre composite laminate structures on modern airplanes.

- The physical testing of fatigue analysis using tensile and flexure methods determined that the use of strain gauges and thermography could be used to determine fairly accurate crack propagation results.

- The FBG sensor was able to detect small incremental micro-cracks however this sensor system wasn't really the best medium for crack propagation detection with this dissertation due to the availability of only one sensor.

- FEA analysis really did not provide accurate results for this dissertation. Physical modelling of components and subsequent testing using FBG, strain gauges and thermostress analysis proved better mediums for results.

- Thermography and thermostress analysis provided the best way to detect crack propagation in the samples tested, due to the visual indications of micro cracks forming. These could be easily analysed and plotted in graphical form.

- Strain gauge analysis proved the best medium to compare the ultimate tensile strength of a fibre laminate to results gained by flexure testing.

15.2 Conclusion

In conclusion, there were three main areas that this project focussed on. These are discussed below under the established aims.

1. *The best methods of crack propagation accumulation progression and detection via fatigue testing by the use of tensile and flexure methods on fibre composite laminates.*

   Under tensile testing: optical, thermography and embedded Fibre Bragg Grating (FBG) sensors were the best methods for detecting crack propagation.

   Under Flexure Testing: Strain gauges proved to be the best method of detecting crack propagation.

2. *To compare the established tensile strength of the fibre composite laminates with results from testing and detect how much earlier the samples start crack propagation.*

   Under tensile loading of 5Hz, the First and Second tensile samples started crack propagation between 80-93% of the ultimate tensile strength of the fibre laminate as determined by material property testing in Chapter 12.0 of 37.5KN

   Under flexure testing of 1Hz the flexure sample started crack propagation at 64% of the of the ultimate tensile strength of the fibre laminate as determined by material property testing in Chapter 12.2 of 3.148KN.

3. *If time permitted: Investigate crack propagation through composite laminates through the use of a Thermography and Thermoelastic stresses.*

   As discussed in section 15.1, thermography and thermostress analysis proved to be the most viable, accurate and most importantly, easiest form of crack propagation detection medium in this dissertation.

   Unfortunately there wasn't enough time to continue looking into this area for flexure or three point bending testing.

15.3 Recommendations for Future Research

As a result of this undergraduate project into the "Investigation into the Delamination of Composite Laminates on Aircraft Rudders due to Fluid Ingress and Icing", a number of experiments and areas discussed in this thesis could be further investigated in future research.

1. Further experimentation of fatigue analysis in crack propagation

   - Between the ranges of 70% to 80% of Ultimate Tensile Strength
   - Larger range of cyclic testing beyond 0-5000 cycles
   - A finer ratio range of under 0.1 to gain more accurate data.

2. A comprehensive FEA analysis of where to place strain gauges, FBG sensors and thermographic cameras on a fibre composite panel prior to testing.

3. The use of more than one FBG sensor to gain more data on multiple icing locations throughout a structure.

4. Further research into the use of Thermography and Thermostress Analysis for the detection of cracks in fibre composite laminates.

Chapter 16.0: References

Adams, R & Cawley, P 1988, 'A review of defect types and nondestructive testing techniques for composites and bonded joints', *NDT international*, vol. 21, no. 4, pp. 208-22.

Airbus 2002, 'A310 - Airplane Characteristics for Aircraft Planning AC', viewed 16/03/2015.

Ali, M 2015, *Advancements of Composite Materials in Aerospace Industry*, viewed 11/03/2015.

Australia, C 2015, *Benefits of Composites*, 9/03/2015, <http://www.compositesaustralia.com.au/benefits-of-composites/>.

Authority, CAS 2010, *Maintaining ageing composite-material aircraft*, viewed 27/10/2014, <http://www.casa.gov.au/wcmswr/_assets/main/lib91145/31-32_41.com>.

Avionics, C 2000, *Mission Analysis*, viewed 14/03/2015, <http://flightdeck.ie.orst.edu/ElectronicChecklist/HTML/mission.html>.

Baker, AAB & Kelly, DW 2004, *Composite materials for aircraft structures*, AIAA.

Benson, T 2014, *Vertical Stabilisers - Rudder*, <http://www.grc.nasa.gov/WWW/k-12/airplane/rud.html>.

Board, TS 2005, *Aviation Investigation Report - A05F0047, Loss of Rudder in Flight*.

Boyce, BR 1999, 'Steps to modern thermoelastic stress analysis', in *ATEM Conference Japan, Stess Photonics Inc, Madison, USA*: *proceedings of theATEM Conference Japan, Stess Photonics Inc, Madison, USA*.

Brischetto, S & Carrera, E 2008, 'Thermal stress analysis by refined multilayered composite shell theories', *Journal of Thermal Stresses*, vol. 32, no. 1-2, pp. 165-86.

Bureau, ATS 2007, *Fibre composite aircraft – capability and safety*, viewed 27/10/2014.

BV, TA 2015, *Thermografisch Adviesbureau BV*, viewed 14/03/2015, <http://www.thermography.nl/index.php/home>.

Canada, TSBo 2005, *Aviation Investigation Report A05F0047*.

Chaddha, S 2011, 'CSLAA and FAA's Rules: Incorporating a 'Risk Management'Framework to Minimise Commercial Human Space Flight Risks', *Available at SSRN 1832322*.

Choi, HS & Jang, YH 2010, 'Bondline strength evaluation of cocure/precured honeycomb sandwich structures under aircraft hygro and repair environments', *Composites Part A: Applied Science and Manufacturing*, vol. 41, no. 9, pp. 1138-47.

Composites, F 2014, *Fibremax Composites - Product Catalog*, viewed 28/04/2015, <http://www.fibermaxcomposites.com/shop/index.php?osCsid=e33b8b90b7457f6bb0fd5f4a1b758b64>.

Composites, F 2014, *Nomex honeycomb applications*, viewed 28/04/2015, <http://www.fibermaxcomposites.com/shop/index_files/honeycombappl.html>.

Cook, RM-P 2010, *History of the de Havilland Mosquito*, viewed 11/03/2015, <http://www.airforce.gov.au/raafmuseum/exhibitions/restoration/dh_98.htm>.

Dutton, A 2004, 'Thermoelastic stress measurement and acoustic emission monitoring in wind turbine blade testing', in *European Wind Energy Conference London*: *proceedings of theEuropean Wind Energy Conference London* pp. 22-5.

Edwards, AK, Savage, S, Hungler, PL & Krause, TW 2011, 'Examination of F/A-18 honeycomb composite rudders for disbond due to water using through-transmission ultrasonics', *Ultragarsas" Ultrasound"*, vol. 66, no. 2, pp. 36-44.

Environment, Aat 2014, 'Advanced aerospace materials: past, present and future', in viewed 24/10/2014, <http://www.chriscarey.co.uk/a&e_materials>.

Evonik 2015, *ROHACELL® for aerospace*, viewed 28/04/2015, <http://www.rohacell.com/product/rohacell/en/markets/aviation-aerospace/pages/default.aspx>.

Gas, B 2014, *ICEBITZZZ™ Dry Ice Slice*, <http://www.boc.com.au/shop/en/au-boc-industrial-store/dry-ice/dry-ice-slice>.

Gray, CF 2015, *Flying Machines*, viewed 11/03/2015, <http://www.flyingmachines.org/>.

Hibbeler, R *Mechanics of Materials (2000)*, Prentice Hall, Upper Saddle River.

History, Et 2015, *The Wright Brothers - First Flight, 1903*, <http://www.eyewitnesstohistory.com/wright.htm>.

IFALPA 2010, 'Use of Rudder on AIrbus A300-600/A310', viewed 23/03/2015.

ISO, B 1998, '14125. Fibre Reinforced Plastic Composites—Determination of Flexural Properties', *Geneva, Switzerland: International Standard*.

ISO, E 1996, *527-1*, Plastics-determination of tensile properties-Part, 1.

ISO, U *527-4: 1997*, Plastics. Determination of tensile properties. Part, 4.

Kutin, M, Ristić, S, Puharić, M, Vilotijević, M & Krmar, M 2011, 'Thermographic Testing of Epoxy-Glass Composite Tensile Properties', *Contemporary Materials*, vol. 2, no. 1, pp. 88-93.

Leng, J & Asundi, A 2003, 'Structural health monitoring of smart composite materials by using EFPI and FBG sensors', *Sensors and Actuators A: Physical*, vol. 103, no. 3, pp. 330-40.

Leybovich, ME 2009, 'A technoregulatory analysis of government regulation and oversight in the United States for the protection of passenger safety in commercial human spaceflight', Massachusetts Institute of Technology.

Lobo Ribeiro, A, Ferreira, L, Santos, J & Jackson, D 1997, 'Analysis of the reflective-matched fiber Bragg grating sensing interrogation scheme', *Applied optics*, vol. 36, no. 4, pp. 934-9.

Lomax, TL 1996, *Structural Loads Analysis: Theory and Practice for Commercial Aircraft*, AIAA.

Minakuchi, S, Tsukamoto, H & Takeda, N 2009, 'Detection of Water Accumulation in Aircraft Honeycomb Sandwich Structures using Optical Fibre based Distributed Temperature Measurement', in *Materials Forum*: *proceedings of theMaterials Forum*.

Moore, DR, Williams, JG & Pavan, A 2001, *Fracture mechanics testing methods for polymers, adhesives and composites*, vol. 28, Elsevier.

Museum, SNAaS 2014, 'Inventing the Flying MAchine', <http://airandspace.si.edu/exhibitions/wright-brothers/online/fly/1903/index.cfm>.

Network, An 2014, *Australia's Rex Completes Purchase Of 25 Aircraft As Leases Expire*, <http://www.aero-news.net/index.cfm?do=main.textpost&id=de20ff07-438f-4a82-b55c-cfb6407aa661>.

Nguyen, DQ 1998, 'The essential skills and attributes of an engineer: A comparative study of academics, industry personnel and engineering students', *Global J. of Engng. Educ*, vol. 2, no. 1, pp. 65-75.

NSW, T 2010, *Aircraft Structures Summary*, viewed 11/08/2015.

O'Brien, T 2001, 'Fracture mechanics of composite delamination', *Materials Park, OH: ASM International, 2001.*, pp. 241-5.

Pugno, N, Ciavarella, M, Cornetti, P & Carpinteri, A 2006, 'A generalized Paris' law for fatigue crack growth', *Journal of the Mechanics and Physics of Solids*, vol. 54, no. 7, pp. 1333-49.

Roe, KL & Siegmund, T 2003, 'An irreversible cohesive zone model for interface fatigue crack growth simulation', *Engineering Fracture Mechanics*, vol. 70, no. 2, pp. 209-32.

Roylance, D 2001, 'Introduction to fracture mechanics', *Massachusetts Institute of*.

Russell, AJ & Street, KN 1985, 'Moisture and temperature effects on the mixed-mode delamination fracture of unidirectional graphite/epoxy', *Delamination and debonding of materials, ASTM STP*, vol. 876, pp. 349-70.

Schmidt, TA 1994, 'Intoxicated Airline Pilots: A Case-based Ethics Model', *Academic Emergency Medicine*, vol. 1, no. 1, pp. 55-9.

Shafizadeh, JE, Seferis, JC, Chesmar, EF, Frye, BA & Geyer, R 2003, 'Evaluation of the mechanisms of water migration through honeycomb core', *Journal of Materials Science*, vol. 38, no. 11, pp. 2547-55.

Sih, GC & Hsu, S 1987, *Advanced Composite Materials and Structures: Proceedings of an International Conference [on Adanced Composite Materials and Structures]... Taipei, Taiwan, Republic of China, May 19-23, 1986*, VSP.

Smith, DF 2013, 'The Use of composites in aerospace: Past, present and future challenges.', viewed 24/03/2015.

Standard, A 2000, 'D2344/D2344M, 2006,"', *Standard Test Method for Short-Beam Strength of Polymer Matrix Composite Materials and Their Laminates." West Conshohoncken, PA*.

Talay, TA 1975, 'Introduction to the Aerodynamics of Flight [NASA SP-367]'.

University, F 2013, *Lecture 12.13: Fracture Mechanics Applied to Fatigue*, http://www.fgg.uni-lj.si/~/pmoze/ESDEP/master/wg12/l1300.htm#SEC_2>.

Vergani, L, Colombo, C & Libonati, F 2014, 'A review of thermographic techniques for damage investigation in composites', *Frattura ed Integrità Strutturale: Annals 2014: Fracture and Structural Integrity: Annals 2014*, vol. 8.

Appendix A – Project Specification

University of Southern Queensland

FACULTY OF ENGINEERING AND SURVEYING

ENG4111/ENG4112 Research Project

Project Specification

For: Samuel Pike

Topic: Investigation into the Delamination of Composite Structure on an Aircraft Rudder due to Fluid Ingress and Icing

Supervisors: Dr Jayantha Epaarachchi

Enrolment: ENG4111 – S1, 2015
ENG4112 – S2, 2015

Project Aim: To investigate fluid ingress into composite aircraft structure, which can lead to the delamination of the primary structure due to icing.

Programme: **Issue B; 14th September 2015**

1. Research background information relating to fluid ingress into composite structure.

2. Research the icing effects of fluid ingress on high altitude flight on laminated composite primary structures.

3. Research on the mechanisms of damage propagation in laminated composites due to absorbed fluids during GAG cycle.

4. Create an appropriate Finite Element Analysis (FEA) model using Abaqus or other packages (as available) to model delaminations in an aircraft composite laminate.

5. Create a composite panel utilising embedded FBG sensors and strain gauges to laboratory level investigation of how damage accumulation progresses through the GAG cycle of an aircraft.

6. Carry out laboratory experimentations to investigate damage propagation in water absorbed composite panel.

7. Carry out Data Analysis to compile, plot and evaluate the collected data obtained from the test samples.

8. Write up the project dissertation.

If time permits:

9. Investigate crack propagation through composite laminates through the use of a Thermography and Thermoelastic stresses.

AGREED

Student Date Supervisor

Appendix B – Risk Assessment

University of Southern Queensland

Generic Risk Management Plan

Workplace (Division/Faculty/Section):		
Assessment No (if applicable):	Assessment Date:	Review Date: (5 years maximum)
1	1/05/2015	1/05/2020
Context: What is being assessed? Describe the item, job, process, work arrangement, event etc:		
ENG4111 and ENG4112 Thesis Experiments		
Assessment Team – who is conducting the assessment?		
Assessor(s):		
Samuel Pike		
Others consulted: (eg elected health and safety representative, other personnel exposed to risks)		

The Risk Management Process

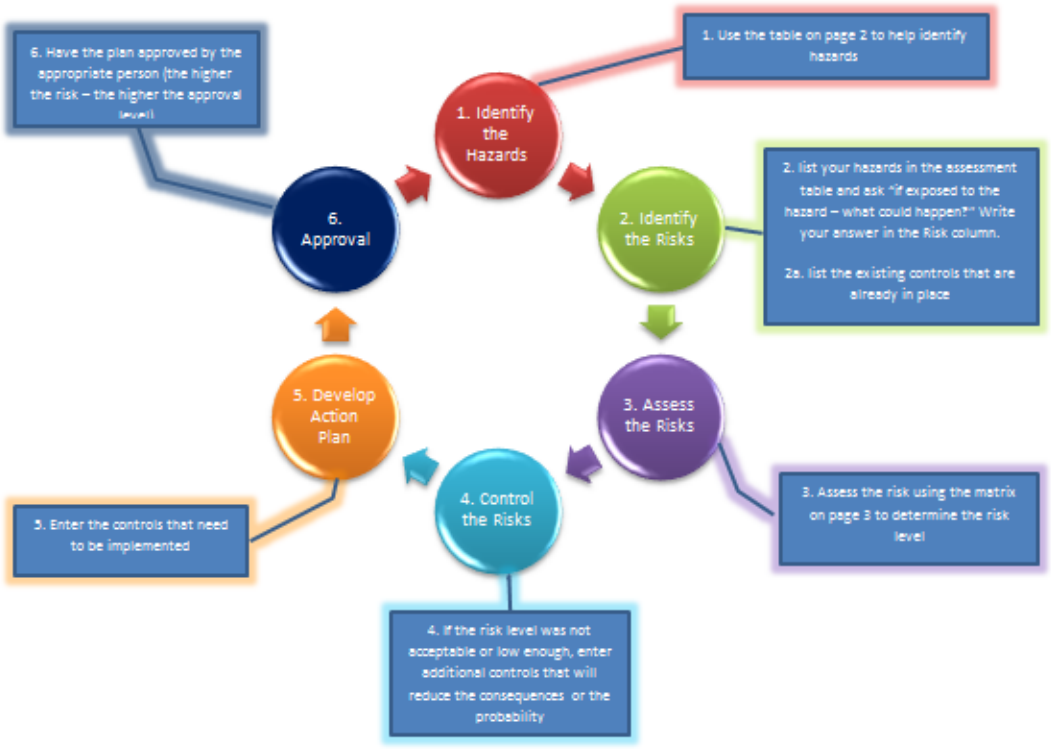

Step 1 - Identify the hazards (use this table to help identify hazards then list all hazards in the risk table)		
General Work Environment		
☐ Sun exposure	☐ Water (creek, river, beach, dam)	☒ Sound / Noise
☐ Animals / Insects	☐ Storms / Weather/Wind/Lightning	☐ Temperature (heat, cold)
☐ Air Quality	☐ Lighting	☐ Uneven Walking Surface
☐ Trip Hazards	☐ Confined Spaces	☐ Restricted access/egress
☐ Pressure (Diving/Altitude)	☐ Smoke	☐
Other/Details:		
Machinery, Plant and Equipment		
☐ Machinery (fixed plant)	☐ Machinery (portable)	☒ Hand tools
☐ Laser (Class 2 or above)	☐ Elevated work platforms	☐ Traffic Control
☐ Non-powered equipment	☐ Pressure Vessel	☐ Electrical
☐ Vibration	☐ Moving Parts	☐ Acoustic/Noise
☐ Vehicles	☐ Trailers	☐ Hand tools
Other/Details:		
Manual Tasks / Ergonomics		
☐ Manual tasks (repetitive, heavy)	☐ Working at heights	☐ Restricted space
☐ Vibration	☐ Lifting Carrying	☐ Pushing/pulling
☐ Reaching/Overstretching	☐ Repetitive Movement	☐ Bending
☐ Eye strain	☐ Machinery (portable)	☒ Hand tools
Other/Details:		
Biological (e.g. hygiene, disease, infection)		
☐ Human tissue/fluids	☐ Virus / Disease	☐ Food handling
☐ Microbiological	☐ Animal tissue/fluids	☐ Allergenic
Other/Details:		
Chemicals Note: Refer to the label and Safety Data Sheet (SDS) for the classification and management of all chemicals.		
☐ Non-hazardous chemical(s)	☒ 'Hazardous' chemical (Refer to a completed hazardous chemical risk assessment)	
☐ Engineered nanoparticles	☐ Explosives	☐ Gas Cylinders
Name of chemical(s) / Details: Kinetix R246TX and H180		
Critical Incident – resulting in:		
☐ Lockdown	☐ Evacuation	☐ Disruption
☐ Public Image/Adverse Media Issue	☐ Violence	☐ Environmental Issue
Other/Details:		
Radiation		
☐ Ionising radiation	☐ Ultraviolet (UV) radiation	☐ Radio frequency/microwave
☐ infrared (IR) radiation	☐ Laser (class 2 or above)	☐
Other/Details:		
Energy Systems – incident / issues involving:		
☐ Electricity (incl. Mains and Solar)	☐ LPG Gas	☐ Gas / Pressurised containers
Other/Details:		
Facilities / Built Environment		
☐ Buildings and fixtures	☐ Driveway / Paths	☐ Workshops / Work rooms
☐ Playground equipment	☐ Furniture	☐ Swimming pool
Other/Details:		
People issues		
☒ Students	☒ Staff	☐ Visitors / Others
☐ Physical	☐ Psychological / Stress	☐ Contractors
☐ Fatigue	☐ Workload	☐ Organisational Change
☐ Workplace Violence/Bullying	☐ Inexperienced/new personnel	☐
Other/Details:		

Step 1 (cont) Other Hazards / Details (enter other hazards not identified on the table)

Risk Matrix

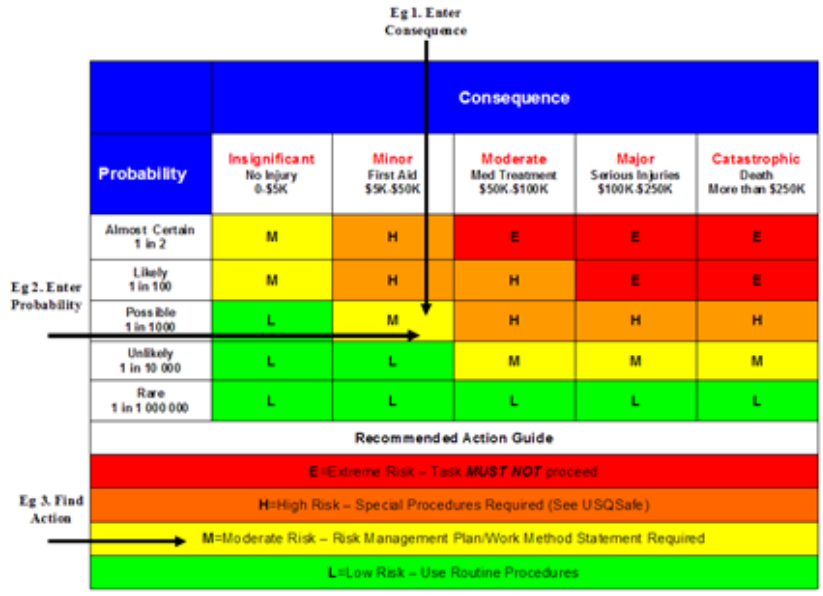

Risk register and Analysis

Step 1 (cont)	Step 2	Step 2a	Step 3			Step 4				
Hazards: From step 1 or more if identified	The Risk: What can happen if exposed to the hazard with existing controls in place?	Existing Controls: What are the existing controls that are already in place?	Risk Assessment: (use the Risk Matrix on p3) Consequence x Probability = Risk Level			Additional controls: Enter additional controls if required to reduce the risk level	Risk assessment with additional controls: (use the Risk Matrix on p3 – has the consequence or probability changed?)			Controls Implemented? Yes/No
			Consequence	Probability	Risk Level		Consequence	Probability	Risk Level	
Example										
Working in temperatures over 35º c	Heat stress/heat stroke/exhaustion leading to serious personal injury/death	Regular breaks, chilled water available, loose clothing, fatigue management policy.	catastrophic	possible	high	temporary shade shelters, essential tasks only, close supervision, buddy system	catastrophic	unlikely	mod	Yes
Preparation of Samples	Fumes	PPE to be worn at all Times	Moderate	Rare	Low		Select a consequence	Select a probability	Select a Risk Level	Yes or No
Working with cold samples	Cold Burns	PPE to be worn at all Times	Minor	Unlikely	Low		Select a consequence	Select a probability	Select a Risk Level	Yes or No
Using FBGs	Eye Damage	PPE to be worn at all Times	Minor	Unlikely	Low		Select a consequence	Select a probability	Select a Risk Level	Yes or No
			Select a consequence	Select a probability	Select a Risk Level		Select a consequence	Select a probability	Select a Risk Level	Yes or No
			Select a consequence	Select a probability	Select a Risk Level		Select a consequence	Select a probability	Select a Risk Level	Yes or No
			Select a consequence	Select a probability	Select a Risk Level		Select a consequence	Select a probability	Select a Risk Level	Yes or No
			Select a consequence	Select a probability	Select a Risk Level		Select a consequence	Select a probability	Select a Risk Level	Yes or No
			Select a consequence	Select a probability	Select a Risk Level		Select a consequence	Select a probability	Select a Risk Level	Yes or No
			Select a consequence	Select a probability	Select a Risk Level		Select a consequence	Select a probability	Select a Risk Level	Yes or No
			Select a consequence	Select a probability	Select a Risk Level		Select a consequence	Select a probability	Select a Risk Level	Yes or No
			Select a consequence	Select a probability	Select a Risk Level		Select a consequence	Select a probability	Select a Risk Level	Yes or No
			Select a consequence	Select a probability	Select a Risk Level		Select a consequence	Select a probability	Select a Risk Level	Yes or No
			Select a consequence	Select a probability	Select a Risk Level		Select a consequence	Select a probability	Select a Risk Level	Yes or No
			Select a consequence	Select a probability	Select a Risk Level		Select a consequence	Select a probability	Select a Risk Level	Yes or No
			Select a consequence	Select a probability	Select a Risk Level		Select a consequence	Select a probability	Select a Risk Level	Yes or No
			Select a consequence	Select a probability	Select a Risk Level		Select a consequence	Select a probability	Select a Risk Level	Yes or No

Step 5 – Action Plan (for controls not already in place)			
Control Option	Resources	Person(s) responsible	Proposed implementation date

Step 6 – Approval

Drafter's Comments:

Drafter Details:

Name: Samuel Pike Signature: Date: 1/05/2015

Assessment Approval: (Extreme or High = VC, Moderate = Cat 4 delegate or above, Low = Manager/Supervisor)

I am satisfied that the risks are as low as reasonably practicable and that the resources required will be provided.

Name: Signature: Date: / /

Position Title:

The University of Southern Queensland

USQSafe
Enquiries: (07) 4631 2520
Facsimile: (07) 4631 2829

Date of Assessment:	1/05/2015	Due Date of Reassessment:	1/05/2020
Assessors Names:		Job:	
Substances:	Kinetix R246TX and H180	Use:	FoES Martin Geach
Location:	Fabrication Room P11		

1 USING THE MSDS AND LABEL, DETERMINE:

Hazards and Health Effects		Potential Routes of Exposure		MSDS Recommended Control Measures	
Corrosive		Inhalation	X	Engineering	
Irritant		Ingestion		Isolation	
Sensitising		Skin/Eye	X	PPE	X
Carcinogenic				Other	
Mutagenic					
Teratogenic					
Toxic	X				
Asphyxiate					
Flammable					
Other					

2 INSPECT THE WORKPLACE AND EVALUATE THE EXPOSURE

	Yes	No
Is the substance used in the work environment?	X	
Is the substance emitted or released into the work area?	X	
Are staff or students exposed to the substance via any of the potential routes of exposure listed:		
• Inhalation	X	
• Ingestion	X	
• Skin Absorption	X	
Have any employees experienced symptoms of exposure?		

If YES, list these:

Have any employees reported any health effects?

If YES, list these:

Looking at the work process, location of workers and considering all persons with the potential for exposure, consider the following:

	Yes	No
Is there evidence of contamination?	☐	☒
• Dusts or fumes visible in the air or on surfaces	☐	☒
• Substances visible on a person's skin or clothing	☐	☒
• Visible leaks, spills or residue	☐	☒
• Other	☐	☒
Is there direct contact with the substance?	☐	☒
Is there a potential for splashes?	☐	☒

What is the time exposure to the substance?

	Number of Times	Period of Each Time (minutes/hours)
• Per day	_____	_____
• Per week	_____	_____
• Per month	_____	_____
• Per year	_____	_____

	Yes	No
Is the substance used in concentrated form?	☒	☐
Is the substance diluted by the user?	☐	☒
Are the health effects different for diluted and undiluted?	☐	☒

If YES what are the health statements for UNDILUTED solution: _____

Are any of the following controls in place and are they properly maintained (cleaned, recorded, follow-up)?

	Present		Maintained	
	Yes	No	Yes	No
• Are there engineering controls in place?	☒	☐	☒	☐
• Are there gen. ventilation & local ventilation systems in Place?	☒	☐	☒	☐
• Are workers trained in the proper use of the substance?	☒	☐	☒	☐
• Do work practices ensure safe handling?	☒	☐	☒	☐
• Is the appropriate PPE used?	☒	☐	☒	☐
• Are there facilities for changing and washing?	☒	☐	☒	☐
• Are good housekeeping practices in place?	☒	☐	☒	☐
• Are hazardous substances stored correctly	☒	☐	☒	☐
• Is waste disposed of properly	☒	☐	☒	☐

• Are there emergency procedures in place?	X		X	
• Is there emergency equipment eg eye wash	X		X	

3 EVALUATE THE RISK

	Low	High
Nature and severity of the hazard/s	X	
Degree of exposure	X	
Are existing control measures adequate?	Yes	

4 ASSESSMENT RESULTS

What is the conclusion about risks?

Conclusion 1	Risks not significant	X
Conclusion 2	Risks significant BUT effectively controlled	
Conclusion 3	Risks significant and NOT adequately controlled	
Conclusion 4	Uncertain about risks, expert opinion required	

NOTE: Conclusion 3 and 4 require **further action.**

5 COMMENTS

Please provide any comments regarding the assessment.

Risk is not significant due to the infrequent use and small quantities held.

6 ACTIONS RESULTING FROM ASSESSMENT RESULTS

(Only further actions that need to be carried out)

Requires no further action	X
Seek expert help	
Requires appropriate control measures	
Requires induction and training	
Requires emergency procedures/first aid	

If Risk is SIGNIFICANT can the substance be:	Yes	No
Eliminated		
Substituted (less hazardous substances)		
Separated (eg relocated from workers)		
Enclosed (isolated)		
Controlled by ventilation/engineering controls		

Isolated (eg restrict entry; organise job rotation; personnel not allowed to work alone)	☐	☐
Controlled by the use of PPE (this is to be used as a last resort only)	☐	☐

7 DO YOU BELIEVE AIR MONITORING IS REQUIRED?

	Yes	No
If the degree of exposure is high and the existing control measures are inadequate, then it is Likely air monitoring is required.	☐	☒

8 DO YOU BELIEVE HEALTH SURVEILLANCE IS REQUIRED?

	Yes	No
If the degree of exposure is high and the substance is listed in column 1 of schedule 6 of the QLD Workplace Hazardous Substances Regulations then health surveillance will be required.	☐	☒

NOTE: THIS RISK ASSESSMENT IS ONLY RELEVANT ON THE CONDITION THAT ALL CONTROLS ARE IN PLACE AND USED AND ALL INSTRUCTIONS AS PROVIDED BY THE MSDS AND RISK ASSESSMENT ARE COMPLIED WITH.

SIGNATURE OF ASSESSOR/S: _____ **Date:** _____

APPROVED BY: _____ **Date:** _____

Appendix C – Thermography Pictures First Tensile Test

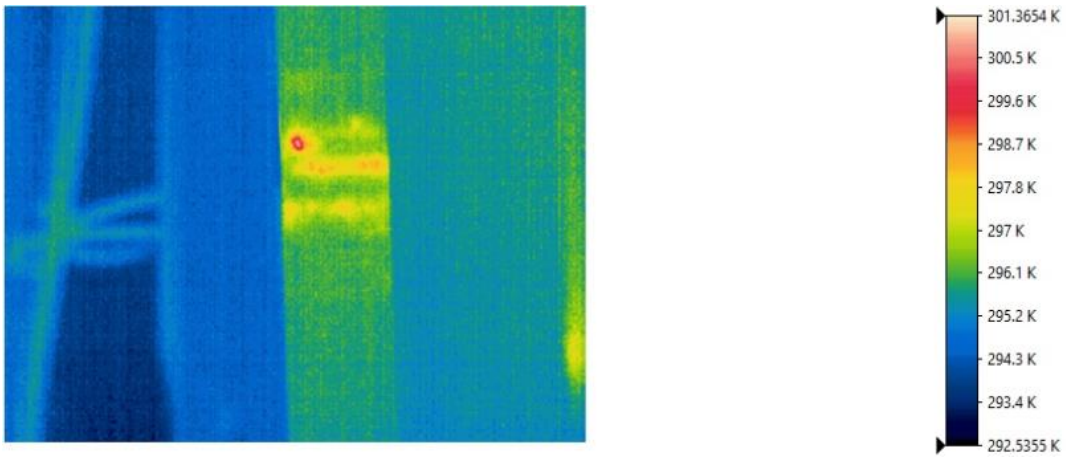

Figure 86: 100 Fatigue Cycles

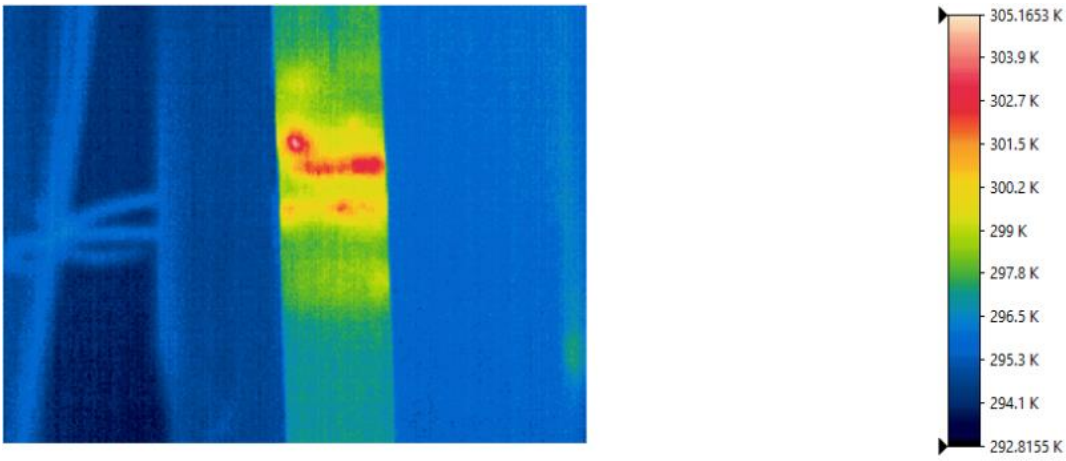

Figure 87: 1000 Fatigue Cycles

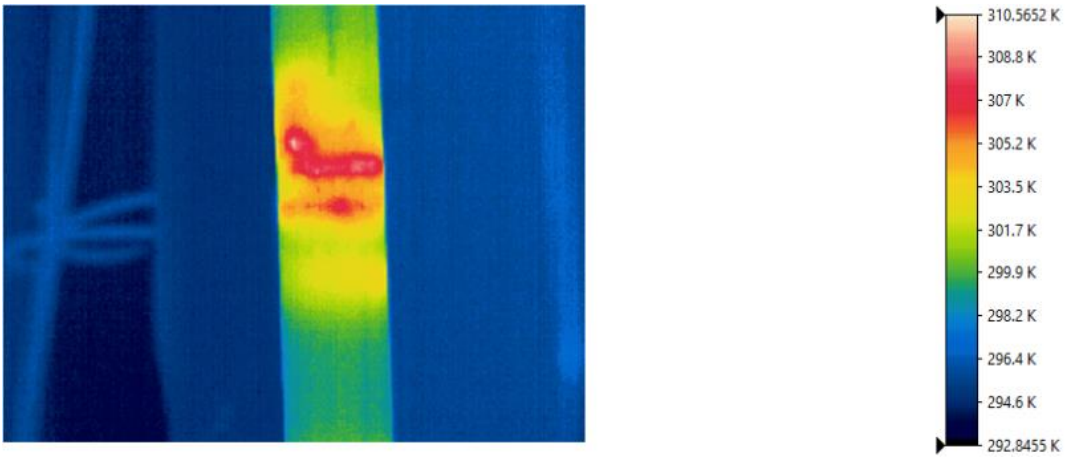

Figure 88: 2000 Fatigue Cycles

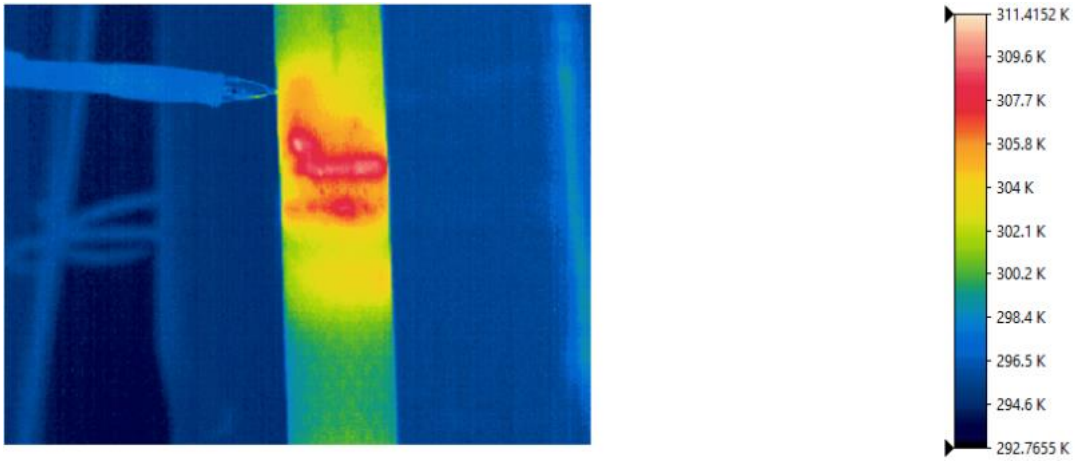

Figure 89: 2300 Fatigue Cycles

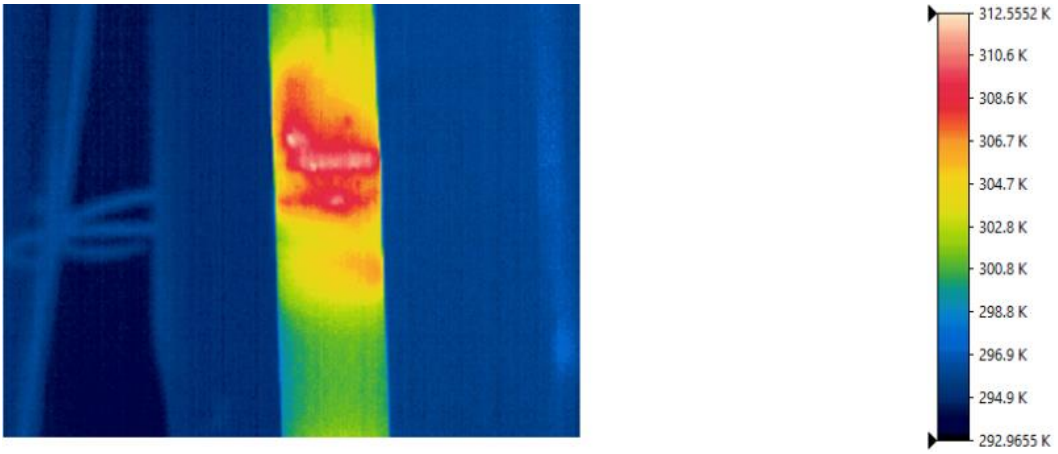

Figure 90: 3000 Fatigue Cycles

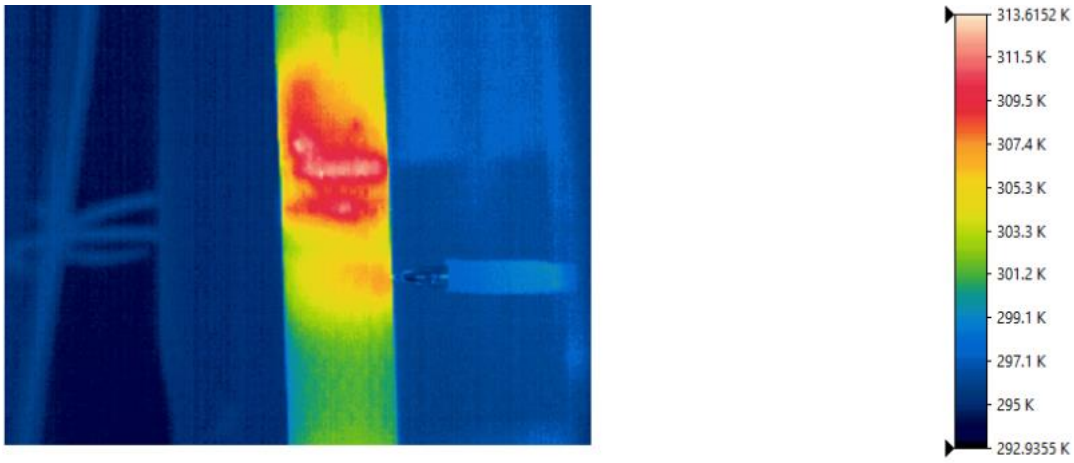

Figure 91: 3500 Fatigue Cycles

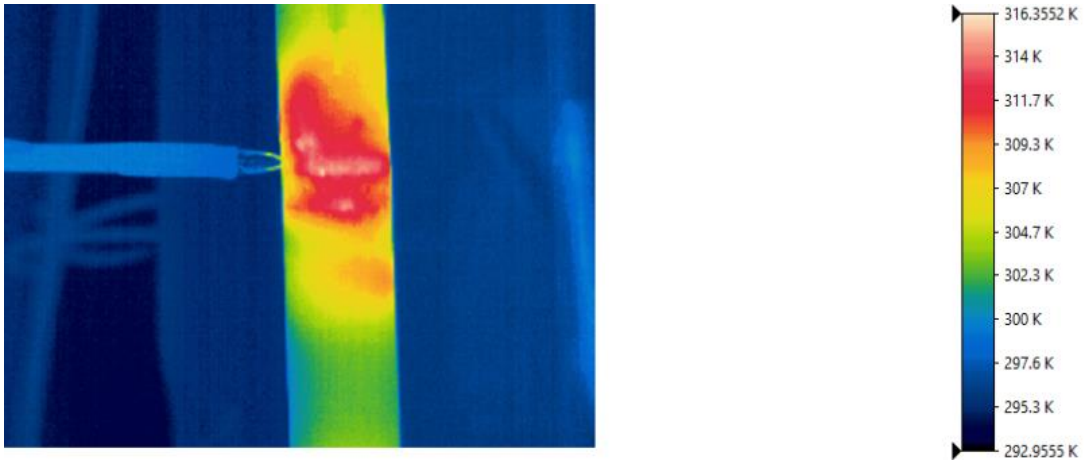

Figure 92: 4600 Fatigue Cycles

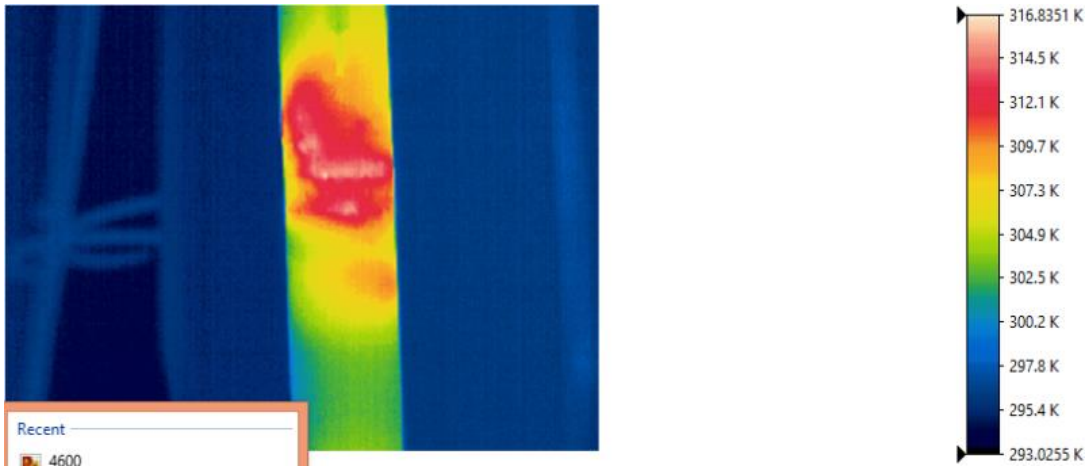

Figure 93: 5000 Fatigue Cycles

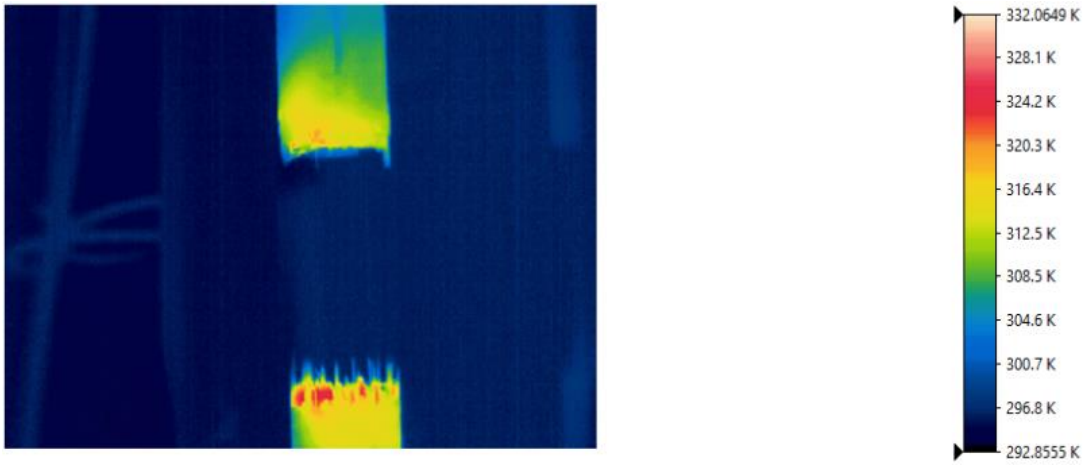

Figure 94: 5200 Fatigue Cycles

Thermography Pictures Second Tensile Test

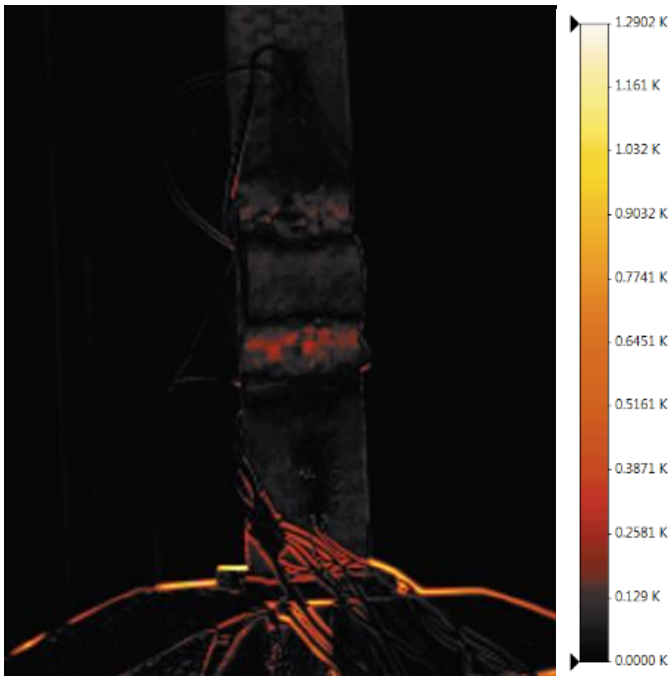

Figure 95: Black Spectrum

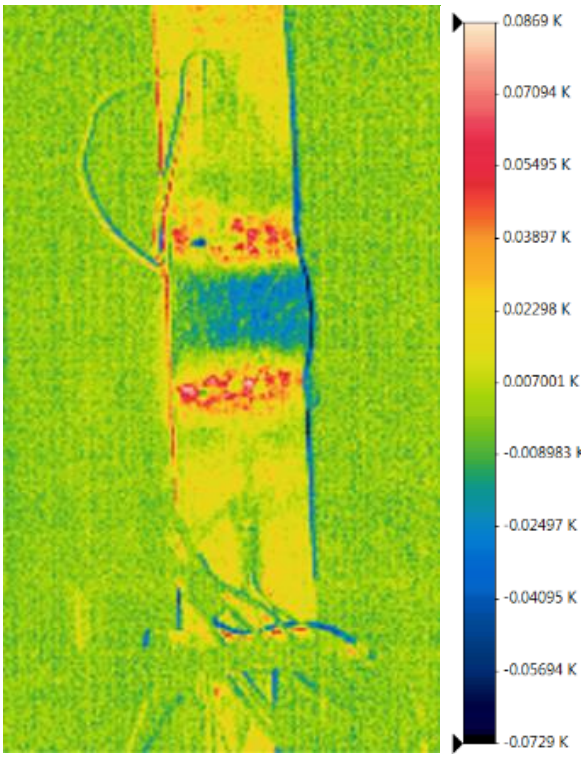

Figure 96: Green Spectrum

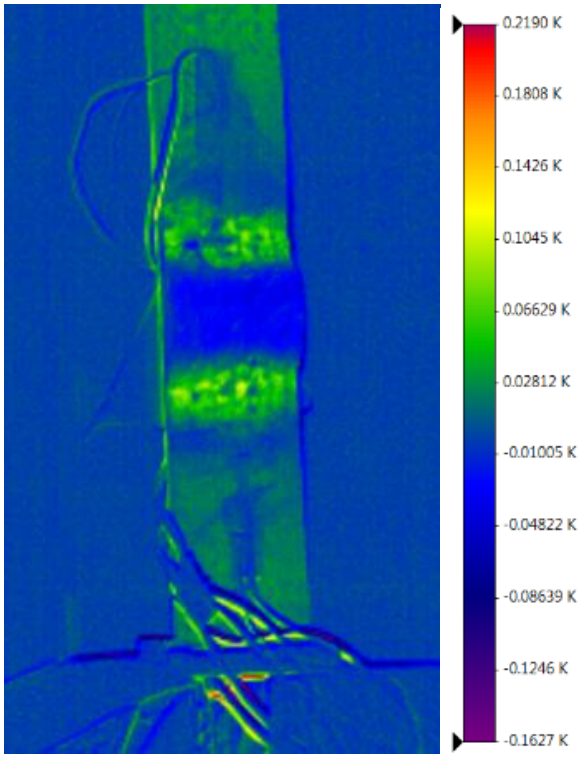

Figure 97: Blue Spectrum

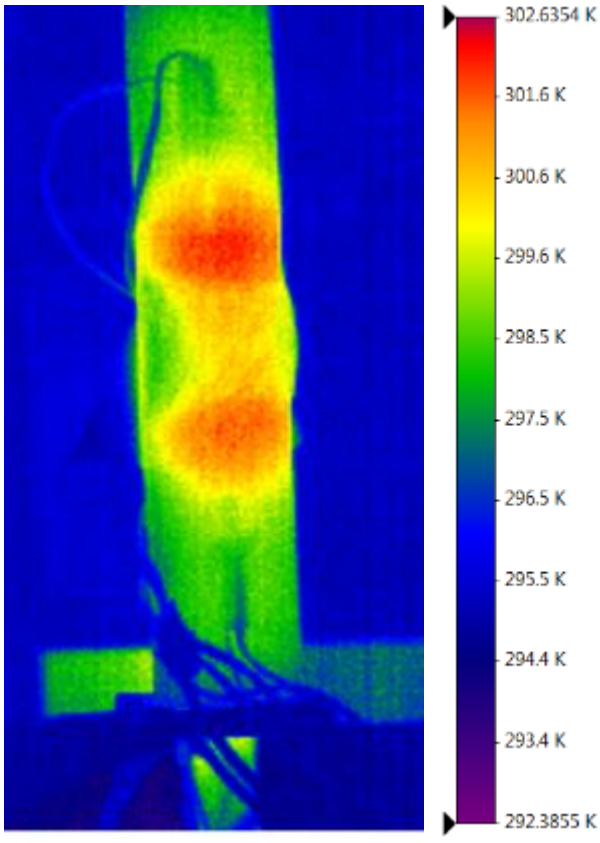

Figure 98: Multi Coloured Spectrum

Appendix D - FBG pictures

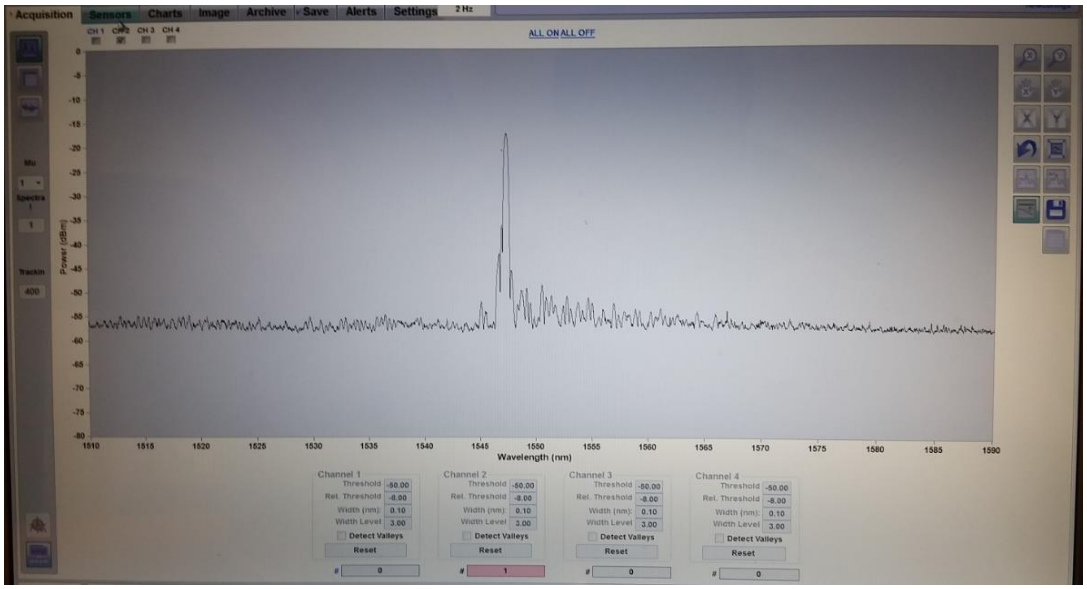

Figure 99: FBG Test Signal

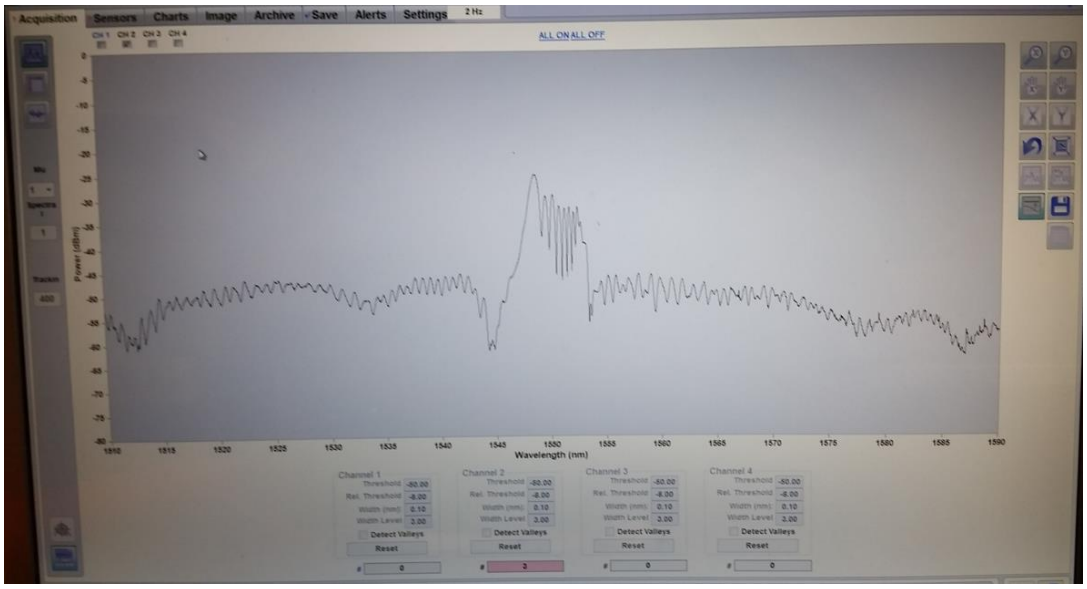

Figure 100: FBG 1000 Cycles

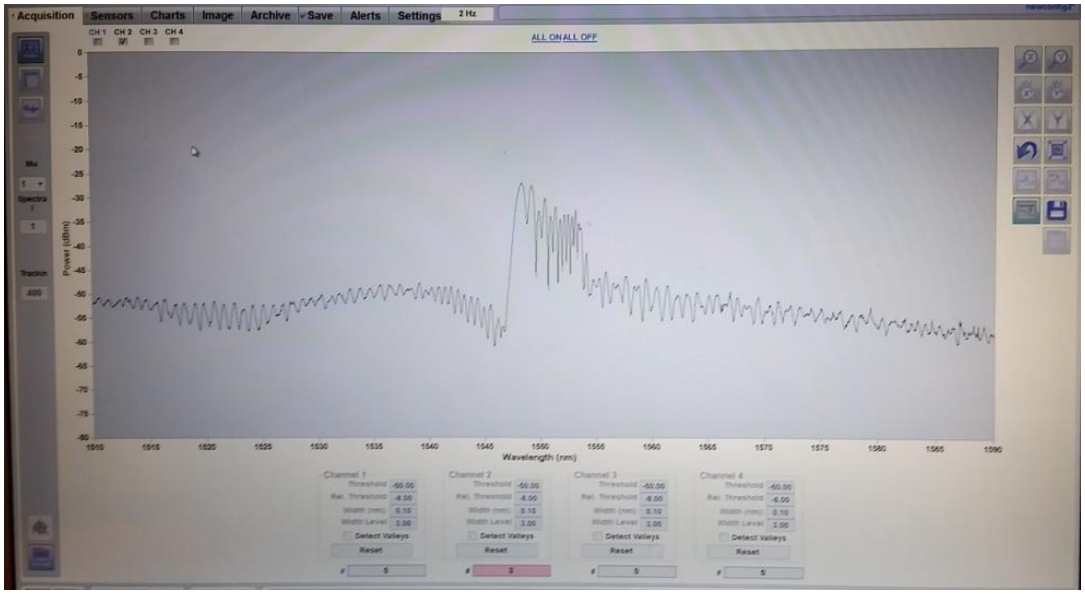

Figure 101: FBG 2000 cycles

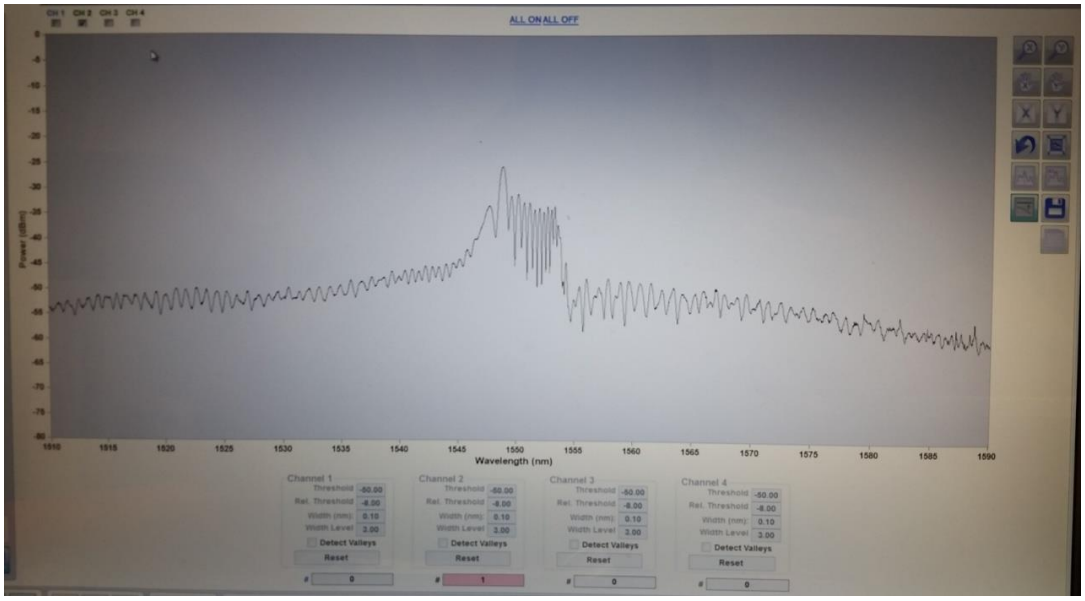

Figure 102: FBG 3000 cycles

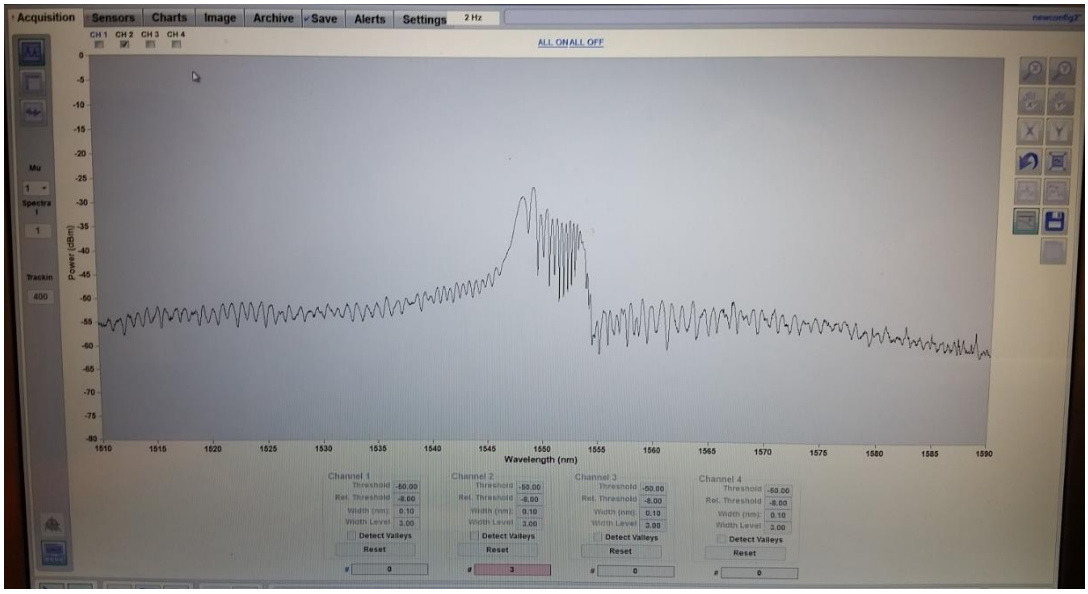

Figure 103: FBG 4000 Cycles

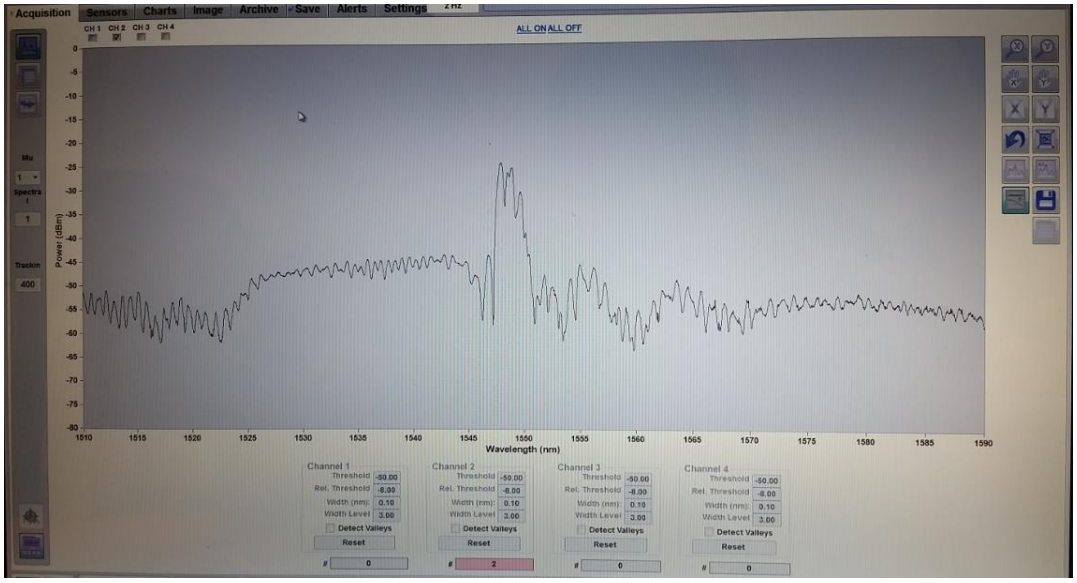

Figure 104: FBG 5000 cycles